UNIVERSITY OF CINCINNATI

March 17 , 20 03

I, Jessica Marlene Phillips ,
hereby submit this as part of the requirements for the degree of:

Master's of Science

in:

Chemical Engineering

It is entitled:

Utilizing Flow Microcalorimetry to Investigate the
Adsorption of Biomolecules on Chromatographic Supports

Approved by:

UTILIZING FLOW MICROCALORIMETRY TO INVESTIGATE THE ADSORPTION OF BIOMOLECULES ON CHROMATOGRAPHIC SUPPORTS

A thesis submitted to the

Division of Research and Advanced Studies
of the University of Cincinnati

in partial fulfillment of the
requirements for the degree of

MASTER OF SCIENCE

in the Department of Chemical and Material Engineering
of the College of Engineering

2003

by

Jessica M. Phillips
M.M., University of Cincinnati College-Conservatory of Music, 2001
B.M., Kansas State University, 1998

Committee Chair:
Dr. Neville G. Pinto
Dr. Jerry Y.S. Lin
Dr. Panagiotis Peter Smirniotis

ABSTRACT

Heats of adsorption for BSA on an ion exchange adsorbent and nitrogen bases, nucleosides, and homo-deoxyoligonucleotides on a hydrophobic adsorbent were collected through flow microcalorimetry in order to ascertain the thermodynamic driving force for adsorption in each case. The heat of adsorption results for BSA on PEI–1000–10 and homo-deoxyoligonucleotides poly(A) and poly(T) on Sepharose CL–6B were analyzed in conjunction with water release data obtained through preferential interaction analysis.

It was determined that for nitrogen bases and nucleosides, enthalpy changes associated with base stacking self-interactions contributed significantly to the observed heats of adsorption. Accordingly, the observed heats were a combination of the heat of adsorption and the enthalpy change associated with base stacking self-interactions. Since base stacking proceeds beyond the dimer stage, multi-layer adsorption of these compounds is likely, even under linear isotherm conditions.

Heat of adsorption data for homo-deoxyoligonucleotides suggest that these biomolecules adsorb in an "end-on" orientation. For the poly(A) 30mer, it was determined that the small charge spacing in this oligonucleotide contributed to the large endothermic heat of adsorption and decrease in retention factor. This implies that the retention factor decreases as the charge spacing decreases for homo-deoxyoligonucleotides. These results indicate that, while hydrophobic interaction typically predominates, other interactions, such as repulsion between the hydrophobic adsorbent and the charged phosphate groups, can significantly alter the thermodynamics of the adsorption process and thus the retention behavior.

Endothermic heats of adsorption were obtained for the BSA/PEI–1000–10 system in the absence of salt and in 0.1 M LiCl, KCl, and NaCl. Analysis of these data, along with water release data, indicates that the endothermic heats result from a combination of surface dehydration, repulsive interactions, and conformational changes/reorientation of the protein on the surface. The entropic driving force likely derives from a combination of water release and conformational changes.

This study demonstrates that by combining heat of adsorption data obtained through flow microcalorimetry with water release data derived from preferential interaction analysis, which utilizes chromatographic retention times, significant contributors to the thermodynamic driving forces for biomolecular adsorption onto chromatographic supports can be uncovered.

To Brian,

for all of his help and support.

ACKNOWLEDGEMENTS

I would like to thank my advisor, Dr. Neville Pinto, for providing his help and expertise whenever needed. Also, thank you to Marvin Thrash—without his guidance and encouragement, I could not have completed this project. Thanks to Malyuba Abu Daabes and Blanca Lapizco-Encinas—our office conversations kept me focused on research, but also helped me see the big picture.

I would also like to express my appreciation to all the Chemical Engineering faculty members for helping me make the transition from the liberal arts to engineering. This has been a challenging but truly rewarding experience for me.

Finally, thanks to my husband, Brian—I couldn't have done it without you; and to my family, for your love and encouragement.

TABLE OF CONTENTS

LIST OF TABLES

LIST OF FIGURES

List of Symbols

$a_{\pm}$	Mean ionic activity (mol solute/kg solvent)
B	Biomolecule
b	Biomolecule stoichiometric coefficient
C	Biomolecule-sorbent complex
c	Biomolecule-sorbent complex stoichiometric coefficient
ΔC_P	Change in heat capacity (kcal/mol·K)
ΔG	Change in Gibb's free energy (kcal/mol)
ΔH	Change in enthalpy (kcal/mol)
K	Equilibrium constant associated with adsorption process
k'	Capacity factor
m_i	Molal concentration of component i (mol solute/kg solvent)
n	Total number of ions associated with the electrolyte
R	Universal gas constant (8.314 J/(mol·K), 0.00198 kcal/(mol·K))
ΔS	Change in entropy (kcal/mol)
S	Sorbent
s	Sorbent stoichiometric coefficient
T	Temperature (K)
T_H	Temperature at which the standard-state enthalpy is zero (K)
T_S	Temperature at which the standard-state entropy is zero (K)
$t_{r,i}$	Retention time of the biomolecule that is intermittently adsorbed (sec)
$t_{m,i}$	Retention time of a solute (of the same size as the biomolecule) that does not adsorb (sec)

Greek Symbols

ε_b	Interstitial void fraction of the column
ε_{pi}	Accessible porosity of the bed for species *i*
Γ_{32}^{m}	Preferential interaction coefficient
ϕ	Phase ratio of the chromatographic column
ν_i	Number of moles of species *i* immediately surrounding the biomolecule per biomolecule (mol)
$\Delta\nu_i$	Stoichiometrically weighted change in the number of moles of species *i*
μ_i	Chemical potential of component *i* (kcal/mol)
$\gamma_{\pm}$	Mean ionic activity coefficient

Subscripts

ads	Adsorption
EQ	Equilibrium
obs	Observed
sol'n	Solution
1	Solvent
2	Biomolecule
3	Solute
+	Cations
-	Anions

Superscripts

°	Standard state

1. Background and Problem Statement

1.1 Introduction

Biomolecules of different types are of vital importance in today's pharmaceutical industry. Drug designers have developed novel methods of protein and nucleic acid production that enable the manufacture of various drugs. A crucial step in the processing of these drugs is purification. For obvious reasons, the purification standards of pharmaceutical products are the highest of any industry. However, with this high level of purification comes a high economic cost in producing large quantities of pharmaceuticals (Ladisch, 2001).

A typical bioseparations purification sequence consists of multiple steps. First, the solids and liquid are separated through sedimentation, centrifugation, and/or filtration. Next, the product is recovered through membrane separation and/or precipitation. Finally, the product is purified through crystallization, adsorption, and/or chromatography (Ladisch, 2001). Although chromatography is only one part of a multi-step procedure, it typically accounts for 50% of the purification costs of a bioproduct (Ladisch, 2001).

Chromatography takes advantage of molecular differences between the target molecules and impurities. For example, ion-exchange chromatography (IEC) exploits differences in electrostatic charge of molecules, while hydrophobic interaction chromatography (HIC) exploits differences in molecular hydrophobicity. Although chromatography has been successfully utilized for biomolecular purification for a number of years, the thermodynamics of the adsorption processes employed in chromatography are not well understood. In fact, the scale-up of chromatographic

separation units is surprisingly unscientific because of this current lack of understanding (Ladisch, 2001).

The first step in optimizing large-scale chromatographic separations is a thorough understanding of the adsorption process. To this end, researchers have sought to quantify the thermodynamic parameters that constitute the driving force for adsorption through various methods, including van't Hoff analysis and direct calorimetric measurements. When the driving forces for adsorption under different conditions are thoroughly understood, an improved model for large-scale chromatographic separations can be developed. The long-term goal of researchers investigating this subject is to improve the economics of chromatography through superior optimization, thus enabling pharmaceutical companies to provide essential products at lower costs to consumers. This improvement could ultimately make currently high-cost medications available to everyone, thus improving the quality of life for millions of people.

1.2 Chromatography

There are several popular chromatographic techniques currently utilized, including IEC, HIC, reversed-phase chromatography (RPC), affinity chromatography (AC), and size-exclusion chromatography (SEC). Each technique exploits specific differences in chemical structure between biomolecules. The purpose of this research is to gain insight on the adsorption thermodynamics of specific biomolecules on IEC and HIC chromatographic supports. Therefore, it is important to have an understanding of IEC and HIC chromatographic procedures in order to interpret the microcalorimetric data obtained.

1.2.1 Ion-Exchange Chromatography (IEC)

Ion-exchange chromatography is one of the most commonly used chromatographic methods (Thrash and Pinto, 2000). In IEC, charged functional groups on the biomolecule interact with charged groups on the adsorbent. The functional groups of the chosen chromatographic support possess a charge opposite that of the target biomolecule at separation conditions. It is generally through the electrostatic interaction between support and biomolecule that separation is achieved. Elution is accomplished by increasing the ionic strength or the pH of the carrier fluid (Thrash and Pinto, 2000).

The strength of the charge on the chromatographic support is an important parameter in IEC. For a strongly charged protein, a weakly charged support is the most suitable. In this instance, using a weakly charged support will help ensure that the protein adsorption is reversible. For a weakly charged protein, a strongly charged support is necessary to ensure that adsorption of the protein does, in fact, take place (Thrash and Pinto, 2000).

As stated above, the elution of the biomolecule in IEC is frequently accomplished through an increasing salt gradient. Generally, as the salt concentration increases, the level of adsorption decreases. As the salt concentration increases, more salt ions are available to bind with sites on the ion-exchange support. These salt ions in effect "trade places" with the adsorbed biomolecules, causing the biomolecules to elute.

The pH of the carrier fluid is often chosen in relation to the target protein's isoelectric point (pI). The isoelectric point is the pH at which the biomolecule has no net charge. By utilizing a carrier fluid with a pH above that of the protein's pI, a net negative charge on the protein is produced. Similarly, choosing a carrier fluid pH below the protein's pI causes the protein to have a net positive charge (Thrash and Pinto, 2000). By altering the charge of the protein in this way, chromatographic separations can be optimized.

1.2.2 Hydrophobic Interaction Chromatography (HIC)

Another method often employed in the purification of biomolecules is HIC. Researchers have successfully separated target proteins from complex biological mixtures through HIC, which exploits differences in hydrophobicity among the biological components to effect separations. In this method of chromatography, the biomolecule of interest adsorbs onto an HIC support and is eluted through a decreasing salt gradient. The carrier fluid typically utilized is an antichaotropic salt such as ammonium sulfate. Antichaotropic salts increase the surface tension of the water, promoting water molecule ordering and enhancing the adsorption of the biomolecule on hydrophobic supports (Gooding and Regnier, ed., 1990).

Because of the presence of the antichaotropic salt in HIC, the biomolecules become preferentially hydrated. This can be explained as follows. The high salt concentration increases the Gibb's free energy of the biomolecule. In order to lower this free energy, water molecules surround the biomolecule and in effect shield the biomolecule from the salt molecules in the bulk liquid. These water molecules

surrounding the biomolecule are highly ordered. However, the free energy of this preferentially hydrated biomolecule is higher than the free energy of the biomolecule adsorbed to the chromatographic support. Therefore, when the preferentially hydrated biomolecule is contacted with a support that is hydrophobic, the biomolecule adsorbs to the support, releasing the ordered water molecules. This release of water molecules causes an increase in the overall entropy of the system. The driving force for adsorption in HIC is generally considered to be this increase in entropy (Lin *et al.*, 2002).

The principle of an increase in adsorption with an increase in salt concentration would seem to imply that an extremely high salt concentration would produce the best adsorptive results. However, if the salt concentration is too high, the biomolecule will precipitate out of solution in order to decrease its interaction with the salt and thus decrease its overall Gibb's free energy (Gooding and Regnier, ed., 1990).

The advantage of HIC over other types of chromatography, such as RPC, is that it generally exposes the biomolecule to a less stressful chemical environment. HIC utilizes a hydrophobic support, but this support is typically less hydrophobic than supports used in RPC. This is one reason the biomolecules are less likely to denature in HIC relative to RPC (Thrash and Pinto, 2000). Since biomolecular function is inherently tied to structure, HIC is attractive for the purification of biomolecules. According to Thrash and Pinto (2000), another advantage of HIC is that it can remove harmful biomolecules such as endotoxins, nucleic acids, and viruses from the sample.

1.3 Biomolecular Structure

In order to meaningfully analyze adsorption equilibria, an understanding of the structure of the target biomolecule is helpful. First, the structure determines the surface area of the biomolecule available for binding on the sorbent. Second, changes in structure may accompany adsorption, and may contribute to changes in the thermodynamic driving force. Third, the ordering of water molecules is dependent on the biomolecular structure. The release of these water molecules upon binding to the adsorbent can increase the overall entropy of the system, which in turn contributes to the thermodynamic favorableness of the process. For these reasons, it is useful to understand the basic structures of the biomolecules of interest.

1.3.1 Proteins

Proteins are biomolecules with highly specific functions and are a common component of biopharmaceuticals. The molecular weights of proteins range from about 5,000 to over a million Daltons (Ritter, 1996). Proteins are polymeric molecules consisting of amino acid monomers. A schematic of an amino acid is shown in Figure 1-1. Each amino acid contains a central carbon atom, or α-carbon, an amine group, a carboxyl group, and a side chain. There are 20 different possible side chains, and each side chain defines a different amino acid. The primary structure of a protein is the sequence of amino acids that are connected in a chain-like fashion through their α-carbons (Mathews and van Holde, 1990). The amino acid monomers are connected through peptide bonds, as shown in Figure 1-2. The three-dimensional

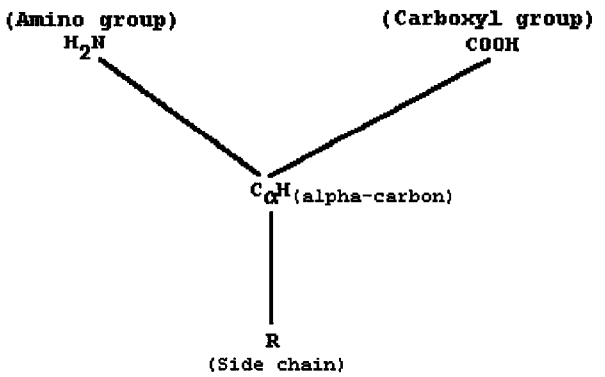

Figure 1-1. Schematic of an amino acid monomer, which includes the primary carbon, or α-carbon, an amino group, a carboxyl group, and a side chain (Friedli, 2000).

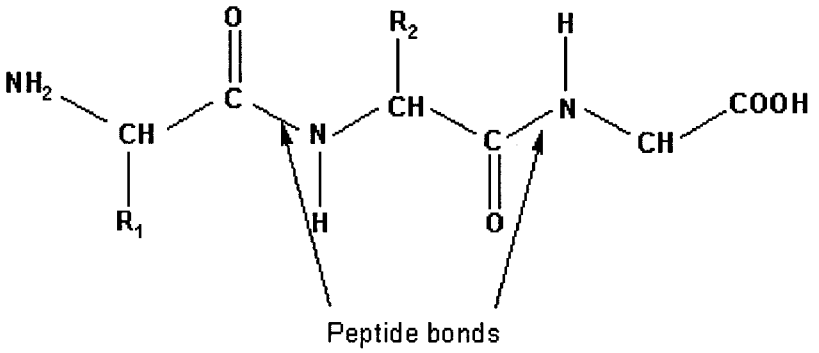

Figure 1-2. Schematic of amino acid monomers connected through peptide bonds. R_1 denotes the side chain of the first amino acid, and R_2 denotes the side chain of the second (Friedli, 2000).

structure of the resulting biopolymer is largely determined by the sequence and particular characteristics of the side chains.

When proteins dissolve in an aqueous solution, their structure is primarily determined by the location of their hydrophobic and hydrophilic moieties. In aqueous solution, the protein typically folds in such as way that it presents its hydrophilic groups to the aqueous environment while protecting its hydrophobic groups within the interior of the structure. However, not all hydrophobic groups are hidden from

the aqueous environment, so HIC can be a viable option for separating proteins (Gooding and Regnier, ed., 1990; Mathews and van Holde, 1990).

Globular proteins have compactly folded polypeptide chains unlike fibrous proteins, which have long, extended chains. The structure of a globular protein typically has a distinct interior and exterior largely determined through the locations of hydrophobic and hydrophilic side chains. When a globular protein denatures, it unfolds and exists in a random coil. This random coil is constantly changing conformation. The three-dimensional structure of many denatured proteins can be regained by manipulating the protein's environment, such as temperature and pH. This is important, since proteins change their structure and thus lose their function upon denaturation.

The protein used in the first set of experiments was bovine serum albumin (BSA; Sigma Product Number A-3675). Albumin is a blood plasma protein whose function is to bind with free fatty acids and deliver them to tissues (Mathews and van Holde, 1990). The structure of BSA can be approximated as a globular ellipsoid with dimensions 14×4×4 nm. The molecular weight of BSA is about 69,000 and its pI is 4.7 (Esquibel-King *et al.*, 1999).

1.3.2 Oligonucleotides

Oligonucleotides are the key components in a relatively new class of drugs that hold promise in combating genetic diseases as well as AIDS and some forms of cancer. Oligonucleotide drugs can inhibit transcription, inhibit translation, or directly bind to undesirable proteins (Kontturi *et al.*, 2002). In the past decade, biochemists

have made great strides in developing methods of synthesizing and purifying oligonucleotides in small quantities. However, as these drugs become available to the public, it is crucial for researchers to develop effective and economical processing and purification methods for large quantities of oligonucleotides.

Oligonucleotides are relatively short nucleic acids. While the double-helical structure of DNA is familiar to most, oligonucleotides generally exist in single, unbound strands. The oligonucleotides used in anti-sense drugs (those that inhibit translation) are typically 15 to 30 bases long with molecular weights ranging from approximately 5000 to 10,000 (Kontturi *et al.*, 2002).

The ability of a single strand to bind to its complementary strand is the feature drug designers exploit in anti-sense drug technology (Ritter, 1996). The oligonucleotide, synthesized to be complementary to a specific nucleic acid called a sense strand, is introduced into the human body. It binds with the complementary nucleic acid, thus rendering it biologically inactive. Researchers are exploring ways to utilize anti-sense oligonucleotides in drug therapies. For example, these drugs make it possible to control production of specific proteins in the body or hinder the reproductive capabilities of some cells or viruses (Ritter, 1996).

Oligonucleotides are biopolymers consisting of monomers connected by phosphodiester links. Each monomer contains a phosphate group, a five-carbon sugar, and a nitrogen base. The five-carbon sugar in RNA is ribose; in DNA it is 2'-deoxyribose. There are two types of nitrogen bases: purines, which include adenine (A) and guanine (G), and pyrimidines, which include cytosine (C), thymine (T), and uracil (U). G, C, A, and T are the bases in DNA, and G, C, A, and U are the bases in

RNA (Mathews and van Holde, 1990). Figure 1-3 shows the structure of various deoxyribonucleotides. Notice that for these compounds the sugar is 2'-deoxyribose

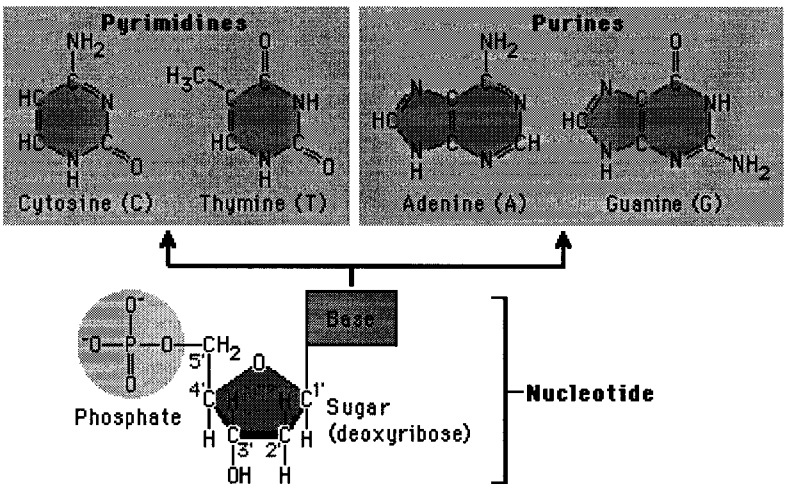

Figure 1-3. 2'-deoxynucleotide structure. Notice that all 2'-deoxynucleotides contain the same sugar (2'-deoxyribose) and phosphate group but vary according to type of nitrogen base. Base types for deoxynucleotides include G, C, A, and T (Russell, 1997).

and the possible bases are G, C, A, and T. For ribonucleotides, the sugar contains an oxygen at the 2'-carbon, and the thymine is replaced by uracil, shown in Figure 1-4.

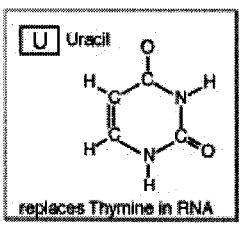

Figure 1-4. Structure of the nitrogen base uracil. For ribonucleotides, base types include G, C, A, and U (National Human Genome Research Institute, Division of Intramural Research, 2003).

Because the primary difference in the monomer unit is the type of base, and because each monomer unit contains one base, the length of these biopolymers is often cited in number of bases. Obviously, the number of bases also corresponds with

the number of monomer units for single-stranded oligonucleotides. (In the case of double-stranded nucleic acids, such as DNA, the length of the biopolymer is usually expressed as the number of base pairs, not the number of individual bases.)

Oligonucleotides containing only one type of monomer, and therefore only one type of base, are called homo-oligonucleotides. Thermodynamic data relating to the homo-deoxyoligonucleotides of adenine and thymine with two different base lengths will be reported in Chapter 5.

The structural properties of oligonucleotides that can be exploited in chromatography are the size/chain length, the negatively charged phosphodiester groups, and the hydrophobic bases and hydrophobic sugar residues. Because the hydrophobic bases and sugar residues are both exposed in single-stranded oligonucleotides, HIC and RPC are the most widely utilized chromatographic methods for oligonucleotide purification (Gooding and Regnier, ed., 1990).

Since oligonucleotides exist in single strands that contain both hydrophobic groups and a negative charge, the conformation of oligonucleotides in aqueous solution can change very quickly and is highly dependent on the conditions. The strand may adopt a three-dimensional coil in which the hydrophobic bases direct themselves into the center of the coil. Oligonucleotides containing different bases may bind to themselves in sections where complementary sequences occur. In general, the structures adopted by single-stranded oligonucleotides in aqueous solution are diverse and constantly changing (Oliver, ed., 1998). Although oligonucleotide conformation in aqueous solution is critical to both drug delivery and

oligonucleotide drug purification processes, it is not well understood (Kontturi *et al.*, 2002).

1.4 Energetics of Adsorption

The expression for the change in Gibb's free energy of adsorption is given by:

$$\Delta G_{ads} = \Delta H_{ads} - T\Delta S_{ads} \qquad (1\text{-A})$$

According to equation (1-A), an increase in entropy or a decrease in enthalpy contributes to a negative ΔG_{ads}. Furthermore, if an endothermic heat of adsorption is detected, it is clear that the adsorption process must be entropically driven, since a large, positive ΔS_{ads} must accompany a positive ΔH_{ads} in order for the overall change in Gibb's free energy to be negative.

Previous calorimetric research indicates that protein adsorption utilizing HIC supports is typically entropically driven. Esquibel-King and coworkers measured endothermic heats of adsorption for BSA and concluded that the adsorption process for BSA on Sepharose CL–6B was entropically driven. These researchers explained the increase in entropy using the preferential interaction model, which takes into account the release of water molecules from the surface and the biomolecule when adsorption occurs (Esquibel-King *et al.*, 1999). According to Thrash and Pinto, the fact that adsorption in HIC is entropically driven may explain why HIC is generally less disruptive to biomolecular structures than other types of chromatography (Thrash and Pinto, 2000).

Calorimetric data for adsorption onto IEC supports have revealed both endothermic and exothermic heats of adsorption. These data imply that IEC

adsorption can generally be driven by enthalpy, entropy, or a combination of both. The driving force for adsorption in IEC is largely dependent on the chosen sorbent and the chromatographic conditions, such as pH and salt concentration (Thrash and Pinto, 2000).

1.4.1 *Van't Hoff Analysis*

Many researchers have utilized van't Hoff plots in order to determine the relative contributions of enthalpy changes and entropy changes to the overall change in Gibb's free energy. The advantage of the van't Hoff approach is that researchers can generate a plethora of data from a relatively small number of measurements. Researchers performing van't Hoff analysis utilize the following equation:

$$\Delta G^\circ = RT \ln K = \Delta H^\circ - T\Delta S^\circ \qquad \text{(1-B)}$$

where ΔG° is the change in Gibb's free energy at standard state, R is the universal gas constant, T is the temperature in Kelvin, K is the equilibrium constant associated with the biomolecular adsorption onto the chromatographic support, ΔH° is the change in enthalpy at standard state, and ΔS° is the change in entropy at standard state (Lin *et al.*, 2002). The relationship between the equilibrium constant and the retention factor is given by:

$$k' = K \times \phi \qquad \text{(1-C)}$$

where k' is the retention factor and ϕ is the phase ratio of the column. Using Equation (1-C), Equation (1-B) can be re-written as:

$$\ln k' = -\frac{\Delta H^\circ}{RT} + \frac{\Delta S^\circ}{R} + \ln \phi \qquad \text{(1-D)}$$

When the enthalpy change and entropy change are independent of temperature, it is typically assumed that the phase ratio is also temperature independent and the resulting van't Hoff plot is linear. From a linear plot, ΔH° can be determined from the slope and ΔS° from the intercept (Lin *et al.*, 2002). ΔG° is then obtained using Equation (1-B) with the known values for ΔH° and ΔS°.

Lin and coauthors (2002) suggest that non-linear van't Hoff plots more accurately describe protein and polypeptide behavior in HIC and RPC. For non-linear plots, equation (1-D) is combined with other equations relating the standard-state enthalpy and entropy changes to the change in heat capacity. The resulting equation, termed the logarithmic relationship, allows researchers to use least square fitting procedures to determine ΔC_P°, the change in standard-state heat capacity and T_H and T_S, the temperatures at which the standard-state enthalpy and entropy changes are zero, respectively. From these parameters, the standard-state enthalpy, entropy, and Gibb's free energy changes can be calculated (Lin *et al.*, 2002).

Van't Hoff analysis has limitations, however. First, the calculated values of ΔG°, ΔH°, and ΔS° are specifically at standard state. Second, the linear and non-linear relationships described above include assumptions, such as constant ΔH° and ΔS° with changing temperature for the linear case, and constant ΔC_P° with changing temperature for the logarithmic relationship (Lin *et al.*, 2002). Because of these assumptions and limitations of van't Hoff analysis, the numerical results obtained through this method must be viewed as estimates.

Esquibel-King and coauthors published one example of the inaccuracy of van't Hoff data. These researchers measured endothermic heats of adsorption for

BSA on Sepharose CL–6B when the van't Hoff data predicted exothermic heats of adsorption (Esquibel-King *et al.*, 1999). As pointed out by Esquibel-King, the heat of adsorption measurements were obtained under chromatographic conditions. Therefore, these measurements represented the thermodynamics of the actual process, while van't Hoff data only provided standard-state values. Consequently, the driving forces for adsorption, particularly under overloaded conditions, cannot be categorically obtained using van't Hoff analysis alone.

1.5 Scope and Objectives

The value of ΔH_{ads} is typically quite small, but can be measured through microcalorimetry. Various calorimetric methods, including isothermal titration calorimetry (ITC), differential scanning calorimetry (DSC), and flow microcalorimetry (FMC) have been utilized in measuring heats of adsorption for various biomolecules (Ladbury and Chowdry, ed., 1998; Thrash and Pinto, 2001, 2002, 2003; Esquibel-King *et al.*, 1999; Lin *et al.*, 2000, 2001; Tsai *et al.*, 2002). Because the aim of this project was to understand adsorption of biomolecules on chromatographic supports in order to improve large-scale purification processes, FMC was the best choice for our endeavors.

Flow microcalorimetry is a valuable technique for chromatographic separations because it replicates the conditions that occur in a chromatographic column. Flow microcalorimetry utilizes a cell packed with sorbent, which is directly analogous to a chromatographic column. In FMC as in chromatography, fluid flows

through the packed cell. Minute temperature changes associated with the adsorption of biomolecules in chromatographic processes can be detected *in situ*.

The goal of this project was to characterize the driving forces for adsorption of specific biomolecules onto chromatographic supports. By better understanding the nature of this adsorption, large-scale chromatographic processes can be improved.

In order to meet this goal, flow microcalorimetry was employed to directly measure heats of adsorption associated with bovine serum albumin (BSA) on PEI–1000–10, an ion-exchange support, and nitrogen bases, nucleosides, and homo-deoxyoligonucleotides on Sepharose CL–6B, a hydrophobic support. The data were analyzed to determine the primary driving force for adsorption in each case.

The applicability of IEC to protein purification has been well documented (Thrash and Pinto, 2002, 2001, 2000; Raje and Pinto, 1997; Bowen and Hughes, 1993; Gooding and Regnier, ed., 1990; Hearn *et al.*, 1988). However, the study of oligonucleotide adsorption onto hydrophobic adsorbents is a more recent development. Diogo and coauthors have demonstrated the applicability of HIC to oligonucleotide purification (Diogo *et al.*, 2003, 2002, 2000). Their research indicated that double-stranded plasmid DNA could be separated from single-stranded nucleic acid impurities using HIC.

Other research groups have studied novel purification techniques, such as displacement chromatography and membrane adsorber chromatography, for synthetic oligonucleotides (Tugcu *et al.*, 2003, 2001; Deshmukh *et al.*, 2000, 1998). The most significant impurities found in synthetic phosphorothiote oligonucleotides are the

(n-1) deletion sequences and the partial phosphodiesters (Tugcu *et al.*, 2003). Clearly, the purification of synthetic oligonucleotides and the purification of oligonucleotides derived from plasmid DNA both present distinct challenges.

Because the focus of this study was to determine the driving forces for HIC of oligonucleotides, one published study was of particular interest. Diogo and coworkers performed HIC on oligonucleotides poly(A), poly(T), and poly(U) (Diogo *et al.*, 2002). For all three base types, these researchers studied strand lengths of 6, 15, and 30 bases. Their results indicated that, for the 6mer, poly(A) was the most strongly retained, followed by poly(T), and the least retained was poly(U). These results were expected, since adenine has been shown to be the most hydrophobic of the three bases studied (Ikuta *et al.*, 1984). However, at longer oligonucleotide lengths, poly(A) was not necessarily the most strongly retained. In fact, the 30mer of poly(T) was the most retained at high ammonium sulfate concentrations, followed by poly(A) and then poly(U) (Diogo *et al.*, 2002). The researchers concluded that, at longer strand lengths, adenine has a higher propensity to form a secondary structure that shields some of its hydrophobic moieties.

The conditions of our study mirrored those used to gather data in the study cited above. The adsorption of homo-deoxyoligonucleotides on hydrophobic supports was studied using flow microcalorimetry to determine the thermodynamic driving forces for the adsorption process. In order to ascertain the effects of base type, salt concentration, and oligonucleotide length on the thermodynamics of this adsorption process, these three parameters were varied.

Generally, the hydrophobicity of an oligomer can be determined using the following expression:

$$H = \sum_{i=1}^{n} B_i n + (n-1)P \qquad \text{(1-E)}$$

where H is the hydrophobicity of the solute, B_i is the hydrophobicity of the base i, n is the chain length, and P is the hydrophobicity (either positive or negative) of the polar groups. In the case of oligonucleotides, P is generally considered the hydrophobic effect of the phosphate group (Ikuta *et al.*, 1984). Therefore, according to this model the oligonucleotide groups primarily responsible for hydrophobic interactions are the nitrogen bases and the phosphate groups. For a homo-oligonucleotide, the above expression can be rewritten as:

$$H = Bn + (n-1)P \qquad \text{(1-F)}$$

Because of the prohibitively high cost of homo-deoxyoligonucleotides, a novel method for determining optimal conditions to collect oligonucleotide adsorption data was employed. As indicated in Equation (1-F) above, the hydrophobicity of the nitrogen base largely determines the homo-oligonucleotide adsorption onto a hydrophobic support. Therefore, the first stage in this research project was to study the adsorption of adenine and thymine on Sepharose CL–6B using flow microcalorimetry. By using these relatively inexpensive materials, the optimal FMC conditions for the study of oligonucleotide adsorption were determined through numerous experiments that were repeated as necessary. Additionally, the ammonium sulfate concentration was varied between 1.0 and 2.0 M in order to examine the effects of salt concentration on the heat of adsorption.

The second stage involved the study of the nucleosides 2'-deoxyadenosine and thymidine. Both of these nucleosides contain the sugar 2'-deoxyribose, as can be seen in Figures 1-5 and 1-6. 2'-deoxyadensine and thymidine were chosen because

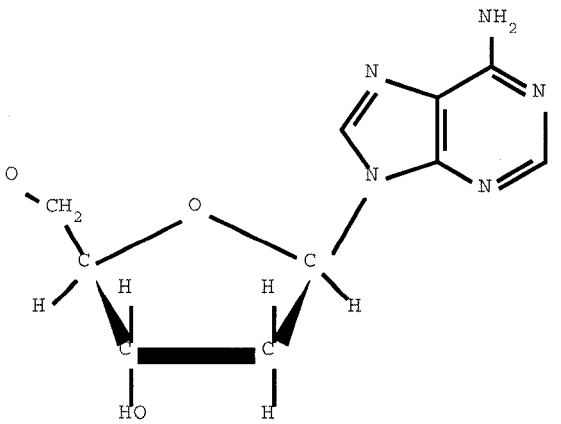

Figure 1-5. The chemical structure of the nucleoside 2'-deoxyadenosine (Ritter, 1996).

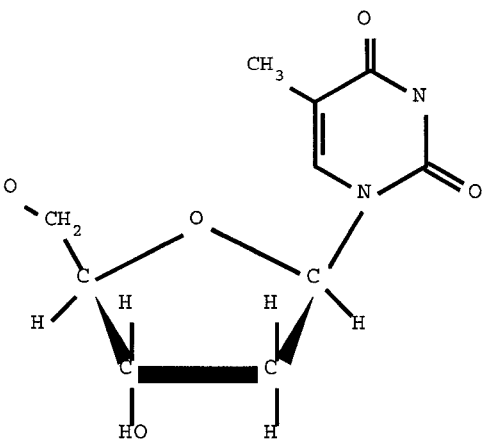

Figure 1-6. The chemical structure of the nucleoside thymidine (Ritter, 1996).

they contain the same sugar as the homo-deoxyoligonucleotides utilized in the final research stage. As in the first stage, the adsorption of these nucleosides onto Sepharose CL–6B was studied while varying the ammonium sulfate concentration. Equation (1-F) suggests that the deoxyribose does not contribute to the hydrophobicity of the oligomer, thus inferring that the adsorption behavior of the bases adenine and thymine should be essentially the same as for the related

nucleosides 2'-deoxyadenosine and thymidine. This assumption was explored by comparing the heats of adsorption for the related compounds.

After completing calorimetric experiments with the bases and nucleosides, heats of adsorption for the homo-deoxyoligonucleotides poly(T) and poly(A) at base lengths of 6 and 30 were collected through flow microcalorimetry. Using these data in conjunction with water release data for the same oligonucleotides, possible contributors to the thermodynamic driving force for adsorption to a hydrophobic adsorbent were uncovered.

2. Experimental Methods and Materials

2.1 Apparatus

Calorimetric data were gathered using a flow microcalorimeter, shown in Figure 2-1 (FMC; Gilson Instruments, Westerville, OH, USA). This instrument is capable of measuring temperature changes as small as 10^{-6}° C. It operates isothermally and includes syringe micropumps to ensure precision fluid delivery. The FMC also includes a vacuum system to evacuate air from the packed cell. Minute temperature changes within the cell are detected through highly sensitive thermistors. These thermistors, along with other details pertaining to the FMC cell, are shown in Figure 2-2. The temperature is monitored and controlled through a block heater.

The FMC is equipped with an injection loop that can be reconfigured to accommodate different sample volumes. The sample is loaded into the injection loop with a small syringe and injected into the packed cell via a multiport valve. The effluent from the cell is typically collected and measured for the biomolecule concentration using a UV spectrophotometer (Milton Roy, Rochester, NY, USA) at a wavelength specific to the target biomolecule.

2.2 Methods and Materials

2.2.1 Materials: Nitrogen Bases and Nucleosides on Sepharose CL–6B

The nitrogen bases adenine (Sigma Product Number A-8626) and thymine (T-0376) and the related nucleosides 2'-deoxyadenosine (D-7400) and thymidine (T-9250) were purchased from Sigma (St. Louis, Missouri, USA) and used without

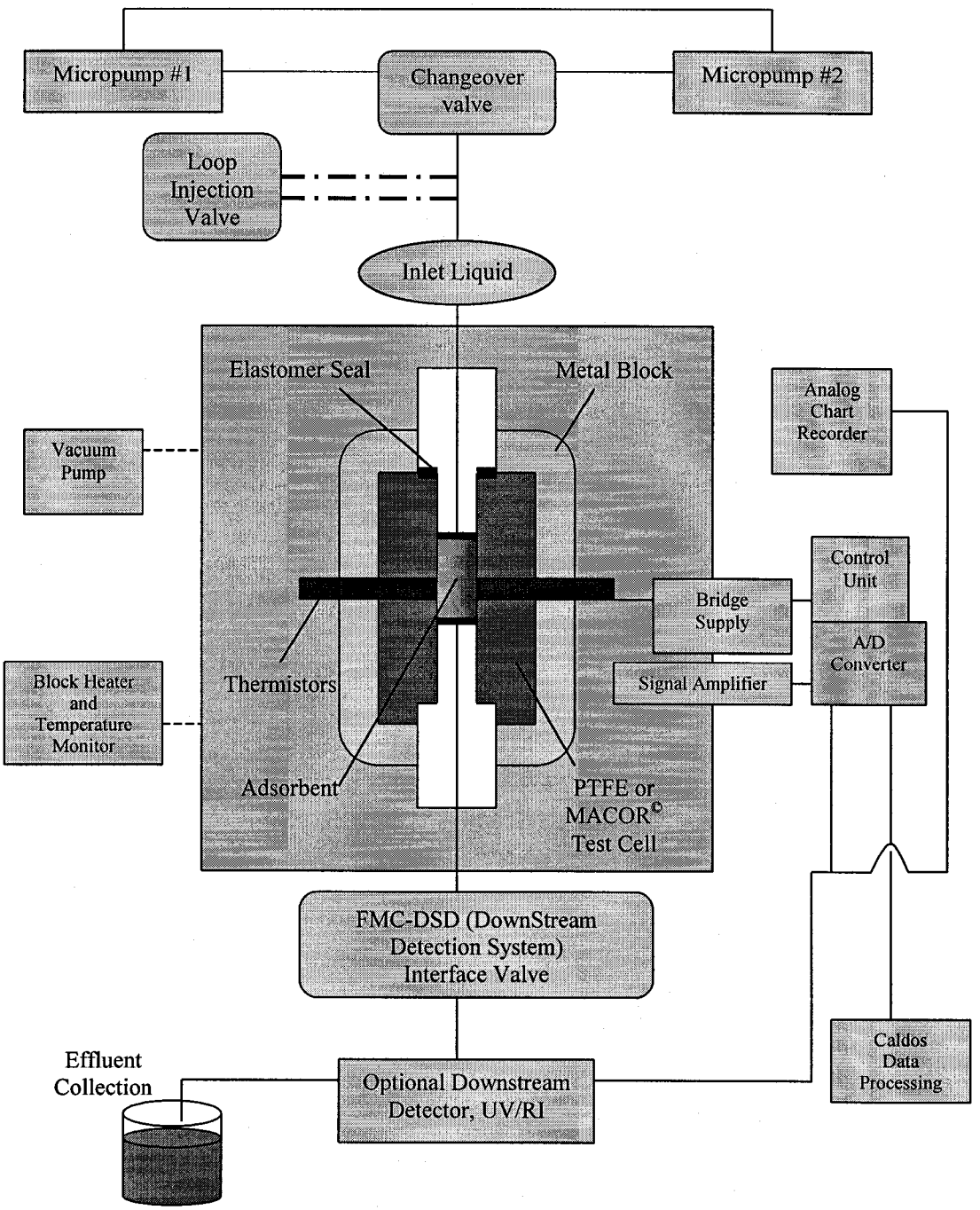

Figure 2-1. A schematic of the Microscal flow microcalorimeter (FMC) (Microscal, 2001).

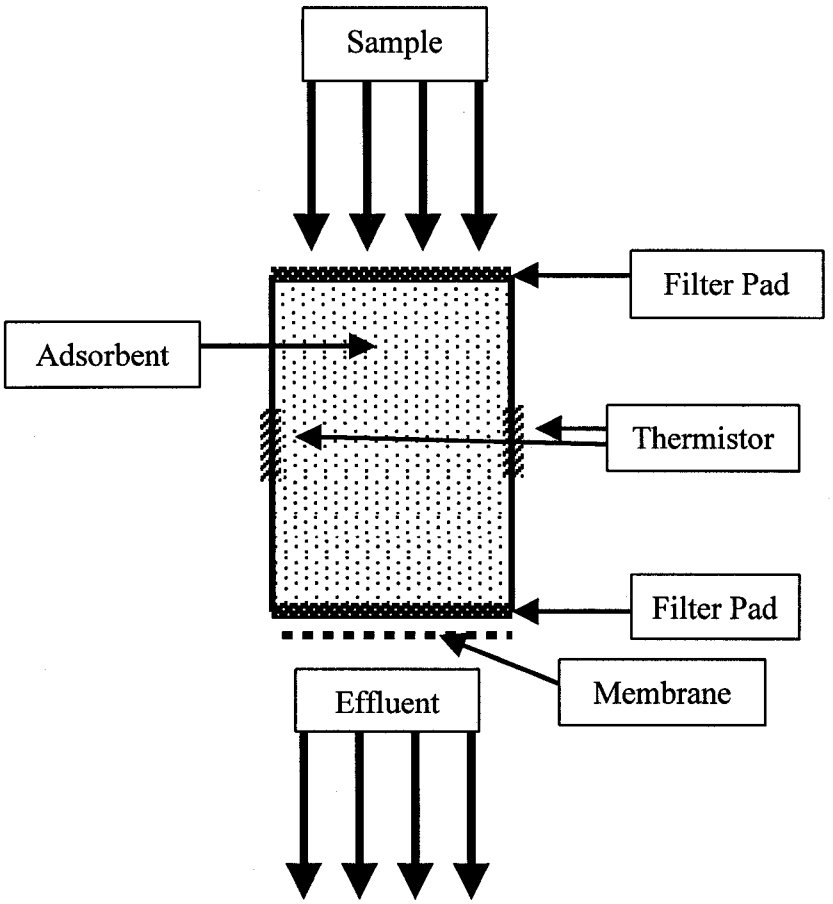

Figure 2-2. An enlarged view of the FMC cell. The cell is packed with adsorbent and minute temperature changes are detected by the thermistors.

further purification. Adenine and thymine were studied at a concentration of 0.25 mg/mL; 2'-deoxyadenosine and thymidine were studied at a concentration of 2 mg/mL. Adenine, thymine, and thymidine solutions were dissolved at room temperature. To aid in dissolution, 2'-deoxyadenosine solutions in 20 mL glass bottles were covered tightly with Parafilm and heated to a temperature of approximately 45° C for about four hours by direct contact with an electric hot plate.

The buffer used was 10 m*M* Trizma buffer purchased from Sigma (St. Louis, Missouri, USA). In order to inhibit bacterial growth, 0.01% (wt.) sodium azide, also purchased from Sigma, was added to the buffer solution. The buffer solution was titrated to a pH of 8.0 using HCl purchased from Fisher Scientific Company (Hanover Park, IL, USA). Analytical grade ammonium sulfate, also purchased from Fisher, was chosen as the modulator. After the addition of the ammonium sulfate, the solution was again titrated to pH 8.0 using NaOH purchased from Fisher.

The chosen hydrophobic support, Sepharose CL–6B, was synthesized by the research group of Dr. J.A. Queiroz, Departamento de Química, Universidade da Beira Interior, Covilha Portugal. It is a Sepharose derivative synthesized by covalent immobilization of the ligand 1,4-butanediol diglycidyl ether on Sepharose CL–6B. The structure of this support is shown in Figure 2-3 (Esquibel-King *et al.*, 1999). The

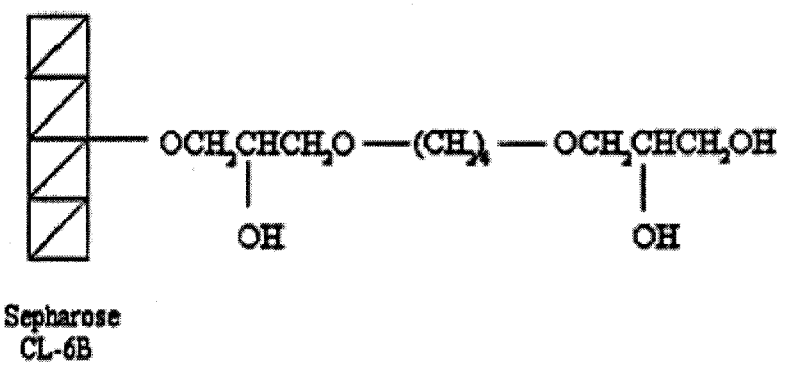

Figure 2-3. Structure of the chosen HIC support, a Sepharose derivative synthesized by covalent immobilization of the ligand 1,4-butanediol diglycidyl ether on Sepharose CL–6B (Esquibel-King *et al.*, 1999).

Sepharose CL–6B was crushed to a fine powder by hand using a mortar and pestle. It has been previously determined that approximately 0.154 g of the adsorbent, when

contacted with carrier fluid, expands to approximately 0.171 mL, the volume of the FMC cell. Accordingly, 0.154 g of the powder was mixed with approximately 1 mL of the buffer solution and allowed to swell in a covered beaker at room temperature for several days.

2.2.2 Flow Microcalorimetry with Bases and Nucleosides on Sepharose CL–6B

The cell was packed with the swelled Sepharose CL–6B powder. It was then equilibrated for several days with buffer from the syringe micropumps at flowrates ranging from 0.33 to 1.65 mL/hr. When equilibrium was attained, the carrier fluid was introduced via the syringe micropumps and the system was allowed to reach thermal equilibrium.

After thermal equilibration, a 0.52 mL sample of the biomolecule dissolved in the carrier fluid was loaded into the injection loop and introduced into the packed cell via the multiport valve. The changes in temperature of the cell were recorded and evaluated against a calibrated heat value. This calibration value was determined by heat dissipation of a known magnitude inside the cell, with the cell packed with adsorbent and carrier fluid passing through the cell. By comparing the calibration peak with the peak obtained during the adsorption process, the total heat of adsorption was determined. Sample calculations using this calibration factor are shown in Appendices A–1 through A–8.

The amount of biomolecule adsorbed onto the support was calculated through a mass balance. Briefly, the concentrations of the injected sample and the effluent were measured using the UV spectrophotometer at a wavelength specific to the

biomolecule of interest. Utilizing the volume of sample introduced into the cell and the volume of effluent collected, the amount of biomolecule retained on the column was determined. By combining the heat associated with the adsorption process and the amount of biomolecule adsorbed, the specific heat of adsorption was obtained. Sample calculations for the bases and nucleosides of interest are shown in Appendices A–1 through A–4.

The UV wavelengths utilized for the bases and nucleosides were as follows: 254 nm for adenine and 2'-deoxyadenosine and 264 nm for thymine and thymidine. In all cases, the mass balances demonstrated that 100±5% of the injected biomolecule was recovered. This indicates that the molecules do not remain adsorbed to the adsorbent. Rather, they adsorb and then desorb, as in an isocratic elution operation.

After each sample was adsorbed and desorbed from the column, the FMC was re-equilibrated with the appropriate carrier fluid to prepare for the next sample injection.

2.2.3 Materials: Homo-deoxyoligonucleotides on Sepharose CL–6B

Synthetic homo-deoxyoligonucleotides of adenine (poly(A)) and thymine (poly(T)) were purchased from Integrated DNA Technologies (Coralville, Iowa). Base lengths of 6 and 30 were studied for both oligonucleotides. The poly(T) 6mers and 30mers were resuspended to a concentration between 0.70 mg/mL and 1.0 mg/mL in the 10 m*M* Trizma buffer described in Section 2.2.1, and utilized without further purification. The poly(A) 6mers and 30mers were also resuspended in the Trizma buffer to a concentration between 0.70 mg/mL and 1.0 mg/mL. Because the

solubility of poly(A) is lower than that of poly(T), the poly(A) samples were heated for approximately 30 seconds in a water bath at 50° C. Additionally, the poly(A) samples contained traces of insoluble material utilized in their synthesis. As was recommended by IDT Technologies technical support, the poly(A) samples were transferred to 8 mL glass bottles (6 cm tall, 1.7 cm diameter), capped, and centrifuged in a Clay Adams Dynac centrifuge at 2500 rpm for approximately 60 seconds. In order for this bottle size to fit the stainless steel centrifuge buckets (12 cm long, 1.8 cm diameter) a piece of foam approximately 8 cm long was inserted into the bottom of each bucket. The supernatant was recovered with a pipette and used for FMC injections. As with the base and nucleoside experiments, analytical grade ammonium sulfate purchased from Fisher Scientific Company (Hanover Park, IL, USA) was the chosen modulator.

2.2.4 Flow Microcalorimetry with Homo-deoxyoligonucleotides on Sepharose CL–6B

Heat of adsorption data were collected using the FMC apparatus as described in Section 2.2.2, except that the injected solution and effluent concentrations were not monitored with the UV spectrophotometer. For the homo-deoxyoligonucleotides, the mass of injected material was calculated from the concentration of the sample solution and the loop volume of 0.52 mL. Sample calculations are shown in Appendices A–4 through A–8. It was assumed that 100% of the material eluted, as was the case for the nitrogen bases and the nucleosides.

2.2.5 Materials: BSA on PEI–1000–10

Bovine serum albumin (BSA; Sigma Product Number A-3675) was purchased from Sigma (St. Louis, MO, USA) and used without further purification. Concentrations of BSA solution varied between 2.5 mg/mL and 20 mg/mL. PEI–1000–10, purchased from Millipore (Bedford, MA, USA) was used as the IEC support. It is a siliceous-based support containing cross-linked polyethylene-imine (PEI) on its surface. The average particle size of the PEI–1000–10 is 10 μm, and the average pore size is 1000 Å.

The buffer utilized was 10 m*M* piperazine (pH 6.0). The piperazine was purchased from Eastman (Kingsport, TN, USA) and titrated with HCl purchased from Fisher Scientific Company (Hanover Park, IL, USA) to a pH of 6.0. To ascertain the effect of different salts on the adsorption of BSA, KCl, LiCl, and NaCl, all at concentration 0.1 *M*, were utilized as modulators. These salts were purchased from Fisher Scientific Company (Hanover Park, IL, USA).

2.2.6 Flow Microcalorimetry with BSA on PEI–1000–10

In this study, the FMC cell was packed with approximately 0.171 mL of the PEI–1000–10 adsorbent. The cell was then evacuated for approximately 12 hours to a pressure of about 30 in. Hg. This evacuation process removed air from the adsorbent surface. The adsorbent was then wetted with carrier fluid and equilibrated for 6 to 12 hours with the carrier fluid at a flow rate of 1.65 mL/hr.

After thermal equilibration, a 0.32 mL sample of protein dissolved in the carrier fluid was injected as previously described. Calibration was performed in the

same manner described in Section 2.2.2, with the cell packed with PEI–1000–10 and buffer flowing through the cell. The calibration factor for this system is used in sample calculations shown in Appendix A–9. For BSA adsorption onto PEI–1000–10, the protein was retained on the adsorbent. The amount of protein retained was calculated through mass balances, as described in Section 2.2.2, with a UV wavelength of 280 nm. A sample calculation is shown in Appendix A–9.

After each sample injection, 1.0 M LiCl was passed through the cell in order to elute the adsorbed protein. The FMC was then re-equilibrated with the appropriate carrier fluid to prepare for the next sample injection.

3. Investigation of Oligonucleotide Adsorption by Preferential Interaction Analysis

3.1 Background

One approach that has been used to analyze the thermodynamic forces for biomolecular adsorption is the preferential interaction model (Perkins *et al.*, 1997; Diogo *et al.*, 2003). Generally, this model allows for calculations of the number of water molecules and ions released from the surface of the adsorbent and the biomolecule upon adsorption of the biomolecule. These calculations typically provide insight into the types of solution molecules that immediately surround the adsorbent ligands and biomolecules. For hydrophobic interactions, the biomolecules and adsorbent ligands are preferentially hydrated, meaning highly ordered water molecules surround them. A decrease in the overall Gibb's free energy of the system is dominated by the increase in entropy associated with the release of these ordered water molecules. Accordingly, it is expected that, for hydrophobic interactions, a larger number of water molecules than ions will be released (Perkins *et al.*, 1997).

Preferential interaction analysis has been utilized in the study of protein adsorption (Thrash and Pinto, 2002; Perkins *et al.*, 1997; Arakawa 1986), and has recently been applied to oligonucleotide adsorption in hydrophobic interaction chromatography (Diogo *et al.*, 2003).

3.2 Theoretical Development

The preferential interaction coefficient, which characterizes the effect that a protein has on the distribution of solvent and solute molecules, is given by:

$$\Gamma_{32}^{m} \equiv \left(\frac{\partial m_3}{\partial m_2}\right)_{T,\mu_1,\mu_2} \tag{3-A}$$

where m_i is the molal concentration of component i, and the subscripts 1, 2, and 3 correspond to the solvent, biomolecule, and solute, respectively. Applying this preferential interaction coefficient to the local region where preferential accumulation or exclusion of solutes occurs gives the following:

$$\Gamma_{32}^{m} = \nu_3 - \frac{m_3}{m_1} \cdot \nu_1 \tag{3-B}$$

where ν_i is the number of moles of species i immediately surrounding the biomolecule per mole of biomolecule. If the value of the preferential interaction coefficient is equal to zero, the biomolecule has no effect on the distribution of solvent and solute molecules in the vicinity of the biomolecule. In other words, the solution composition in the local region surrounding the biomolecule is the same as the composition in the bulk solution.

Similarly, for electrolytes the preferential interaction coefficient is given by:

$$\Gamma_{+,2}^{m} + \Gamma_{-,2}^{m} = (\nu_+ + \nu_-) - \frac{n \cdot m_3}{m_1}\nu_1 \tag{3-C}$$

where n is the total number of ions associated with the electrolyte and + and – signify the cations and anions, respectively.

For a process involving adsorption of a biomolecule onto an adsorbent, an equation for the observed equilibrium constant can be developed. Consider the process:

$$bB + sS \Leftrightarrow cC \tag{3-D}$$

where B is the biomolecule, S is the adsorbent, and C is the biomolecule-sorbent complex. The natural logarithm of the observed equilibrium constant can then be expressed as:

$$\ln K_{OBS} = c\ln(m_C) - b\ln(m_B) - s\ln(m_S) \tag{3-E}$$

For an electrolyte, it can be shown that:

$$SK_{OBS} = \left(\frac{\partial \ln(K_{OBS})}{\partial \ln(a_{\pm})}\right)_{T,P,EQ} = c(\Gamma^m_{+,C} + \Gamma^m_{-,C}) - b(\Gamma^m_{+,B} + \Gamma^m_{-,B}) - s(\Gamma^m_{+,S} + \Gamma^m_{-,S}) \tag{3-F}$$

where $a_{\pm}$ is the mean ionic activity, defined by:

$$a_{\pm} = (n_+^{n_+} n_-^{n_-})^{\frac{1}{n}} \gamma_{\pm} m_3 \tag{3-G}$$

In equation (3-G), $\gamma_{\pm}$ is the mean ionic activity coefficient, n_+ and n_- are the number of cations and anions per unit salt, and n is the total number of anions and cations per formula unit of salt.

Considering the local region surrounding a biomolecule, equation (3-F) can be restated as:

$$SK_{OBS} \equiv \left(\frac{\partial \ln(K_{OBS})}{\partial \ln(a_{\pm})}\right)_{T,P,EQ} = (\Delta\nu_+ + \Delta\nu_-) - \frac{n \cdot m_3}{m_1}\Delta\nu_i \tag{3-H}$$

where $\Delta\nu_i$ is the stoichiometrically weighted change in the number of moles of the species that is present in the local regions of the products and reactants.

The above results can be applied to chromatographic systems through the capacity factor. The capacity factor, k', is a measure of how strongly a target biomolecule is retained in the column under specific conditions. It can be calculated from retention times, which are easily measured in chromatographic systems.

Generally, the capacity factor is related to the observed equilibrium constant through the following equation:

$$k' \equiv \frac{n_{B,ads}}{n_{B,sol'n}} = \frac{t_{r,i} - t_{m,i}}{t_{m,i}} = \frac{K^{m}_{OBS}}{\varepsilon_b + (1-\varepsilon_b)\cdot\varepsilon_{pi}} \qquad \text{(3-I)}$$

where: $n_{B,ads}$ is the number of moles of biomolecule adsorbed on the column, $n_{B,sol'n}$ is the number of moles of biomolecule in solution, $t_{r,i}$ is the retention time of the biomolecule that is intermittently adsorbed, $t_{m,i}$ is the retention time of a solute of the same size that does not adsorb, ε_b is the interstitial void volume of the column, and ε_{pi} is the accessible porosity of the bed for species i. According to Perkins and coauthors, the equilibrium constant and the properties of the fluid are independent of protein concentration in linear chromatography. Furthermore, if the composition of the mobile phase does not affect the phase ratio of the column, the effect of the salt on the observed equilibrium constant for adsorption is responsible for the changes in retention factor as salt concentration varies (Perkins *et al.*, 1997).

Equation (3-H) can be rewritten in terms of the capacity factor as follows:

$$\left(\frac{\partial \ln(k')}{\partial \ln(m_3)}\right)_{T,P,EQ} = \frac{(\Delta\nu_+ + \Delta\nu_-)}{g} - \frac{n\cdot\Delta\nu_1}{m_1 g} m_3 \qquad \text{(3-J)}$$

where:

$$g = \left(\frac{d\ln(m_3)}{d\ln(a_\pm)}\right)_{T,P} \qquad \text{(3-K)}$$

Values for g are commonly calculated using activity coefficients, or more recently by applying thermodynamic models (Perkins *et al.*, 1997).

Because we have made no assumptions regarding the mechanism of adsorption in the derivation of equation (3-J), it is completely general and can be

applied to ion exchange, hydrophobic interaction, and reversed-phase systems. Further examination of equation (3-J) reveals that, at low salt concentrations, the electrostatic interactions represented in the first term dominate. Conversely, at high salt concentrations the second term, which contains the water release term, dominates.

Assuming that the ion and water stoichiometries are independent of the salt concentration, integration of equation (3-J) yields:

$$\ln(k') = c + \frac{(\Delta\nu_+ + \Delta\nu_-)}{g} \cdot \ln(m_3) - \frac{n \cdot \Delta\nu_1}{m_1 \cdot g} m_3 \qquad \text{(3-L)}$$

With capacity factor values at various salt concentrations, we can use equation (3-L) to determine the number of ions and water molecules released per adsorbed biomolecule.

Preferential interaction analysis was applied to the BSA/PEI–1000–10 system by Thrash and Pinto (Thrash and Pinto, 2002). The reported results will be discussed in conjunction with heats of adsorption obtained through flow microcalorimetry in Chapter 6.

For adsorption of oligonucleotides poly(A) and poly(T) onto Sepharose CL–6B, the release of water molecules and ions was calculated using Equation (3-L) with: $n = 3$, $m_1 = 55.15$, and $g = 1.6$, as reported by Diogo and coauthors (2003) for the system of homo-deoxyoligonucleotides on Sepharose CL–6B. These researchers previously measured the retention factors for this system (Diogo *et al.*, 2003). Equation (3-L) was fitted to the retention factor data (Table 3-1) using Curve Expert curve-fitting software, which employs the Leventhal-Marquardt method. From these calculations, the number of water molecules and ions released per biomolecule adsorbed appear in Table 3-2.

		Retention Factors									
		Ammonium Sulfate Concentration (M)									
Oligonucleotide	**T (°C)**	**1.0**	**1.1**	**1.2**	**1.3**	**1.4**	**1.5**	**1.6**	**1.7**	**1.8**	**2.0**
Poly(T) 6mer	15	1.72		2.08			3.12	3.68		5.68	8.60
	25	1.72		2.08			3.12	3.68		5.68	8.60
	30	1.72		2.08			3.12	3.68		5.68	8.60
	35	1.72		2.08			3.12	3.68		5.68	8.60
Poly(T) 15mer	15	1.72		2.44	3.24	4.52	6.36				
	25	1.84		2.88	3.96	5.64	8.00				
	30	1.90		3.00	4.20	6.20	8.60				
	35	1.98		3.20	4.40	6.36	9.16				
Poly(T) 30mer	15	1.98	2.84	4.56	7.00						
	25	2.40	3.78	5.80	10.68						
	30	2.62	4.12	6.60	12.20						
	35	2.80	4.60	7.40	13.96						
Poly(A) 6mer	15	2.04		2.52		3.28	4.12	5.18	6.52		
	25	2.12		2.68		3.52	4.20	5.40	6.86		
	30	2.12		2.76		3.68	4.36	5.64	7.24		
	35	2.12		2.76		3.68	4.36	5.64	7.24		
Poly(A) 15mer	15	2.04	2.44	3.08	4.20	6.04					
	25	2.40	3.04	4.08	5.72	8.44					
	30	2.68	3.28	4.62	6.60	10.12					
	35	2.92	3.76	5.24	7.64	11.60					
Poly(A) 30mer	15	1.24	1.52	2.00	2.70						
	25	1.66	2.16	3.00	4.54						
	30	1.90	2.56	3.80	5.80						
	35	2.12	3.08	4.68	7.80						

Table 3-1. Retention factors for homo-deoxyoligonucleotides of different base lengths on Sepharose CL–6B at 15, 25, 30, and 35° C. The carrier fluid (pH 8.0) contained ammonium sulfate concentrations between 1.0 M and 2.0 M (Diogo *et al.*, 2002).

Oligonucleotide	T (°C)	$(-n*\Delta v_1)/(m_1*g)$	$(-\Delta v_1)$	$(\Delta v_+ + \Delta v_-)/g$	$(-(\Delta v_+ + \Delta v_-))$
PolyA, 6	15	3.95	116	-3.72	6
PolyA, 6	25	3.74	110	-3.43	6
PolyA, 6	30	3.59	105	-3.13	5
PolyA, 6	35	3.59	105	-3.13	5
PolyA, 15	15	7.86	231	-7.14	11
PolyA, 15	25	6.87	202	-5.39	9
PolyA, 15	30	8.66	254	-7.46	12
PolyA, 15	35	7.51	220	-5.86	9
PolyA, 30	15	6.23	183	-4.92	8
PolyA, 30	25	9.22	271	-7.82	13
PolyA, 30	30	8.37	246	-6.35	10
PolyA, 30	35	9.25	271	-6.82	11
PolyT, 6	15	2.90	85	-2.56	4
PolyT, 6	25	2.90	85	-2.56	4
PolyT, 6	30	2.90	85	-2.56	4
PolyT, 6	35	2.90	85	-2.56	4
PolyT, 15	15	6.99	205	-6.37	10
PolyT, 15	25	6.10	179	-4.82	8
PolyT, 15	30	6.18	181	-4.79	8
PolyT, 15	35	6.16	181	-4.75	8
PolyT, 30	15	6.19	182	-3.11	5
PolyT, 30	25	10.38	304	-7.60	12
PolyT, 30	30	10.83	318	-7.97	13
PolyT, 30	35	9.94	292	-6.65	11

Table 3-2. Calculated number of water molecules and ions released for adsorption of homo-deoxyoligonucleotides onto Sepharose CL–6B at pH 8.0 and various temperatures. These data were calculated using the Preferential Interaction Model with retention data shown in Table 3-1.

3.3 Discussion

The values obtained from preferential interaction analysis clearly demonstrate that significantly more water molecules are released than ions for the homo-deoxyoligonucleotide/Sepharose CL–6B system. This is consistent with water release trends for hydrophobic interactions between proteins and hydrophobic adsorbents (Esquibel-King *et al.*, 1999; Perkins *et al.*, 1997). Because the biomolecules and the adsorbent are both hydrophobic, the solution immediately surrounding them largely excludes salt molecules. In other words, the biomolecule and surface are preferentially hydrated, and the water molecules surrounding them are ordered. When the biomolecule and surface come into contact, they form a weak hydrophobic bond and the ordered water molecules are released. This shift from ordered water molecules surrounding the biomolecule and surface to disordered water molecules released into the bulk solution corresponds to an increase in the overall entropy of the system.

In Figures 3-1 and 3-2, the number of water molecules released is plotted against the number of bases in the oligonucleotide. Figures 3-3 and 3-4 show the number of ions released with respect to the number of bases. Notice that the trends for water release and ion release are consistent for both poly(A) and poly(T) at all temperatures. This trend is consistent with the chain-like structure of oligonucleotides. Each monomer contains a phosphate group, around which ions are concentrated, and a nitrogen base, which is preferentially hydrated. Consequently, when the base hydrophobically interacts with the surface, a large number of water molecules are released from the hydrophobic base, accompanied by a small number

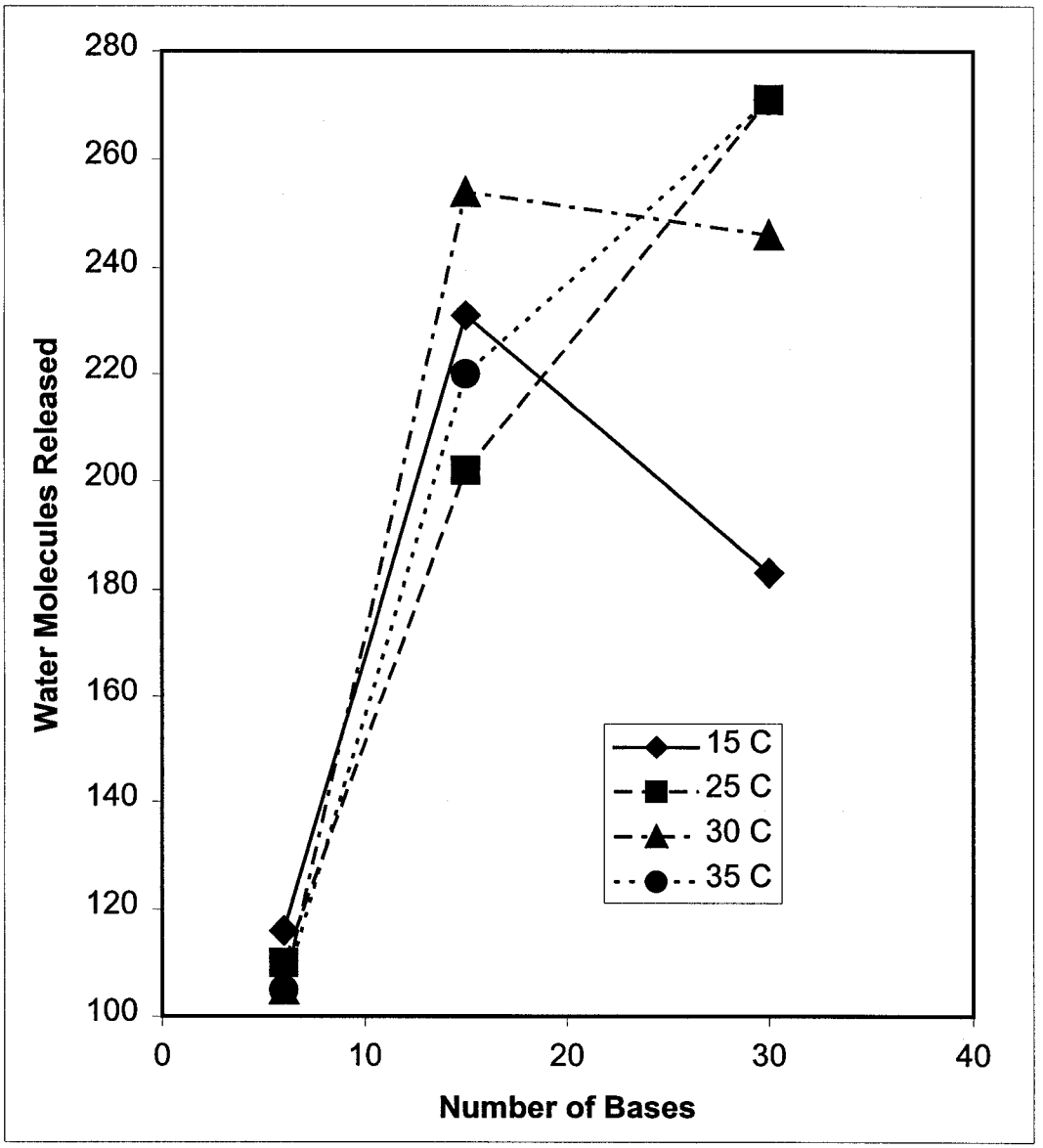

Figure 3-1. Number of water molecules released with respect to the number of bases in the oligonucleotide for poly(A) at 15, 25, 30, and 35° C. (Carrier fluid: ammonium sulfate, 1.0 M to 2.0 M; pH: 8.0)

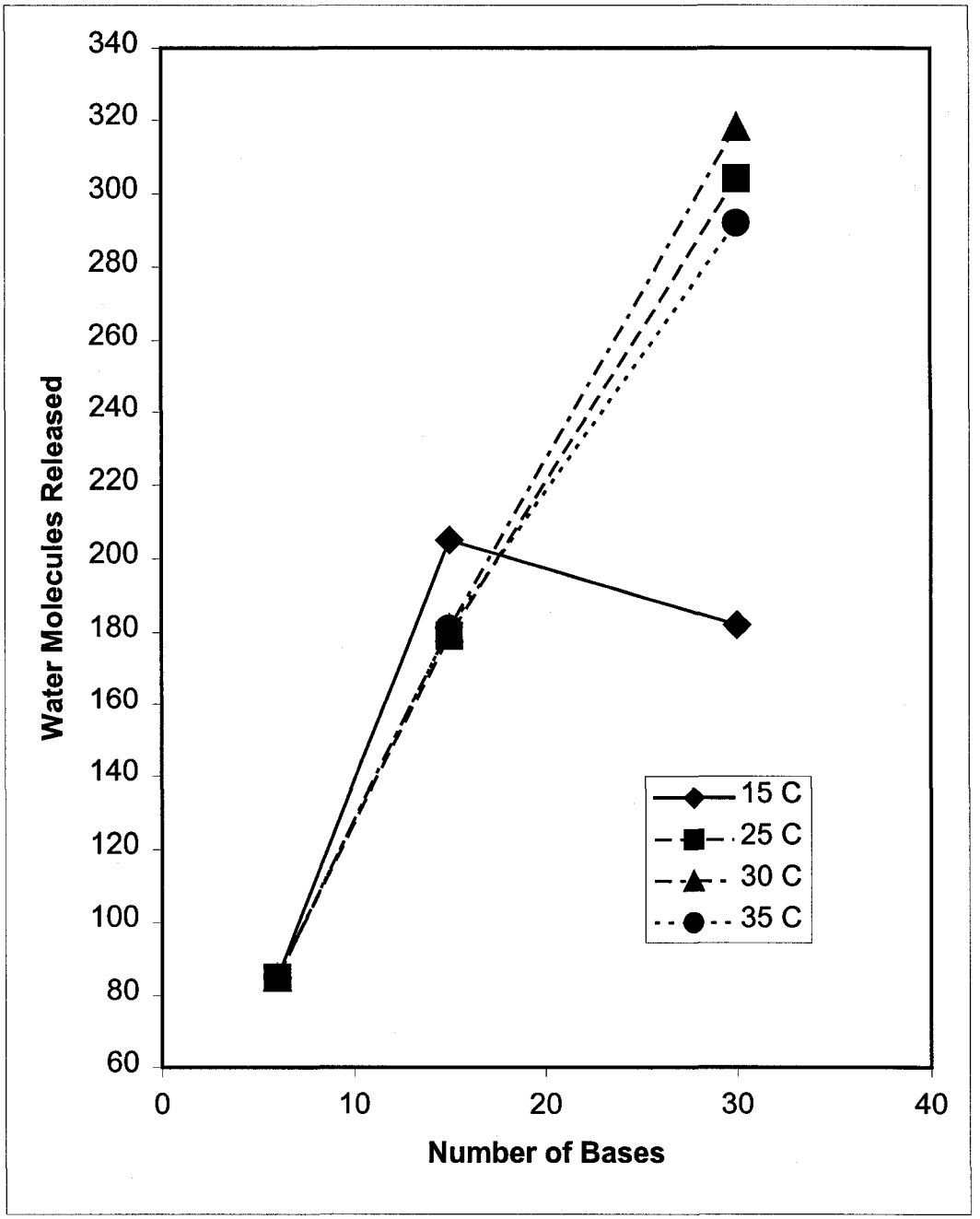

Figure 3-2. Number of water molecules released with respect to the number of bases in the oligonucleotide for poly(T) at 15, 25, 30, and 35° C. (Carrier fluid: ammonium sulfate, 1.0 M to 2.0 M; pH: 8.0)

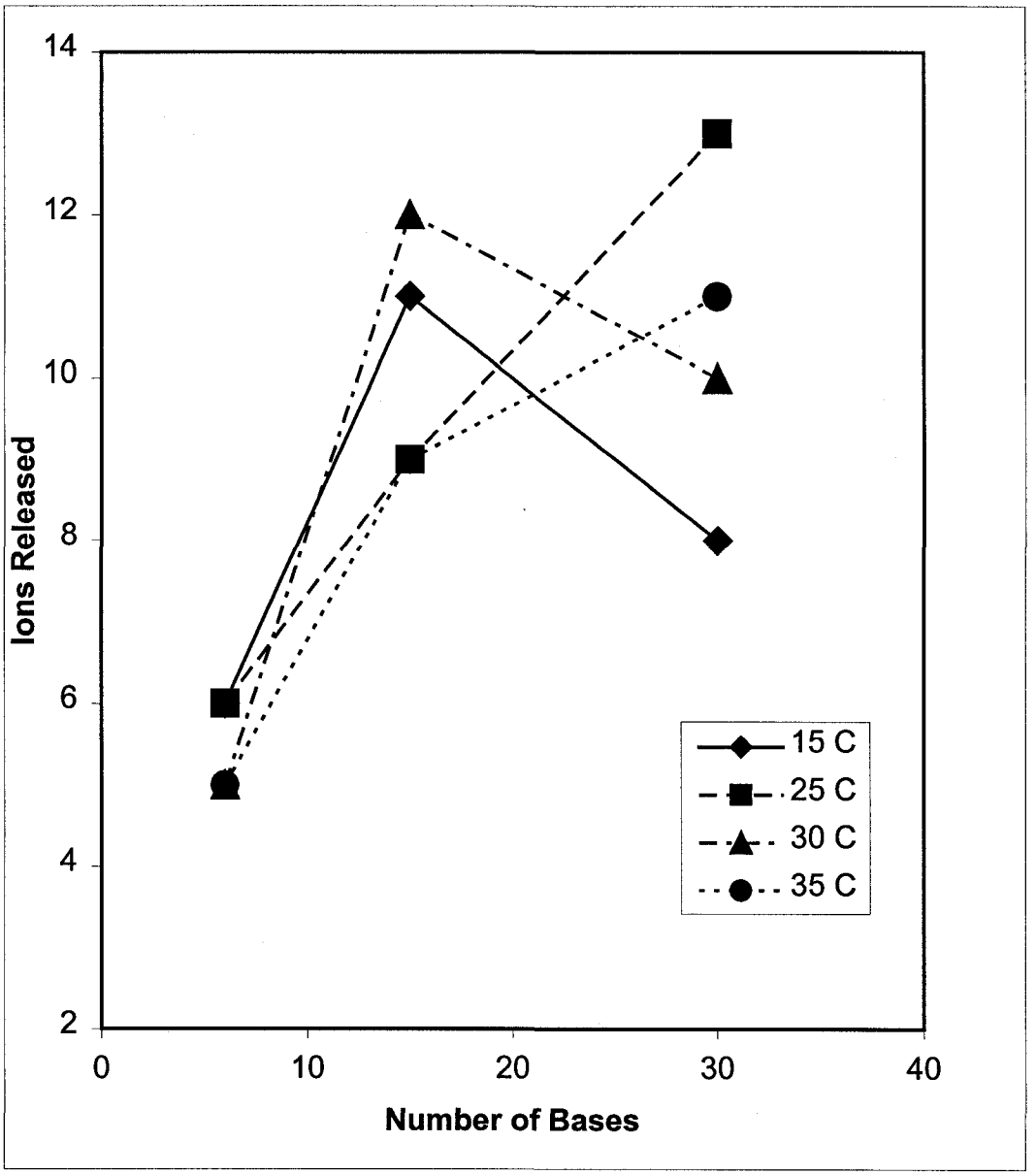

Figure 3-3. Number of ions released with respect to the number of bases in the oligonucleotide for poly(A) at 15, 25, 30, and 35° C. (Carrier fluid: ammonium sulfate, 1.0 M to 2.0 M; pH: 8.0)

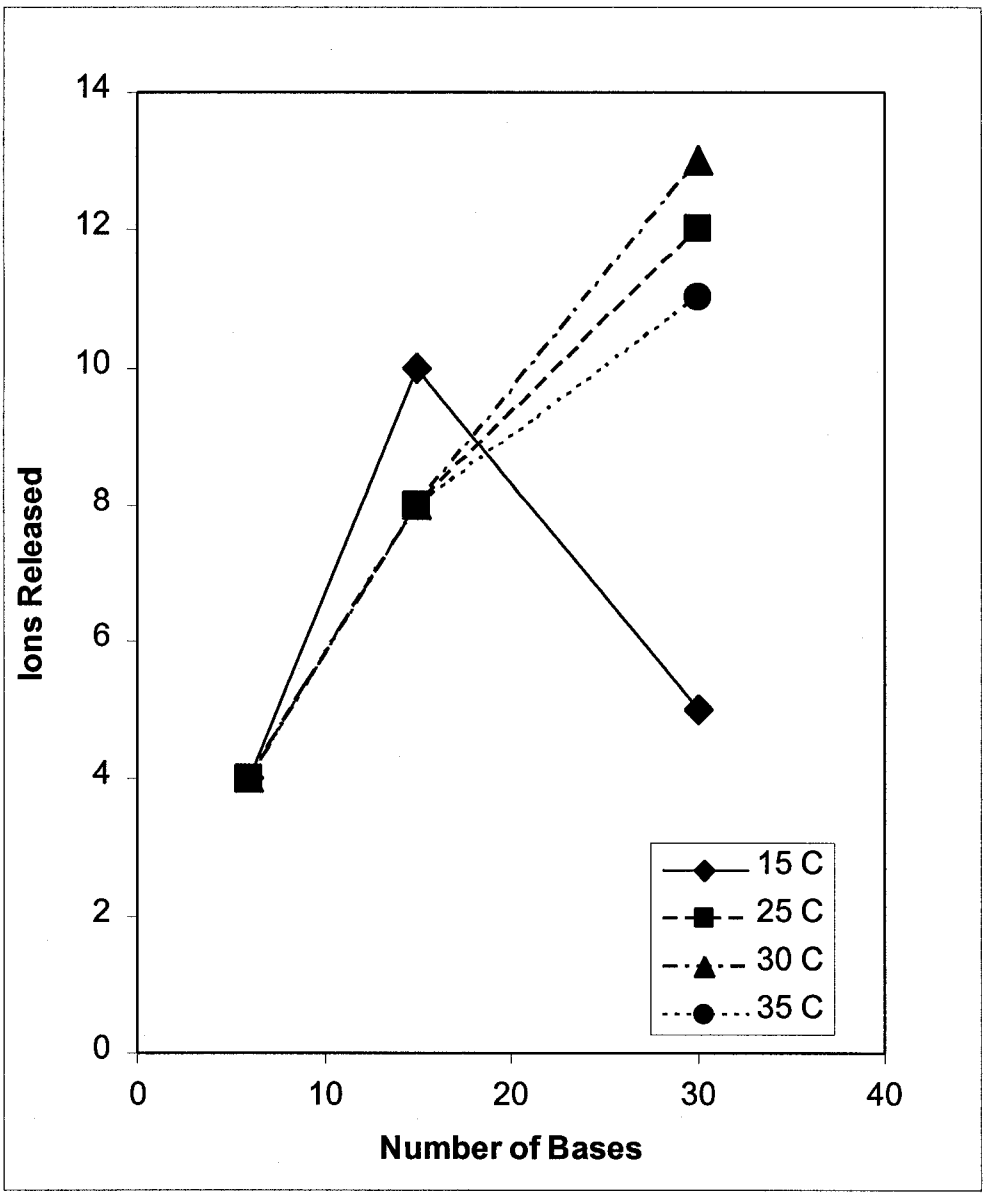

Figure 3-4. Number of ions released with respect to the number of bases in the oligonucleotide for poly(T) at 15, 25, 30, and 35° C. (Carrier fluid: ammonium sulfate, 1.0 M to 2.0 M; pH: 8.0)

of ions from the nearby phosphate group. Therefore, it is expected that the number of ions and water molecules released would be proportional.

For poly(T), the water molecules released increases with the number of bases for the three highest temperatures. However, at 15° C the water release decreases from 205 for the 15mer to 182 for the 30mer. This trend can be explained in terms of secondary structure. At 15° C, the poly(T) 30mer probably has a more tightly coiled secondary structure, which decreases the distance between any single hydrophobic moiety and the phosphate groups adjacent to it (Neidle, ed., 1999). The close proximity of the hydrophilic phosphate groups limits the amount of water released. However, when the temperature is raised just 10° C, the conformation of the oligonucleotide changes significantly. Kontturi and coworkers have shown through diffusion coefficient measurements that oligonucleotide conformation is relatively compact at 20° C and opens up appreciably as the temperature is increased to 40° C (Kontturi *et al.*, 2002). The fact that the number of water molecules released for poly(T) at the three highest temperatures is nearly linear indicates that the change in secondary structure for the poly(T) 30mer becomes less significant as the temperature increases.

The trends for poly(A) demonstrate that a tightly coiled secondary structure also exists for the 30mer at 15° C, since the number of water molecules released decreases from 231 for the 15mer to 183 for the 30mer. Additionally, a slight decrease in water release between the 15mer and 30mer is also observed at 30° C, even though the water release increases from 202 to 271 at 25° C. At 25° C and

35° C, the water release increases with increasing number of bases, but the trend is clearly not linear. These data suggest that the secondary structure of poly(A) may open up slightly between 15° C and 25° C, close appreciably between 25° C and 30° C, then open up again between 30° C and 35° C. Clearly, the secondary structure of poly(A) at longer base lengths is strongly related to temperature (Felsenfeld and Miles, 1967).

It is also useful to compare the water release for poly(T) with that for poly(A). As discussed in Chapter 1, adenine is more hydrophobic than thymine, so it is expected that poly(A) would interact more strongly with the adsorbent than poly(T), thus releasing more water molecules. The data in Table 3-2 show that this was observed at all temperatures for 6mers and 15mers. However, at base lengths of 30, poly(T) released more water molecules than poly(A) at 25°, 30°, and 35° C. This further supports the hypothesis that, while poly(T) may have a secondary structure at 15° C that is lost when the temperature is raised to 25° C, poly(A) maintains its secondary structure up to 35° C, the highest temperature studied.

3.4 Summary

Preferential interaction analysis for the system of homo-deoxyoligonucleotides poly(A) and poly(T) adsorbing onto Sepharose CL–6B has provided further support that adsorption is due to hydrophobic interaction. More importantly, the change in the number of water molecules released with respect to base length demonstrates that, although these biomolecules are chain-like polymers, the strength of the adsorption interaction does not in general scale linearly with the

number of bases. In some cases, however, dependence was observed, particularly for poly(T), at higher temperatures. These observations coupled together provide strong support for the theory that a secondary structure exists and can influence the chromatographic behavior of homo-deoxyoligonucleotides at long base lengths.

As previously mentioned, the preferential interaction model described in Equation (3-J) is completely general and applies to both ion exchange and hydrophobic interaction systems. By combining water release results obtained through preferential interaction analysis with heat of adsorption data obtained through flow microcalorimetry, the thermodynamic driving forces for adsorption can be described more completely.

4. Heat of Adsorption Effects for Nitrogen Bases and Nucleosides on an HIC Adsorbent

4.1 Results

Heats of adsorption for the nitrogen bases adenine and thymine and the nucleosides 2'-deoxyadenosine and thymidine were obtained at ammonium sulfate concentrations varying between 1.0 M and 2.0 M. The adenine and thymine solution concentrations studied were 0.25 mg/mL; the 2'-deoxyadenosine and thymidine solution concentrations were 2.0 mg/mL. The limited solubility of these compounds required the study of low solution concentrations, which correspond to linear isotherm conditions within the column. In all cases, the amount of solute injected and the amount of solute recovered were determined. Mass balances confirmed that 100±5% of the solute injected was recovered for all solutes.

Error analysis was completed for each data point. A sample of the error analysis calculations is provided in Appendix A–10. The calculated error for heats of adsorption and desorption for the nitrogen bases and nucleosides studied was 5% or less of the calculated heat value in all cases. Accordingly, the data reported in Chapter 4 include error bars of 5%.

4.1.1 Thymine and Thymidine

For both thymine and thymidine, bimodal peaks were obtained for all ammonium sulfate concentrations. Each bimodal peak consisted of two parts: an endothermic peak followed by an exothermic peak. Example peaks are shown in Figures 4-1 and 4-2. Because both peaks are Gaussian in shape, it appears that the two peaks do not overlap. Additionally, the areas under the endothermic peak and the

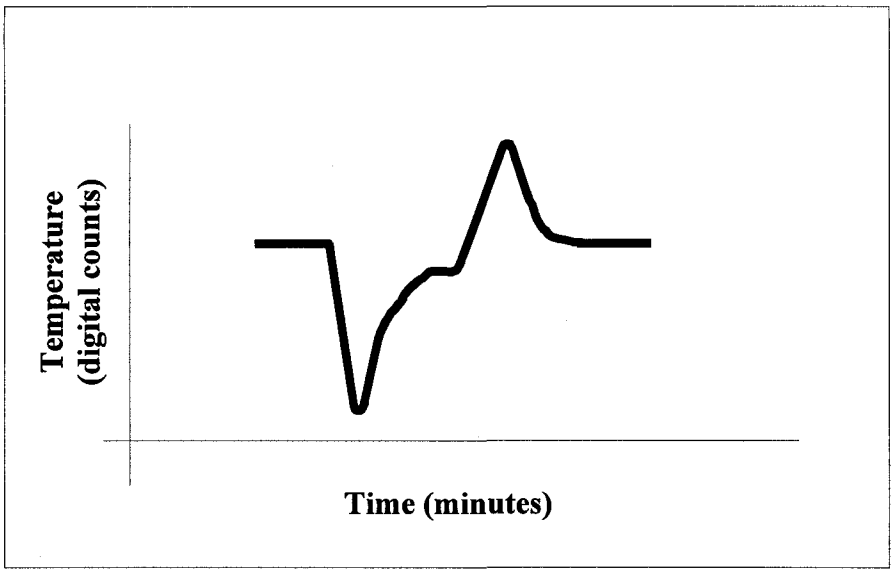

Figure 4-1. Example peak obtained for thymine adsorbing to and desorbing from Sepharose CL–6B. This peak was obtained at the following conditions: flow rate, 1.65 mL/hr; sample, 0.25 mg/mL thymine in 2.0 M ammonium sulfate; pH, 8.0; temperature, 26.9° C.

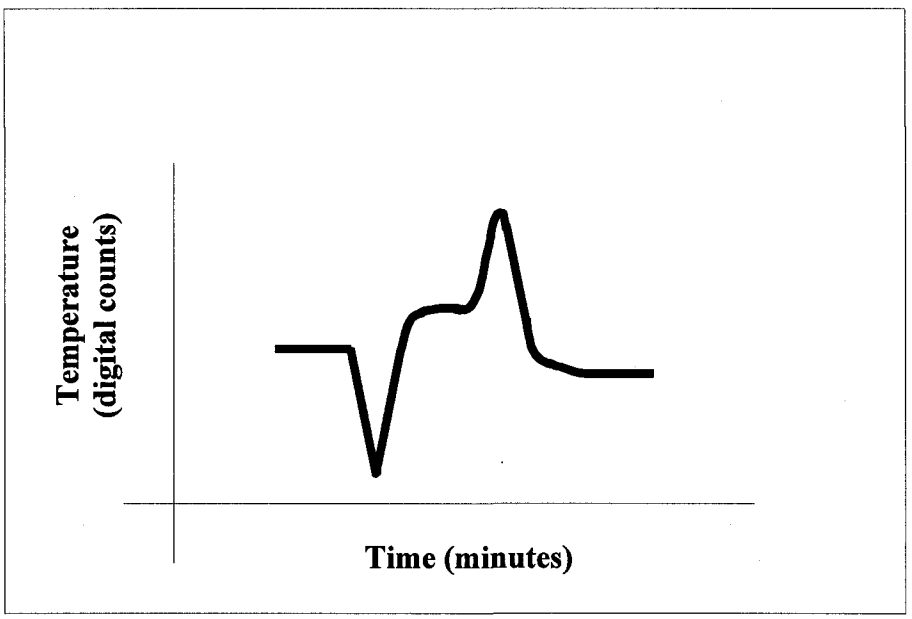

Figure 4-2. Example peak obtained for thymidine adsorbing to and desorbing from Sepharose CL–6B. This peak was obtained at the following conditions: flow rate, 1.65 mL/hr; sample, 2.0 mg/mL thymidine in 1.5 M ammonium sulfate; pH, 8.0; temperature, 26.2° C.

exothermic peak have approximately the same magnitude in all cases. For these reasons, and because 100±5% of the injected target biomolecule was recovered in all cases, it can be concluded that the endothermic peak corresponds to the adsorption peak, while the exothermic peak corresponds to the desorption peak.

The peaks were analyzed by determining the area of the peak and comparing it to a calibration peak of known magnitude, as discussed in Section 2.2.2. The observed heat of adsorption and heat of desorption values for thymine are shown in Figures 4-3 and 4-4, respectively. Similarly, the observed heat of adsorption and heat of desorption values for thymidine are shown in Figures 4-5 and 4-6. Thymine sample calculations are shown in Appendix A–1; thymidine sample calculations are shown in Appendix A–2.

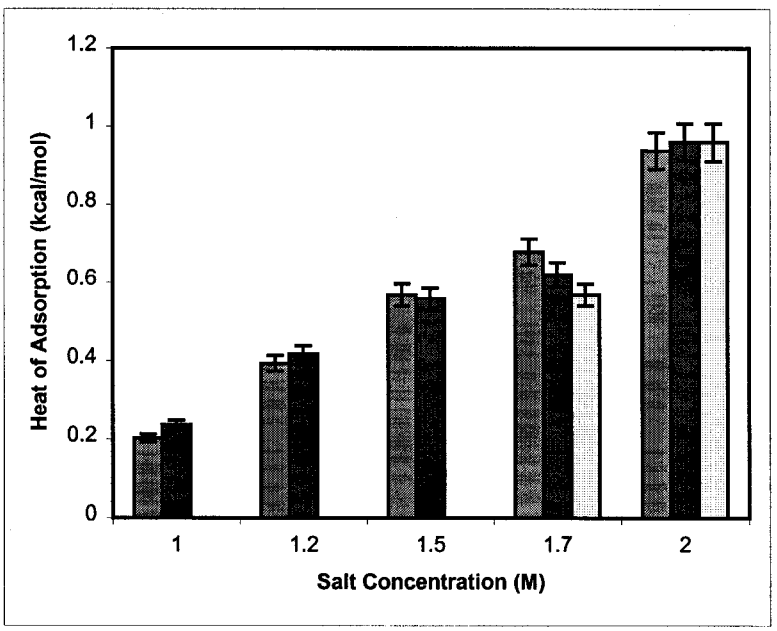

Figure 4-3. Observed heats of adsorption for thymine on Sepharose CL–6B at varying ammonium sulfate concentrations. Data were collected at 26±1.0°C, a flow rate of 1.65 mL/hr, a solution pH of 8.0, and a thymine concentration of 0.25 mg/mL.

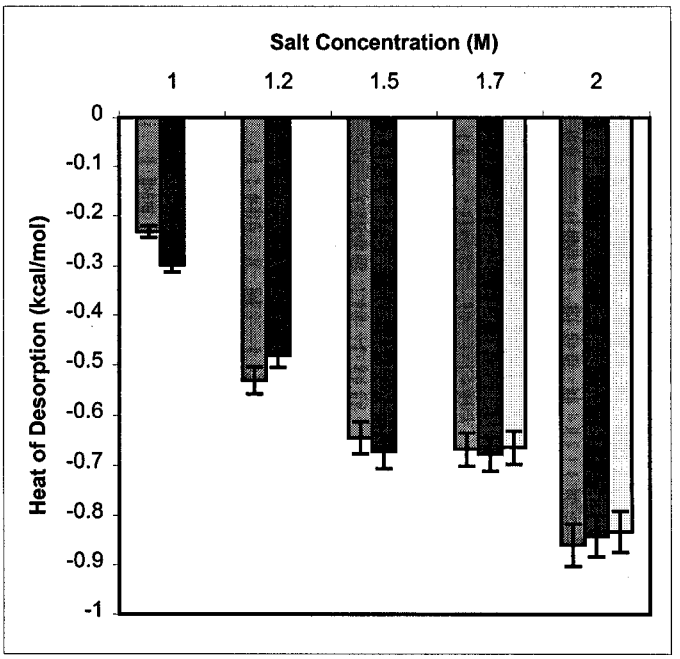

Figure 4-4. Observed heats of desorption for thymine from Sepharose CL–6B at varying ammonium sulfate concentrations. Data were collected at 26±1.0°C, a flow rate of 1.65 mL/hr, a solution pH of 8.0, and a thymine concentration of 0.25 mg/mL.

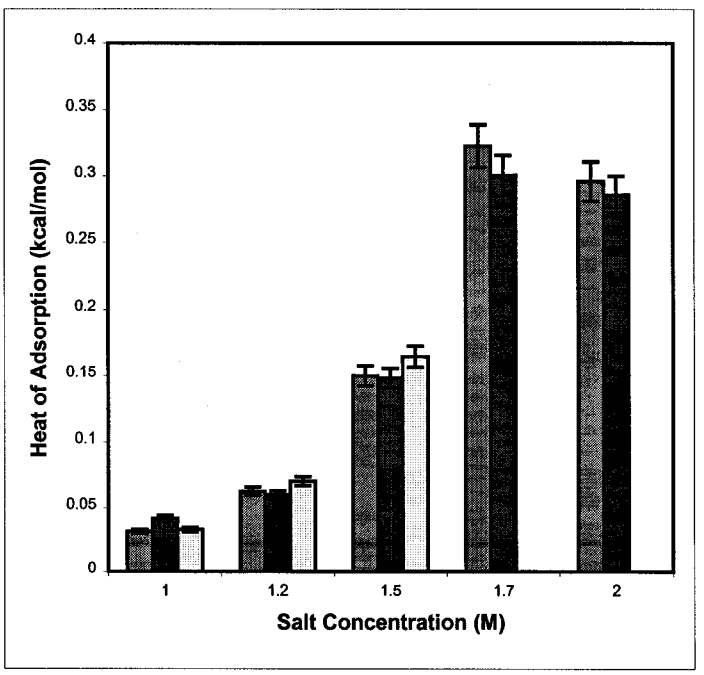

Figure 4-5. Observed heats of adsorption for thymidine on Sepharose CL–6B at varying ammonium sulfate concentrations. Data were collected at 26±1.0°C, a flow rate of 1.65 mL/hr, a solution pH of 8.0, and a thymidine concentration of 2.0 mg/mL.

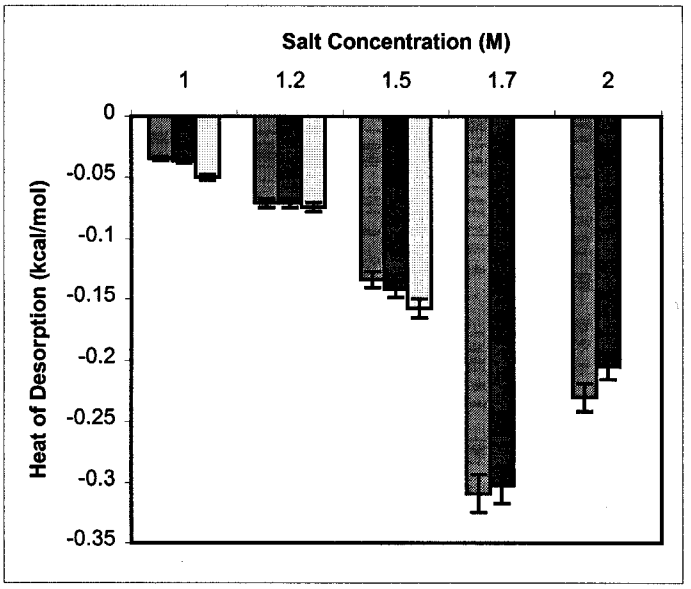

Figure 4-6. Observed heats of desorption for thymidine from Sepharose CL–6B at varying ammonium sulfate concentrations. Data were collected at 26±1.0°C, a flow rate of 1.65 mL/hr, a solution pH of 8.0, and a thymidine concentration of 2.0 mg/mL.

For thymine the observed heats of adsorption increase nearly linearly with increasing ammonium sulfate concentration. This behavior is consistent with that expected for hydrophobic interactions (Queiroz *et al.*, 2001). Similarly, the observed heats of adsorption for thymidine also generally increase as the ammonium sulfate concentration increases. Although the heat of adsorption for thymidine at 1.7 M ammonium sulfate is greater than that at 2.0 M, the value is within experimental error, suggesting that the heats of adsorption for 1.7 M and 2.0 M are likely equivalent.

4.1.2 Adenine and 2'-deoxyadenosine

As with the thymine and thymidine peaks, the adenine peaks were bimodal with an endothermic peak followed by an exothermic peak. An example peak is shown in Figure 4-7. The peaks are Gaussian in shape, indicating that they do not

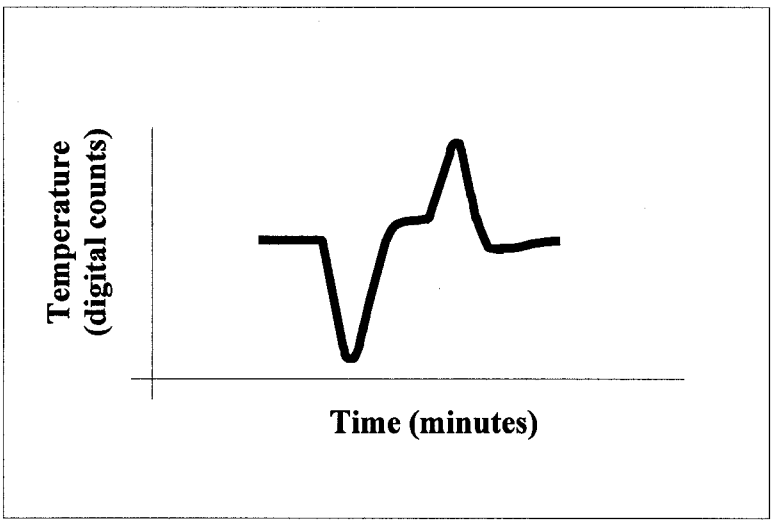

Figure 4-7. Example peak obtained for adenine adsorbing to and desorbing from Sepharose CL–6B. This peak was obtained at the following conditions: flow rate, 1.65 mL/hr; sample, 0.25 mg/mL adenine in 1.7 M ammonium sulfate; pH, 8.0; temperature, 26.7° C.

overlap, and magnitudes of the endothermic and exothermic peaks are approximately equal. Thus, as with the thymine and thymidine peaks, it was concluded that the endothermic peak corresponds to the adsorption peak and the exothermic peak corresponds to the desorption peak.

The observed heats of adsorption and heats of desorption for adenine are shown in Figures 4-8 and 4-9, respectively. Sample calculations showing how these values were obtained are given in Appendix A–3. The heats of adsorption decrease slightly with increasing ammonium sulfate concentration. This behavior is opposite of that expected for hydrophobic interactions.

Data obtained for 2'-deoxyadenosine was quite different from that of the other three solutes. The 2'-deoxyadenosine peaks were bimodal with the exothermic peak followed by the endothermic peak. Furthermore, the shape of the exothermic peak

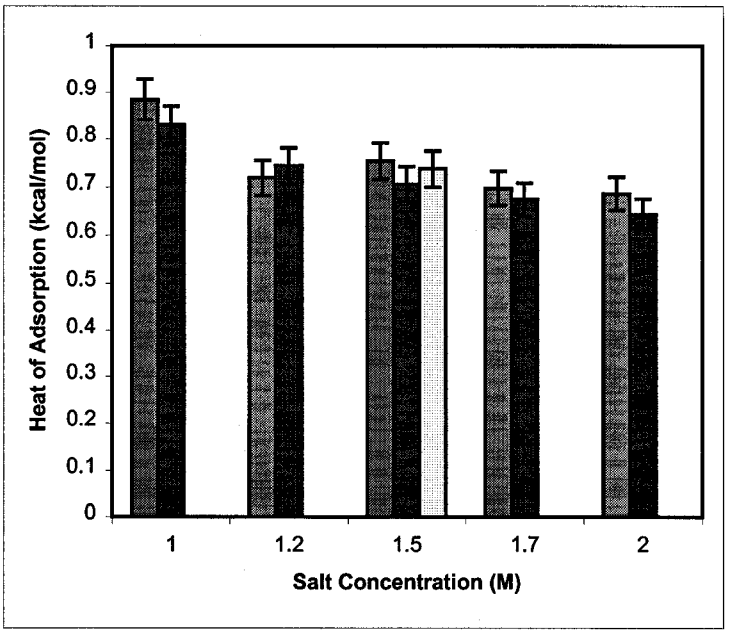

Figure 4-8. Observed heats of adsorption for adenine on Sepharose CL–6B at varying ammonium sulfate concentrations. Data were collected at 26±1.0°C, a flow rate of 1.65 mL/hr, a solution pH of 8.0, and an adenine concentration of 0.25 mg/mL.

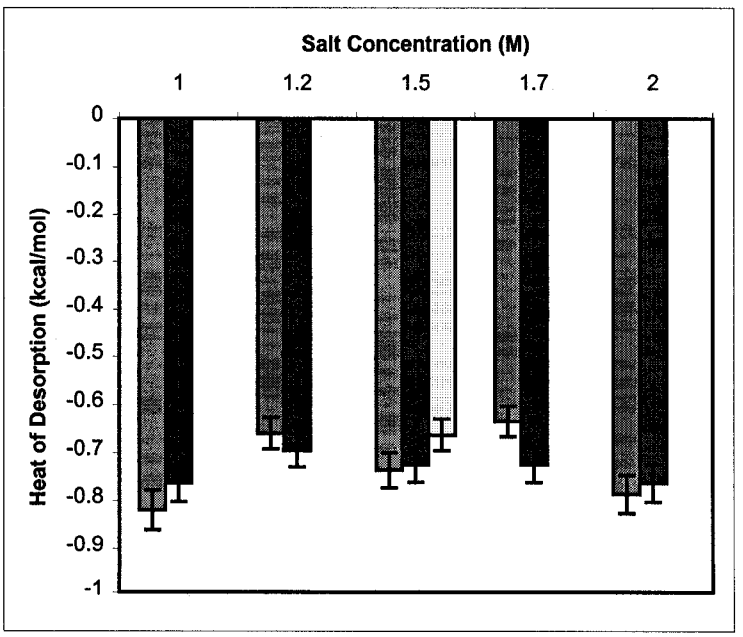

Figure 4-9. Observed heats of desorption for adenine from Sepharose CL–6B at varying ammonium sulfate concentrations. Data were collected at 26±1.0°C, a flow rate of 1.65 mL/hr, a solution pH of 8.0, and an adenine concentration of 0.25 mg/mL.

was slightly skewed, as shown in Figure 4-10, indicating an overlap of separate

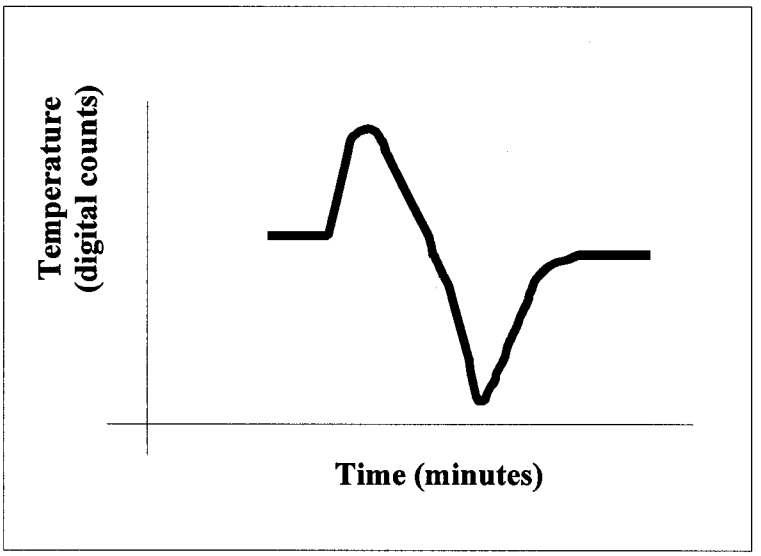

Figure 4-10. Example peak obtained for 2'-deoxyadenosine adsorbing to and desorbing from Sepharose CL–6B. This peak was obtained at the following conditions: flow rate, 1.65 mL/hr; sample, 2.0 mg/mL 2'-deoxyadenosine in 1.7 M ammonium sulfate; pH, 8.0; temperature, 26.2° C.

effects progressing at different rates. Mass balances indicated that, as with the other three solutes, all the solute injected was recovered within approximately 5%.

The observed heats of adsorption and heats of desorption for 2'-deoxyadenosine are shown in Figures 4-11 and 4-12, respectively. Unlike the three previous solutes discussed, for 2'-deoxyadenosine the heats of adsorption are exothermic and the heats of desorption are endothermic. The magnitude of these heat values increases with increasing ammonium sulfate concentration.

4.2 Discussion

The driving force for adsorption due to weak hydrophobic interactions is considered to be the increase in entropy that results with the release of water

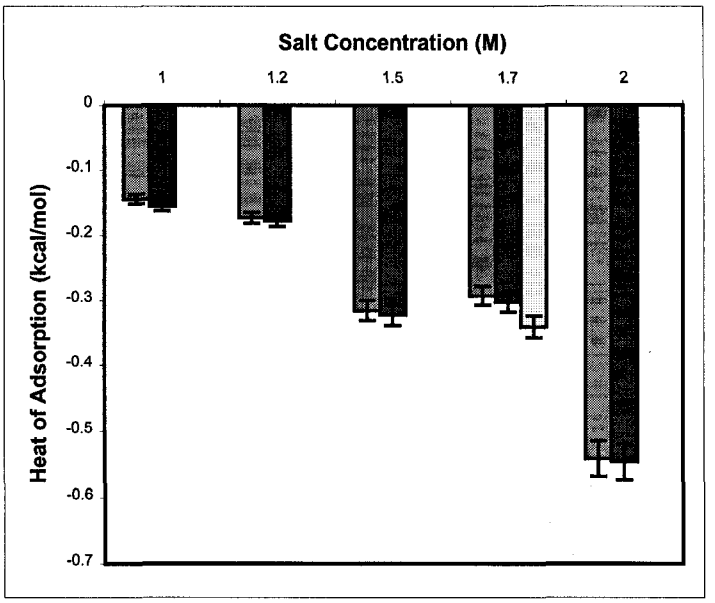

Figure 4-11. Observed heats of adsorption for 2'-deoxyadenosine on Sepharose CL–6B at varying ammonium sulfate concentrations. Data were collected at 26±1.0°C, a flow rate of 1.65 mL/hr, a solution pH of 8.0, and a 2'-deoxyadenosine concentration of 2.0 mg/mL.

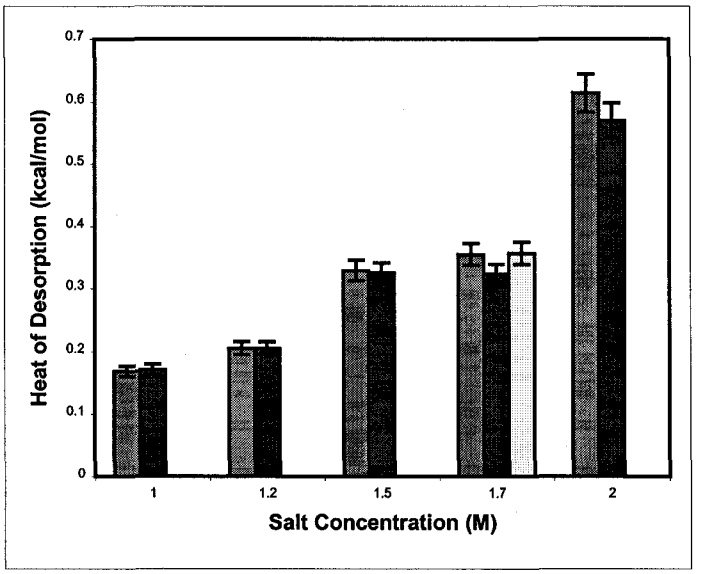

Figure 4-12. Observed heats of desorption for 2'-deoxyadenosine from Sepharose CL–6B at varying ammonium sulfate concentrations. Data were collected at 26±1.0 °C, a flow rate of 1.65 mL/hr, a solution pH of 8.0, and a 2'-deoxyadenosine concentration of 2.0 mg/mL.

molecules from both the biomolecule and the surface of the adsorbent (Lin *et al.*, 2002; Gooding and Regnier, ed., 1990). Therefore, an energetically unfavorable enthalpic effect, manifested through an endothermic heat of adsorption, can be overcome by the large positive entropy change due to water release, thus rendering the process energetically favorable. As stated above, endothermic heats of adsorption were, in fact, observed for three of the four solutes studied here: thymine, thymidine, and adenine.

Figures 4-3 and 4-5 show that the observed endothermic heat of adsorption increases with increasing ammonium sulfate concentration for both thymine and thymidine. These data are consistent with results reported in the literature for biomolecules adsorbing onto weak hydrophobic adsorbents in the presence of ammonium sulfate (Esquibel-King, *et al.*, 1999; Perkins, *et al.*, 1997). As the ammonium sulfate concentration increases, hydrophobic interactions between biomolecules and weak hydrophobic adsorbents increase because the surface tension of the carrier fluid increases. This increase in surface tension creates a more hydrophobic solution environment, thus promoting hydrophobic interactions between the solute and the surface (Tsai *et al.*, 2002).

According to Lin and coworkers, adsorption of a biomolecule to a hydrophobic adsorbent can be divided into five subprocesses: a) exclusion of water molecules or ions from the biomolecule surface (dehydration or deionization of the biomolecule); b) exclusion of water molecules or ions from the adsorbent surface (dehydration or deionization of the surface); c) hydrophobic interactions between the biomolecule and the hydrophobic adsorbent; d) structural rearrangement of the

biomolecule upon adsorption; and e) structural rearrangement of the excluded water molecules or ions into the bulk solvent (Lin *et al.*, 2001). For thymine and thymidine adsorption onto Sepharose CL–6B, the observed endothermic heats of adsorption probably derive from a combination of biomolecule dehydration (subprocess a), surface dehydration (subprocess b), and hydrophobic interaction (subprocess c). Norde (1998) demonstrated that the free energy associated with dehydration that accompanies protein adsorption onto solid surfaces ranges between 5 and 12 mJ/m^2. Clearly, a relatively large endothermic contribution due to dehydration, coupled with a small exothermic contribution due to hydrophobic interaction, results in a small net endothermic heat of adsorption. Furthermore, because these molecules have a relatively inflexible structure and are very small in comparison with other biomolecules commonly purified through chromatography, i.e. proteins, endothermic effects due to structural rearrangement of nitrogen bases and nucleosides upon adsorption (subprocess d) are negligible. Additionally, neither the solutes nor the adsorbent utilized in this study carry an electrostatic charge, so no endothermic effects due to deionization would be observed for this system.

In the case of adenine, the observed heat of adsorption decreases with increasing ammonium sulfate concentration. This behavior is opposite that reported in the literature for solutes undergoing hydrophobic interactions in the presence of ammonium sulfate (Esquibel-King, *et al.*, 1999; Perkins, *et al.*, 1997). Additionally, the observed heats of adsorption for 2'-deoxyadenosine are exothermic, and also decrease slightly with increasing ammonium sulfate concentration. The thermodynamic data collected for adenine and 2'-deoxyadenosine can be explained

when the effect of base stacking is taken into account. It is probable that each of these measured heats of adsorption is actually the composite of the heat of adsorption and the heat associated with molecular base stacking for several reasons.

In the 1960's several research groups studied the interactions between purines, pyrimidines, and nucleosides. Ts'o and coworkers reported in a series of papers that nitrogen bases and nucleosides not only interact heterogeneously in aqueous solutions, but also self-associate. After further study, the researchers concluded that the interactions between these molecules are not due to lateral hydrogen bonding but base stacking (Ts'o *et al.*, 1963, 1964, 1969; Chan *et al.*, 1964; Schweizer *et al.*, 1965; Broom *et al.*, 1967). Furthermore, it was determined that these interactions proceed beyond the dimer stage, creating stacks containing numerous bases (Ts'o *et al.*, 1963). In fact, the base stacking of these molecules is nearly identical to that observed in oligonucleotides and DNA. According to Solie and Schellman (1968), "the asymmetric stacking is the stablest form of interaction and is not forced upon the system by the presence of the sugar-phosphate chain," which connects the monomers in DNA and RNA.

Through thermal osmometry studies, researchers determined the association constants for thymidine and 2'-deoxyadenosine to be in the range of 0.91 $molal^{-1}$ and 4.7–7.5 $molal^{-1}$, respectively (Broom *et al.*, 1967). The changes in free energies associated with base stacking were then calculated and determined to be approximately 0.060 kcal/mol for thymidine and between –0.92 to –1.195 kcal/mol for 2'-deoxyadenosine (Broom *et al.*, 1967). Through microcalorimetry, Gill and coworkers determined that both enthalpic and entropic effects in self-association were

negative, and both contributed significantly to the free energy change (Gill *et al.*, 1967). Ts'o (1974) utilized the calorimetric data reported by Gill and coworkers and Farquhar and coworkers (1968) to determine the change in enthalpy due to self-association for thymidine and deoxyadenosine. He reported values of –2.4±0.3 kcal/mol and –6.5±1.0 kcal/mol, respectively. Unfortunately, self-association enthalpic changes for thymine and adenine have not been studied, though the trend of decreasing ΔH_{ads} with increasing ionic strength for adenine suggests that these enthalpic contributions may not be negligible for all bases. In the case of adenine it is postulated, based on results in the literature that will be discussed later, that base stacking effects, which lead to exothermic heats, increase with an increase in salt concentration. However, the adsorbate/adsorbent interaction dominates the overall process to give the net endothermic heats of adsorption reported in Figure 4-8.

The mechanism for base stacking was initially considered to be primarily hydrophobic interactions because the phenomenon was observed only in aqueous solutions (Bugg, 1972). However, it was concluded that bases and nucleosides self-interact due to a combination of hydrophobic interactions, van der Waals forces, and π-electron interactions (Ts'o *et al.*, 1964). Clearly a combination of these forces would, in fact, result in significant enthalpic and entropic contributions to the overall free energy change.

Base stacking was observed by the researchers cited above at relatively high concentrations in aqueous solution. Although lower concentrations were utilized in this study, it is still probable that the peaks observed were due to a combination of base stacking and adsorption heats. The postulated process is demonstrated in

Figure 4-13. As the first solute enters the column, it adsorbs to the adsorbent, as shown

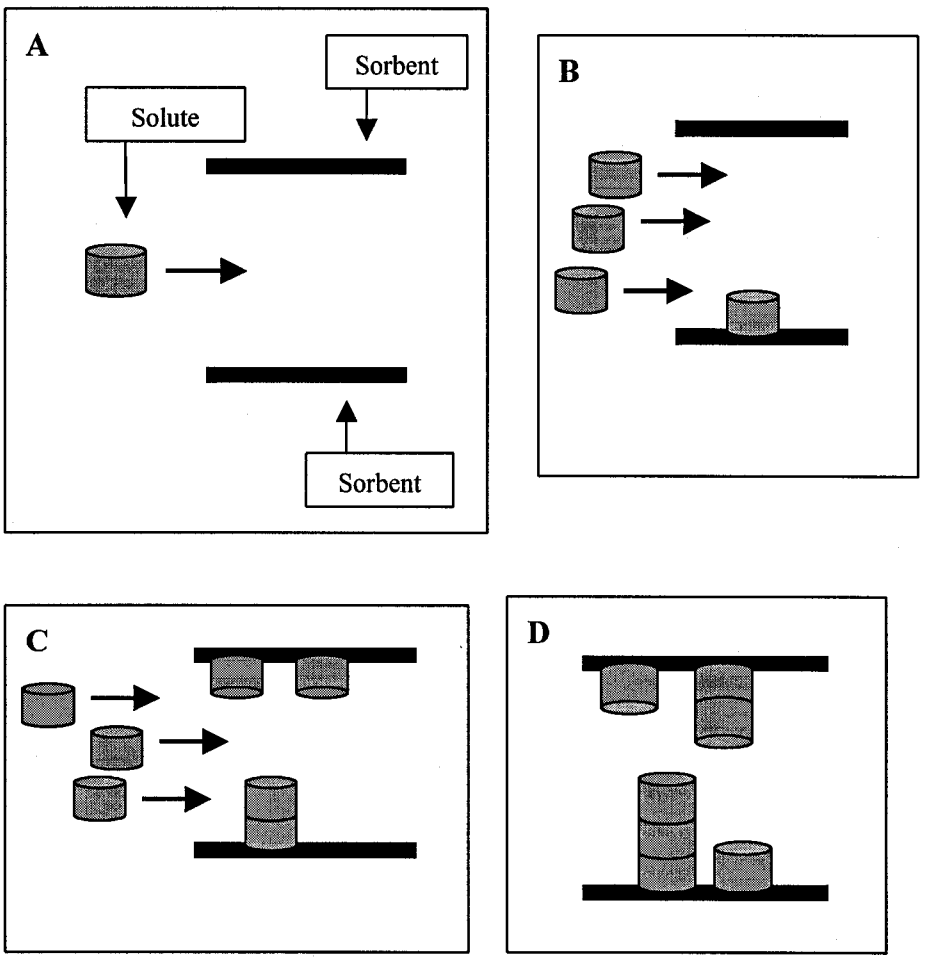

Figure 4-13. Schematics demonstrating the proposed simultaneous adsorption and base stacking processes. Notice that base stacking only occurs on the surface, not in solution. Schematic A shows the first solute molecule entering the column. In schematic B, this solute molecule has adsorbed to the surface as more solute molecules enter. Schematic C shows that some of the subsequent solute molecules adsorbed to the surface, while others interacted with previously adsorbed molecules through base stacking. Schematic D demonstrates that this process continues, and that the sizes of the base stacks proceed beyond the dimer stage.

in schematics A and B. As additional solute subsequently enters, as shown in schematic B, it may base stack with the adsorbed solute or adsorb to the adsorbent surface, demonstrated in schematic C. This process proceeds, as shown in schematic D, with subsequent solute molecules either adsorbing to the surface or base stacking

with molecules that are already adsorbed to the surface. Consequently, base stacking only occurs on the surface, not in solution. As previously mentioned, base stacking can proceed beyond the dimer stage, so the number of bases in any given stack would not hinder further stacking of incoming solute, as demonstrated by the various stack sizes shown in schematic D. Furthermore, the high association constant of 2'-deoxyadenosine suggests that its affinity to self-interact may be as significant as its affinity to adsorb to the selected adsorbent, or even more so. In fact, all reported values for the self-association constant of deoxyadenosine are at least four times that of thymidine (Solie and Schellman, 1968; Ts'o, ed., 1974). This high association constant could also explain why slightly skewed peaks were obtained for 2'-deoxyadenosine but not for the other three compounds studied. As previously mentioned, skewed peaks result from a combination of processes occurring concurrently, but at different rates. For thymine, adenine, and thymidine, the peaks are Gaussian in shape, either indicating that one process dominates overall or that the rates of all processes are the same. However, the peaks for 2'-deoxyadenosine are skewed, indicating that more than one process contributes to the observed heats of adsorption, and furthermore that the processes proceed at different rates. The data suggest that base stacking is not negligible for thymine, adenine, and thymidine, as will be discussed later. However, base stacking effects are as significant as adsorption effects for 2'-deoxyadenosine. This observation is supported by the fact that the self-association constant for 2'-deoxyadenosine is significantly greater than that for thymidine.

In examining the observed heats of adsorption for 2'-deoxyadenosine and adenine, it is clear that enthalpic contributions due to base stacking are indeed significant. All the peaks obtained for 2'-deoxyadenosine were exothermic, which is uncharacteristic for weak hydrophobic interactions in the presence of ammonium sulfate. Although exothermic heats of adsorption have been observed in the case of strong attractive forces between the adsorbate and adsorbent, there is no evidence that such strong interactions occur in this case. It is expected that the hydrophobicity of adenine and 2'-deoxyadenosine are approximately equal, since the nitrogen base provides the primary hydrophobic contribution. As discussed in Chapter 1, the strength of a hydrophobic interaction is largely determined by the hydrophobicity of the adsorbing molecule. 2'-deoxyadenosine only differs from adenine in that it contains the sugar 2'-deoxyribose. If the addition of the 2'-deoxyribose to the base caused the adsorbate/adsorbent interaction to become strongly attractive, exothermic peaks would have also been observed for the nucleoside thymidine. This was not the case, however, which supports the claim that the large discrepancy in the 2'-deoxyadenosine peaks and the adenine peaks is due to at least one effect besides interactions with the surface.

Because the reported enthalpies of base stacking are on the same order of magnitude as most of the observed heats of adsorption, and because those enthalpies are exothermic and hydrophobic interactions between weak hydrophobic adsorbents and biomolecules typically produce endothermic heats of adsorption, it is reasonable to hypothesize that the observed heats of adsorption are a combination of a negative enthalpy change due to base stacking and a positive enthalpy change due to

hydrophobic interaction. As previously stated, the relative contributions of these two effects would largely be determined by the relative affinities for adsorption to the selected adsorbent and self-association. Unfortunately, the discrete contributions of base stacking and adsorption to the overall observed heat of adsorption could not be determined from the data collected in these experiments.

Further support for the hypothesis that the enthalpy change of base stacking significantly contributes to the overall observed heats comes from an examination of the adenine and 2'-deoxyadenosine data. It has been reported that base stacking self-interactions vary with salt concentration (Neidle, ed., 1999). Robinson and Grant found that self-interaction effects in 2 M salt solutions were up to 50% greater than those in 1 M salt solutions (Robinson and Grant, 1966). The fact that self-interactions increase with increasing salt concentration explains the decrease in observed heats of adsorption for adenine and 2'-deoxyadenosine with increasing salt concentration. If we view the observed heat of adsorption as a combination of the heat of adsorption and the enthalpy change of base stacking, it is possible that the observed heat of adsorption may actually decrease with salt concentration. According to Scoble (1984), changing the ionic strength of the mobile phase only slightly affects the retention behavior of nucleosides and bases. This implies that the adsorption characteristics of these biomolecules would also change only slightly with a change in mobile phase salt concentration. Coupling a slightly increasing endothermic heat of adsorption with an increasingly exothermic heat of base stacking results in a decrease in the overall observed heat. This is, in fact, the trend observed for adenine and 2'-deoxyadenosine.

Since the association constant and the enthalpy change of base stacking for thymidine are significantly smaller than those for 2'-deoxyadenosine, it is likely that base stacking makes a smaller contribution to the observed heats of adsorption for thymidine. A comparison of the thymine and thymidine data reveals that all observed heats are endothermic, and they increase slightly with increasing salt concentration. In addition, the magnitudes of the endothermic peaks for thymidine are consistently smaller than those for thymine. This relatively small discrepancy in heats of adsorption for thymine and thymidine is likely due to differences in the base stacking self-interactions of these compounds. The fact that the observed heats of adsorption for both thymine and thymidine increase with increasing ammonium sulfate concentration (as is expected for weak hydrophobic interactions) further suggests that the contribution of adsorption to enthalpy change is more significant than that for base stacking for these compounds.

Combining the fact that the enthalpy change of base stacking is significantly larger for deoxyadenosine than thymidine with the observation that the observed heats of adsorption for 2'-deoxyadenosine are exothermic while those for thymidine are endothermic indicates that, indeed, enthalpic contributions due to self-interactions cannot be ignored. Assuming that the observed endothermic heats are a combination of the adsorption heat and the enthalpy change of base stacking, the differences between the observed heats of thymine versus thymidine and adenine versus 2'-deoxyadenosine could be entirely due to differences in their respective enthalpies of base stacking.

4.2.1 Hydrophobicity Equation

As discussed in Chapter 1, the hydrophobicity of a homo-oligonucleotide is given by:

$$H = Bn + (n-1)P \qquad \text{(1-F)}$$

where H is the hydrophobicity of the solute, B is the hydrophobicity of the base, n is the chain length, and P is the hydrophobicity of the phosphate group (Ikuta *et al.*, 1984). An assumption of this equation is that the effect of the sugar, in this case 2'-deoxyribose, is not significant for calculating the hydrophobicity of an oligonucleotide. This assumption was examined by comparing the heats of adsorption, which are assumed to correlate proportionally with the hydrophobicity, for two nitrogen bases and their related nucleosides, specifically thymine with thymidine and adenine with 2'-deoxyadenosine. The results of this study do not strongly indicate that the addition of 2'-deoxyribose to the nitrogen base significantly affects the hydrophobicity of the molecule. The differences observed between the heats of adsorption for the nitrogen bases and their related nucleosides can be attributed to base stacking self-interaction effects that occur with nitrogen bases and nucleosides, but not with oligonucleotides. Thus, the assumption in Equation (1-F) that the sugar does not contribute to the hydrophobicity of an oligonucleotide cannot be contested. However, the addition of the sugar clearly alters other important properties related to the adsorption of nitrogen bases and nucleosides, such as the solubility and the propensity to base stack.

4.3 Summary

Microcalorimetric data revealed that the adsorption behavior of nitrogen bases and nucleosides in aqueous solution is a complex phenomenon. Although hydrophobic interactions appear to be the primary mechanism for adsorption to the hydrophobic adsorbent, these biomolecules exhibited base stacking behavior on the adsorbent even at low solution concentrations.

The technique of flow microcalorimetry proved vital in this study. It is likely that the effects of base stacking due to contact between adsorbed biomolecules and biomolecules in solution would not have been observed through analyses using chromatographic techniques or static calorimetric techniques such as ITC or DSC.

These results have strong implications for chromatographic separations of bases and nucleosides. As discussed above, nitrogen bases and nucleosides self-interact through base stacking when in close contact. Even when the adsorbent surface is completely saturated, the molecules in solution are likely to base stack with the adsorbed molecules, creating multi-layer adsorption. This knowledge can be utilized to optimize packed bed separation processes for bases and nucleosides.

5. Heats of Adsorption of Homo-deoxyoligonucleotides on Sepharose CL–6B

5.1 Results

Heats of adsorption for the homo-deoxyoligonucleotides poly(A) and poly(T) at base lengths of 6 and 30 were obtained at ammonium sulfate concentrations varying between 1.0 M and 2.0 M. The oligonucleotide solution concentrations studied varied between 0.70 mg/mL and 1.0 mg/mL. The limited solubility of these compounds required the study of low solution concentrations, which correspond to linear isotherm conditions within the column. Sample calculations are shown in Appendices A–5 through A–8. As with the nitrogen base and nucleoside data reported in Chapter 4, the data reported in this chapter include 5% error bars.

5.1.1 Poly(T)

For both poly(T) 6mer and 30mer, bimodal peaks were obtained at all salt concentrations. Each bimodal peak consisted of an endothermic peak followed by an exothermic peak, as was observed for thymine and thymidine. An example peak is shown in Figure 5-1. In all cases, the magnitudes of the endothermic and exothermic peaks were approximately equal, supporting our assumption that the poly(T) was adsorbed and then desorbed in an elution operation. The peaks were analyzed as discussed in Section 2.2.2. Poly(T) 6mer heats of adsorption and heats of desorption are shown in Figures 5-2 and 5-3, respectively, and sample calculations are provided in Appendix A–5. Similarly, heats of adsorption and desorption for poly(T) 30mer

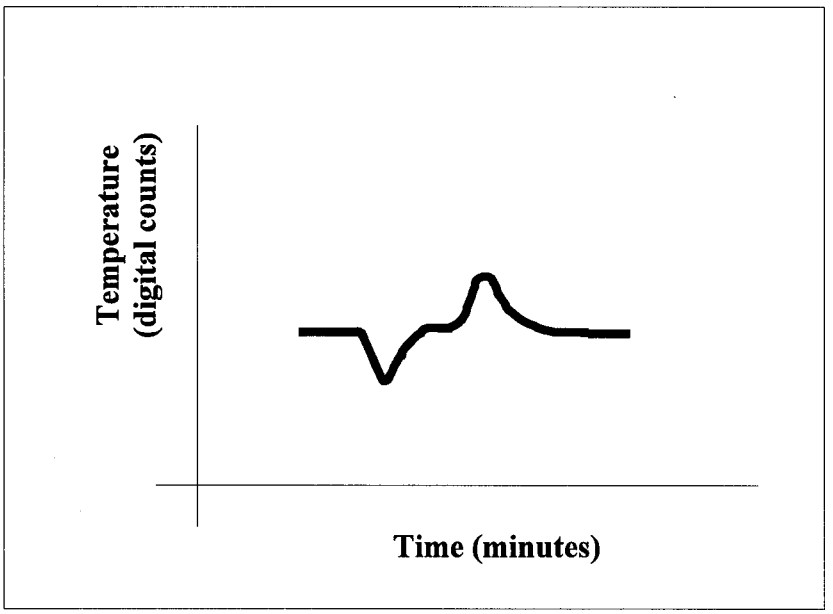

Figure 5-1. Example peak obtained for poly(T) 6mer adsorbing to and desorbing from Sepharose CL–6B. This peak was obtained at the following conditions: flow rate, 1.65 mL/hr; sample, 1.0 mg/mL poly(T) 6mer in 1.0 M ammonium sulfate; pH, 8.0; temperature, 26.1° C.

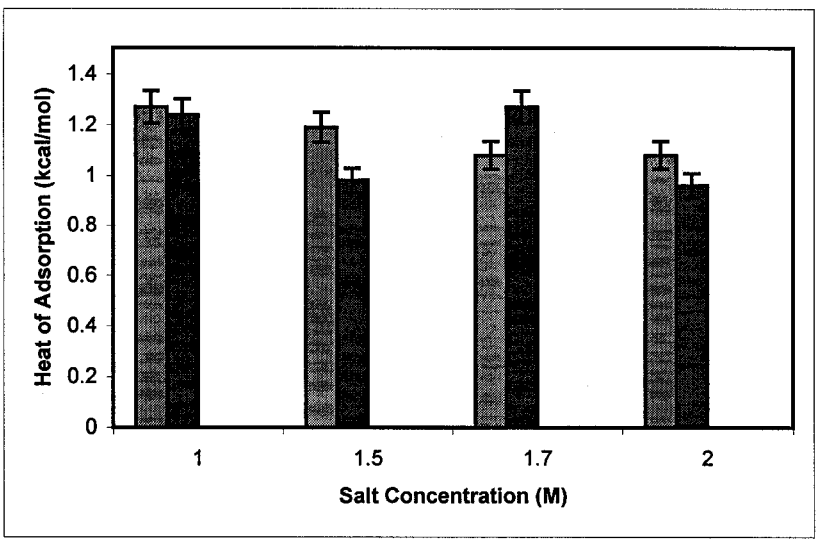

Figure 5-2. Observed heats of adsorption for poly(T) 6mer on Sepharose CL–6B at varying ammonium sulfate concentrations. Data were collected at 26±1.0° C, a flow rate of 1.65 mL/hr, a solution pH of 8.0, and poly(T) 6mer concentrations ranging from 0.70 mg/mL to 1.0 mg/mL.

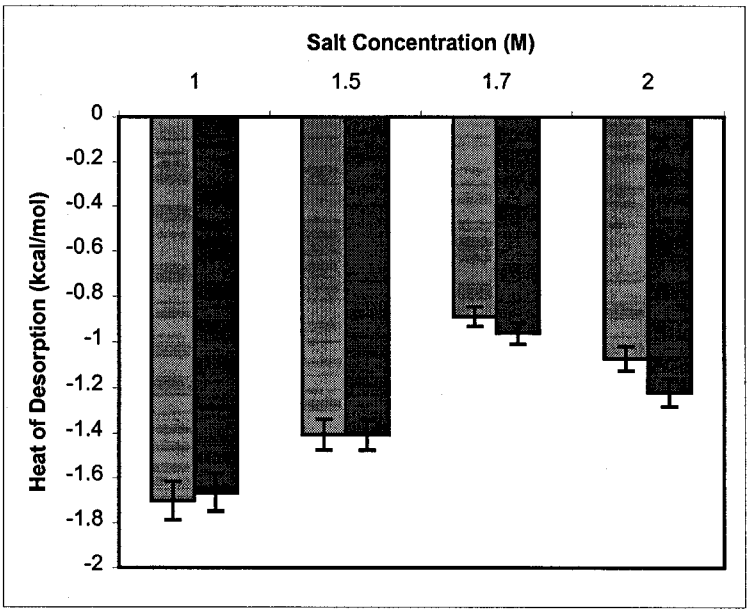

Figure 5-3. Observed heats of desorption for poly(T) 6mer from Sepharose CL–6B at varying ammonium sulfate concentrations. Data were collected at 26±1.0° C, a flow rate of 1.65 mL/hr, a solution pH of 8.0, and poly(T) 6mer concentrations ranging from 0.70 mg/mL to 1.0 mg/mL.

are given in Figures 5-4 and 5-5, and sample calculations are shown in Appendix A–7.

5.1.2 Poly(A)

For poly(A) 6mer, bimodal peaks were obtained at all salt concentrations. Each bimodal peak consisted of an endothermic peak followed by an exothermic peak, as was observed for adenine. As with the poly(T), the magnitudes of the endothermic and exothermic peaks were approximately equal for poly(A) 6mer, and both peaks were analyzed as discussed in Section 2.2.2. An example peak appears in Figure 5-6. The heats of adsorption and heats of desorption for Poly(A) 6mer are shown in Figures 5-7 and 5-8, respectively, and sample calculations appear in Appendix A–6.

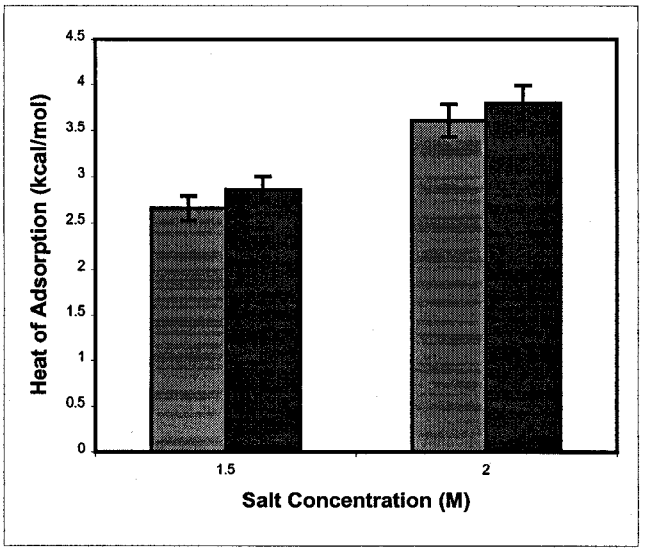

Figure 5-4. Observed heats of adsorption for poly(T) 30mer on Sepharose CL–6B at varying ammonium sulfate concentrations. Data were collected at 26±1.0° C, a flow rate of 1.65 mL/hr, a solution pH of 8.0, and poly(T) 30mer concentrations ranging from 0.70 mg/mL to 1.0 mg/mL.

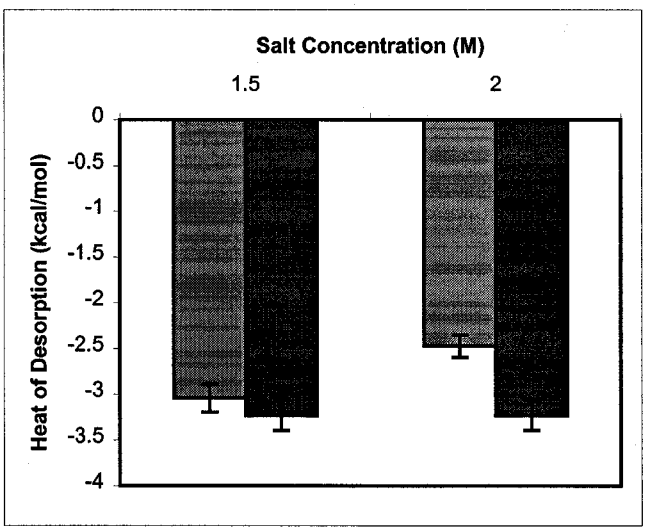

Figure 5-5. Observed heats of desorption for poly(T) 30mer from Sepharose CL–6B at varying ammonium sulfate concentrations. Data were collected at 26±1.0° C, a flow rate of 1.65 mL/hr, a solution pH of 8.0, and poly(T) 30mer concentrations ranging from 0.70 mg/mL to 1.0 mg/mL.

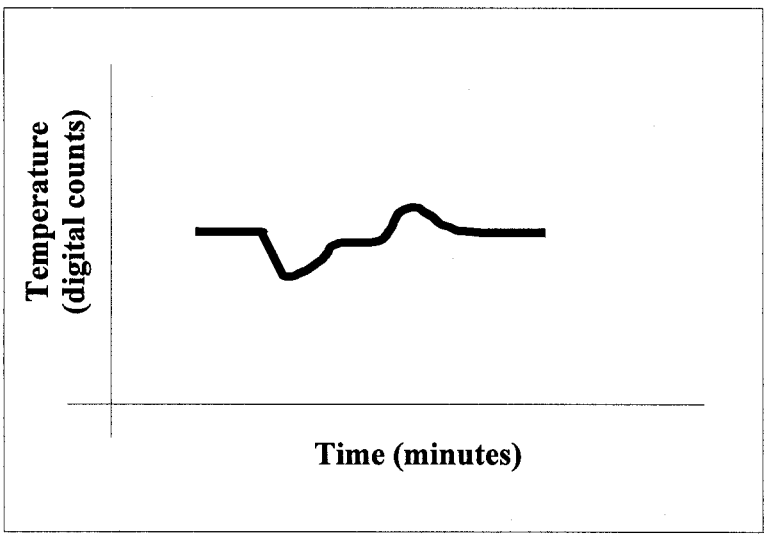

Figure 5-6. Example peak obtained for poly(A) 6mer adsorbing to and desorbing from Sepharose CL–6B. This peak was obtained at the following conditions: flow rate, 1.65 mL/hr; sample, 1.0 mg/mL poly(A) 6mer in 1.7 M ammonium sulfate; pH, 8.0; temperature, 25.9° C.

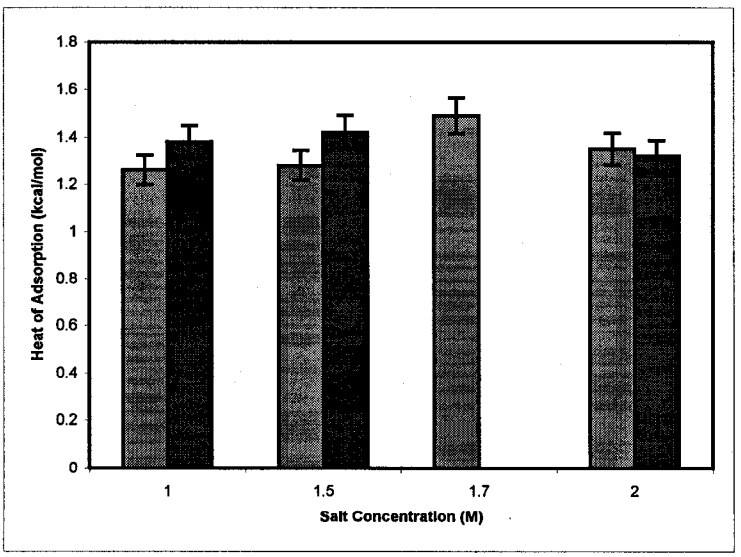

Figure 5-7. Observed heats of adsorption for poly(A) 6mer on Sepharose CL–6B at varying ammonium sulfate concentrations. Data were collected at 26±1.0° C, a flow rate of 1.65 mL/hr, a solution pH of 8.0, and poly(A) 6mer concentrations ranging from 0.70 mg/mL to 1.0 mg/mL.

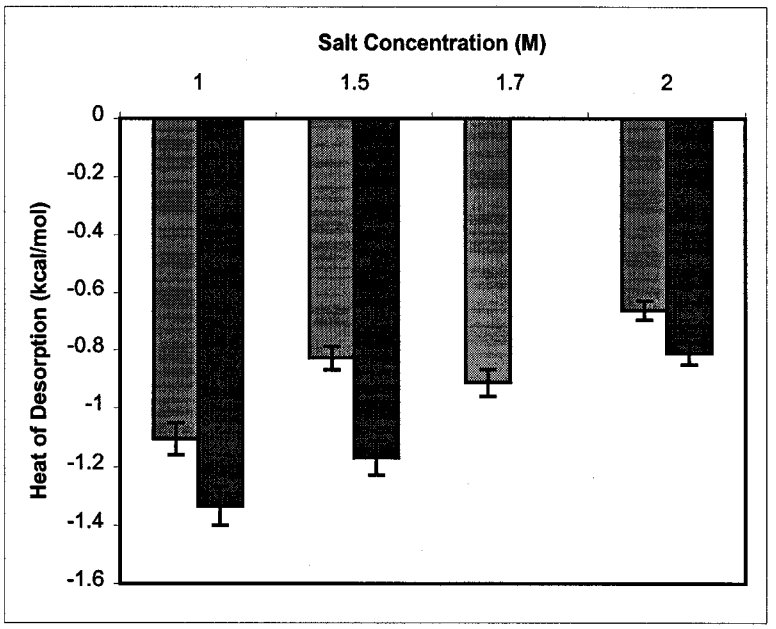

Figure 5-8. Observed heats of desorption for poly(A) 6mer from Sepharose CL–6B at varying ammonium sulfate concentrations. Data were collected at 26±1.0° C, a flow rate of 1.65 mL/hr, a solution pH of 8.0, and poly(A) 6mer concentrations ranging from 0.70 mg/mL to 1.0 mg/mL.

The adsorption peaks obtained for poly(A) 30mer were endothermic, but clear desorption peaks were not evident. Additionally, the peaks were not Gaussian in shape, but more smooth and rounded as shown in Figure 5-9. This peak shape suggests that overlapping effects progressing at different rates contribute to the observed endothermic heat of adsorption. The heats of adsorption for poly(A) 30mer are shown in Figure 5-10, and sample calculations are provided in Appendix A–8. Since there were no clear desorption peaks for poly(A) 30mer, heats of desorption were not calculated for this homo-deoxyoligonucleotide. Clearly, the endothermic heats of adsorption for poly(A) 30mer are significantly larger than those for the other three oligonucleotides studied.

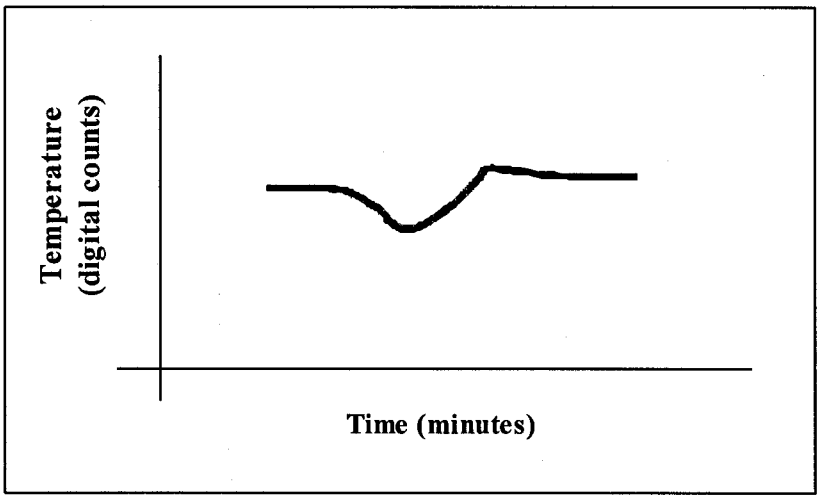

Figure 5-9. Example peak obtained for poly(A) 30mer adsorbing to Sepharose CL–6B. This peak was obtained at the following conditions: flow rate, 1.65 mL/hr; sample, 0.72 mg/mL poly(A) 30mer in 1.5 M ammonium sulfate; pH, 8.0; temperature, 25.9° C.

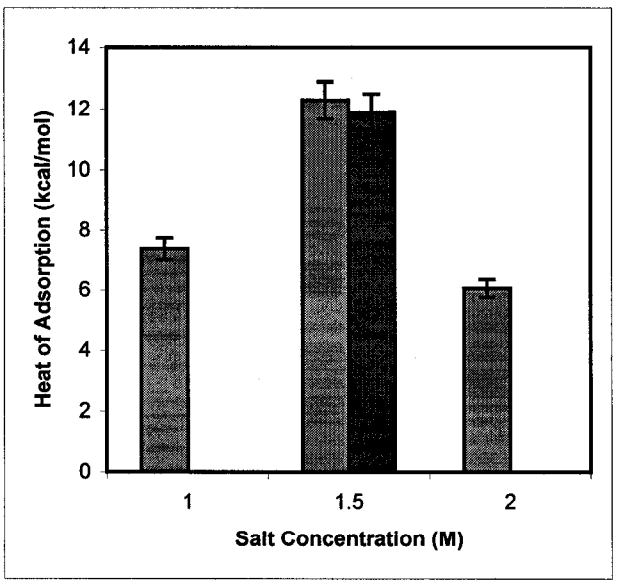

Figure 5-10. Observed heats of adsorption for poly(A) 30mer on Sepharose CL–6B at varying ammonium sulfate concentrations. Data were collected at 26±1.0° C, a flow rate of 1.65 mL/hr, a solution pH of 8.0, and poly(A) 30mer concentrations ranging from 0.70 mg/mL to 1.0 mg/mL.

Generally, it was more difficult to obtain reproducible results using poly(A) 30mer than the other three oligonucleotides. This is probably due to the difficulties associated with the synthesis of this homo-deoxyoligonucleotide. Because of the strong hydrophobicity of adenine, synthesizing relatively long oligonucleotides using only this base is more problematic than other homo-oligonucleotides or heterogeneous oligonucleotides. Gilar and Bouvier (2000) reported crude purities for several oligonucleotides. Although they did not purchase these materials from IDT Technologies, as we did, the fact that they reported the crude purity of poly(A) 15mer to be 72.6% as compared with poly(T) 15mer at 89.1% and poly(T) 30mer at 79.0% demonstrates that synthesis of high purity poly(A) homo-oligonucleotides is more difficult than poly(T) or heterogeneous oligonucleotides.

5.2 Discussion

In all cases, endothermic heats of adsorption were observed. These findings are consistent with calorimetric measurements for weak hydrophobic interactions reported in the literature (Esquibel-King *et al.*, 1999; Perkins *et al.*, 1997). Heat of adsorption values ranged from 0.96 to 1.49 kcal/mol for the 6mers, and 2.66 to 12.30 kcal/mol for the 30mers. Although this is the first known calorimetric study of hydrophobic adsorption for homo-deoxyoligonucleotides onto hydrophobic supports, these values appear to be reasonable. As discussed in Chapter 1, the hydrophobic constituent bases provide the primary contribution to the hydrophobicity of an oligonucleotide. Accordingly, if hydrophobic interaction is the primary source of the observed heat of adsorption, we expect heats of adsorption for oligonucleotides to be

no less than the heat of adsorption for one constituent base and no more than the heat of adsorption for one constituent base multiplied by the number of monomers in a given oligonucleotide. Indeed, for both 6mers and 30mers studied here, this was the case.

Unfortunately, the exact number of oligonucleotide bases interacting with the adsorbent cannot be unequivocally determined from the heats of adsorption for the oligonucleotide and its constituent bases. As discussed in Chapter 5, the observed heats of adsorption for the bases probably include not only the heat associated with adsorption due to hydrophobic interaction, but also the enthalpy change associated with base stacking self-interactions. Since base stacking does not occur between two discrete oligonucleotides, as it does between two discrete nitrogen base molecules, the correlation between the observed heats of adsorption for homo-deoxyoligonucleotides and the observed heats of adsorption for their constituent bases (reported in Chapter 4) is not a direct one. However, the relative magnitudes of the measured heats of adsorption provide a qualitative indication of oligonucleotide adsorption behavior.

The endothermic heats of adsorption for all four oligonucleotides studied are relatively insensitive to small changes in mobile phase concentration. However, retention data for these biomolecules (see Chapter 3, Table 3-1) demonstrate that retention clearly increases with increasing salt concentration for all oligonucleotides studied. Since the enthalpic contribution to the overall change in Gibb's free energy is approximately constant, the entropic term must increase with increasing

ammonium sulfate concentration in order for the interactions at higher salt concentrations to be more favorable than those at lower salt concentrations.

For the poly(A) 6mers, the heats of adsorption are approximately 1.3 kcal/mol, independent of salt concentration. These measured heats of adsorption are only one to two times greater than those observed for adenine alone. Furthermore, at the short base length of 6, little secondary structure exists for oligonucleotides, as will be discussed later. These poly(A) 6mer data suggest that the adsorbed orientation is more likely to be "end-on" as opposed to "side-on" against the adsorbent surface for these oligonucleotides.

For the poly(T) 6mers studied, the heats of adsorption are approximately 1.0 kcal/mol, independent of salt concentration. This heat of adsorption value is approximately six times greater than the heat of adsorption value for thymine in 1.0 M ammonium sulfate, but approximately equal to the heat of adsorption value for thymine in 2.0 M ammonium sulfate. However, as discussed in Chapter 4, the overall observed heats of adsorption for thymine are a combination of the heat of adsorption and the enthalpy change associated with base stacking self-interactions. Since the enthalpy change associated with thymine base stacking self-interactions has not been quantified, the true heat of adsorption value for thymine on Sepharose CL–6B is unknown. Accordingly, it is not clear whether the adsorbed orientation of this oligonucleotide is "end-on" or "side-on" against the adsorbent surface, since the data indicate that any number of the six bases may be interacting with the surface. However, since the poly(A) 6mer is more hydrophobic than the poly(T) 6mer, and

because the poly(A) 6mer clearly adsorbs in an "end-on" orientation, it is likely that the poly(T) 6mer also adsorbs in an "end-on" orientation.

If the adsorbed orientation is, in fact, "end-on," the measured heats of adsorption will not correlate linearly with the hydrophobicity of the oligonucleotide. Specifically, if the oligonucleotide adsorbs "end-on," then approximately the same number of constituent bases will be adsorbed to the surface of the adsorbent regardless of the oligonucleotide length. Accordingly, the measured heats of adsorption will not increase significantly as the number of bases, and therefore the hydrophobicity, increases.

This is, in fact, the trend we observe for poly(T). As shown in Figure 5-11,

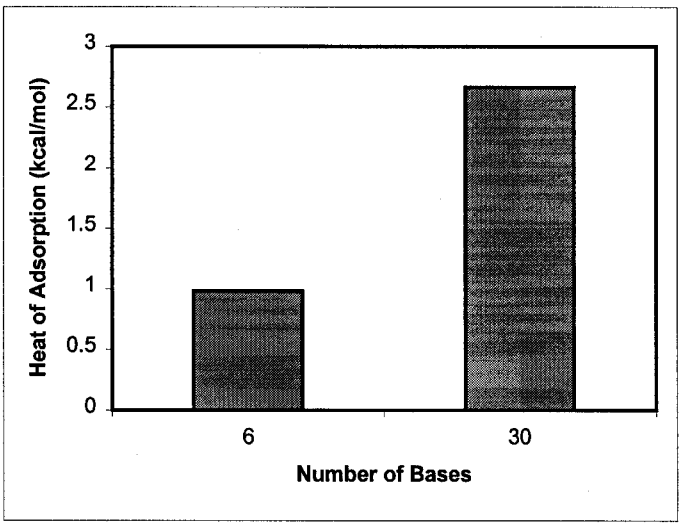

Figure 5-11. Relative heats of adsorption for poly(T) on Sepharose CL–6B at base lengths of 6 and 30. Data were collected at 26±1.0° C, a flow rate of 1.65 mL/hr, an ammonium sulfate concentration of 1.5 M, a solution pH of 8.0, and poly(T) concentrations of 1.0 mg/mL.

the heat of adsorption for poly(T) increases by a factor of approximately 2.5 when the number of bases increases by a factor of 5. Assuming that the heat of adsorption for thymine is approximately 0.54 kcal/mol (the average value of the measured heats of

adsorption for thymine reported in Chapter 4, Figure 4-3), two bases would be interacting with the adsorbent in the case of the 6mer, and five bases would be interacting with the adsorbent in the case of the 30mer. This small number of interacting bases for poly(T) 30mer cannot be attributed to shielding of the hydrophobic bases due to secondary structure at 26±1.0° C, the temperature at which calorimetric data were collected. As discussed in Chapter 3, the linearity of Figure 3-2 demonstrates that little secondary structure exists for poly(T) at 25° C and base lengths of 6, 15, and 30. Therefore, the small number of bases interacting with the adsorbent surface indicate that the adsorption is "end-on," with either one or both ends interacting with the surface, as shown in Figure 5-12.

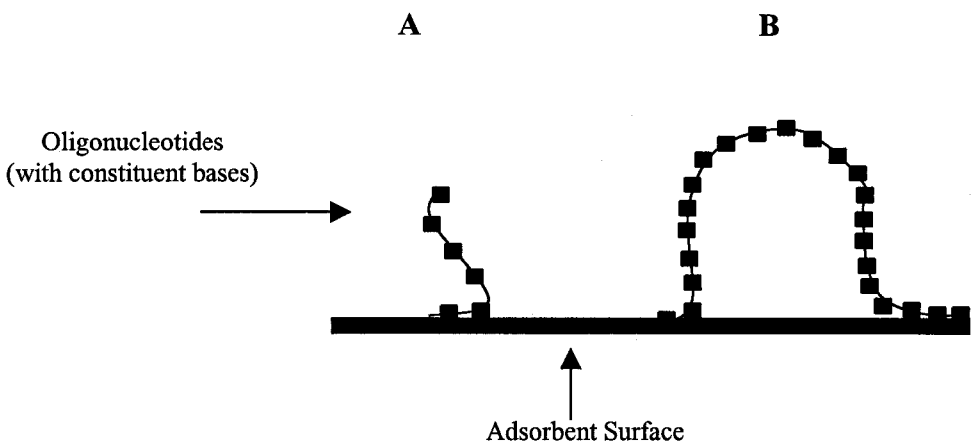

Figure 5-12. Schematic of the proposed adsorbed orientation for homo-deoxyoligonucleotides on Sepharose CL–6B. In A, one end of a relatively short oligonucleotide interacts with the adsorbent surface. In B, both ends of a longer oligonucleotide are adsorbed.

Assuming this proposed "end-on" adsorbed orientation is correct, the measured heat of adsorption will not correlate linearly with the hydrophobicity of an

oligonucleotide. As previously stated, the hydrophobicity of an oligonucleotide is given by:

$$H = Bn + (n-1)P \qquad \text{(1-F)}$$

where B is the hydrophobicity of the nitrogen base, n is the base length, and P is the hydrophobicity (either positive or negative) of one phosphate group. Clearly, this relationship shows that the hydrophobicity is related to the number of bases in a linear fashion. However, the observed heats of adsorption for the homo-deoxyoligonucleotides studied do not correlate linearly with the number of bases. These data demonstrate that the heat of adsorption does not accurately reflect the true hydrophobicity of homo-deoxyoligonucleotides.

The endothermic heat of adsorption of 12.30 kcal/mol, obtained for poly(A) 30mer at 1.5 M ammonium sulfate, was by far the largest recorded. The other dissimilarity between the poly(A) 30mer results and the results for the other three oligonucleotides studied is the non-Gaussian peak shape of the thermograms for poly(A) 30mer. This suggests that at least one effect in addition to adsorption contributes significantly to the endothermic heat observed.

It is interesting to note that the most unusual retention behavior reported by Diogo and coworkers occurred for poly(A) 30mer also. They reported higher retention factors for poly(A) than poly(T) at base lengths of 6 and 15, but lower retention factors for poly(A) 30mer than poly(T) 30mer. Moreover, the retention factors for poly(A) 30mer were lower than those for poly(A) 15mer (Diogo *et al.*, 2003). They concluded this decrease in retention factors for poly(A) 30mer was due

to a secondary structure of the oligonucleotide that shields some of the hydrophobic moieties.

Our data support the premise that secondary structure causes the observed decrease in retention time for poly(A) 30mer, but not due to a reduction in the hydrophobic surface area. It is clear from the enthalpic data obtained in this study that only some of the constituent bases on each oligonucleotide interact with the surface. Therefore, a slight decrease in the overall hydrophobicity of the molecule would not greatly affect the adsorption characteristics, since not all the bases of each oligonucleotide interact with the adsorbent. Furthermore, if poly(A) 30mer were less retained because of a relative decrease in its hydrophobicity, we would also expect a decrease in the observed heat of adsorption. In fact, the largest heats of adsorption were collected for poly(A) 30mer.

However, a closer examination of the secondary structure of poly(A) 30mer reveals that the hydrophobicity of the molecule is not the only consideration. Neidle (1999) describes the secondary structure of single-stranded RNA in terms of stacking. Using his terminology, base stacking for oligonucleotides occurs between constituent bases within a single oligonucleotide. This is distinct from the base stacking discussed in Chapter 4, in which base stacking interactions for nitrogen bases and nucleosides occur when two discrete molecules of the same type come into contact and interact.

According to Neidle (1999), the bases within any single oligonucleotide are generally stacked at low temperatures, meaning they are in close contact and are therefore interacting due to a combination of hydrophobic interactions, van der Waals

forces, and π-electron interactions. As the temperature increases, the stacking decreases, which causes the chain-like structure of the molecule to spread out and the secondary structure to diminish. Thus, the molecule exists as a random coil at higher temperatures (Neidle, ed., 1999). Kontturi and coworkers (2002) determined through diffusion coefficient measurements that the conformation of oligonucleotides is compact at 20° C, but opens to a random coil as the temperature increases.

As discussed in Chapter 4, 2'-deoxyadenosine has a higher propensity for base stacking than thymidine. According to Neidle (1999), this holds true not only for interactions between discrete nucleosides, but also for interactions between constituent bases within a single oligonucleotide. Specifically, adenine and guanine have the highest stacking propensity, followed by cytosine and uracil. Thymine is structurally similar to uracil, with an additional hydrophobic methyl group. Therefore, thymine probably stacks slightly more than uracil, but significantly less than adenine.

Kontturi and coworkers (2002) also reported that the heterogeneous oligonucleotides they studied exhibited very compact, tightly coiled structures, which made the distance between phosphate groups very short. The statement made by Neidle (1999), that "stacking decreases the average phosphate–phosphate distance" supports this finding. Furthermore, Kontturi and coworkers reported the smallest charge spacing (1.5–1.7 Å) for oligonucleotides with base lengths greater than 15, and their results indicate that charge spacing decreases with increasing base length. Because of adenine's high propensity to base stack, the relatively long base length of 30, and the temperature at which data were collected (26±1.0° C), it is likely that the

charge spacing for poly(A) 30mer was the smallest of any of the homo-oligonucleotides used in this study.

A small charge spacing distance also implies that the distance between any given hydrophobic moiety and the adjacent phosphate groups, which are negatively charged, is small. Accordingly, in order for a hydrophobic moiety to interact with the surface, the repulsion between the hydrophobic surface and the adjacent charged phosphate groups (which favor solvation in aqueous solution) must be overcome. Overcoming this repulsion increases the observed endothermic heat of adsorption. In fact, the unusual shape of the poly(A) 30mer peaks probably derives from the overlapping effects of hydrophobic interactions and repulsion between the phosphate groups and the adsorbent surface.

The hypothesis that the charge spacing makes a significant contribution to the observed heat of adsorption for poly(A) 30mer is further supported by preferential interaction analysis. In addition to the increase in the endothermic heat observed through flow microcalorimetry, the amount of water released decreases for poly(A) 30mer (see Chapter 3, Table 3-2), again because the hydrophilic phosphate group is very close to the hydrophobic base involved in adsorption and thus limits the water release. As Figure 5-13 shows, preferential interaction analysis demonstrates that the release of water for poly(A) 30mer is less than that for poly(T) 30mer, even though the release of water for poly(A) is significantly greater than that for poly(T) at shorter base lengths. Additionally, water release for poly(A) 30mer is also less than that for

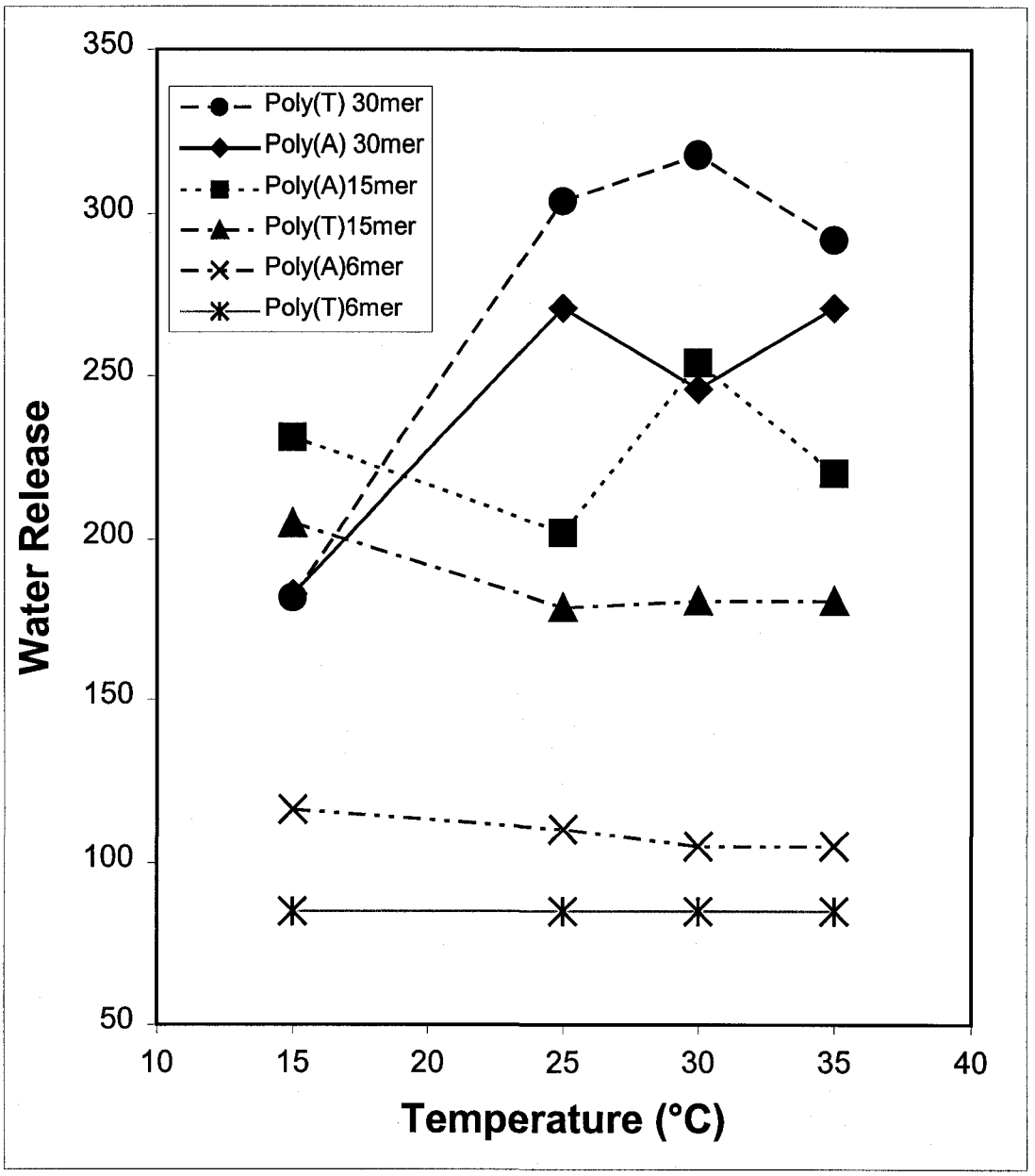

Figure 5-13. Water release data for adsorption of homo-deoxyoligonucleotides poly(A) and poly(T) on Sepharose CL–6B with respect to temperature. Water release data were calculated using the Preferential Interaction Model, as described in Chapter 3.

poly(A) 15mer at 15° C. The fact that water release for poly(A) 30mer is greater than that for poly(A) 15mer only at higher temperatures further indicates that the secondary structure of poly(A) 30mer is significant.

Although the hydrophobicity of an oligonucleotide can be easily calculated using Equation (1-F), data from this study demonstrate that heats of adsorption and retention behavior of homo-deoxyoligonucleotides on the hydrophobic adsorbent Sepharose CL–6B cannot be predicted through relative hydrophobicities alone. The heat of adsorption data indicate that oligonucleotides adsorb to this adsorbent in an "end-on" orientation. Thus, the hydrophobicity, largely determined by the base length, does not correlate linearly with the heat of adsorption, since approximately the same number of bases interacts with the adsorbent surface regardless of base length.

Additionally, the secondary structure of homo-deoxyoligonucleotides, particularly the charge spacing, significantly affects retention behavior. The results of this study indicate that, as the charge spacing decreases, the amount of water released decreases and the heat of adsorption increases. These combined effects (a decrease in the positive entropy change and an increase in the positive enthalpy change) cause the adsorption process to be less energetically favorable. Thus, the retention factor for the homo-deoxyoligonucleotide decreases as the charge spacing decreases.

5.3 Summary

Heat of adsorption data obtained through flow microcalorimetry demonstrate that the homo-deoxyoligonucleotides studied adsorb in an "end-on" orientation as opposed to "side-on" against the adsorbent surface. Therefore, a slight decrease in

the overall hydrophobicity of the molecule probably does not significantly affect adsorption behavior. Additionally, the heats of adsorption varied little with increasing ammonium sulfate concentration, suggesting that the reported increase in retention factors is due to an increase in the entropic contribution to the overall Gibb's free energy as ammonium sulfate concentration increases.

For poly(T) 6mer, poly(A) 6mer, and poly(T) 30mer the heat of adsorption peaks obtained were Gaussian in shape, which is expected when all effects proceed at the same rate. For these homo-deoxyoligonucleotides adsorbing onto Sepharose CL–6B, the effect of hydrophobic interaction likely predominates. In contrast, the poly(A) 30mer peaks were not Gaussian, suggesting the presence of more than one type of interaction. After examining the secondary structure of poly(A) 30mer, specifically the charge spacing, it was determined that the poly(A) 30mer peaks represented a combination of hydrophobic interactions and repulsion between the charged phosphate groups and the hydrophobic surface. This explanation is also consistent with the decrease in water release and reported retention factors for poly(A) 30mer.

Flow microcalorimetry proved vital in understanding the underlying thermodynamics for the adsorption of homo-deoxyoligonucleotides to Sepharose CL–6B. The results of this study suggest that hydrophobic interactions are the primary interactions between the biomolecules and adsorbent, but that secondary structure, particularly charge spacing, significantly affects retention behavior of homo-deoxyoligonucleotides.

6. Effects of Salt on Adsorption of BSA on an Ion-Exchange Support

Whereas adsorption of oligonucleotides is a relatively new area of research, adsorption of proteins has been studied for several years by numerous researchers (Thrash and Pinto, 2003, 2002, 2001; Lin *et al.*, 2002, 2001, 2001; Raje and Pinto, 1998, 1997; Norde, 1998; Haynes and Norde, 1995). As previously stated, one of the most common methods of chromatographic separation of proteins is IEC. In this study, heats of adsorption for BSA adsorbing onto PEI–1000–10, an ion-exchange support, were collected through flow microcalorimetry. These data were analyzed in conjunction with water release data obtained through preferential interaction analysis to determine the primary driving force for adsorption.

6.1 Results

Heats of adsorption for BSA on PEI–1000–10 were obtained for BSA concentrations ranging from 2.5 mg/mL to 20 mg/mL. These relatively high concentrations of BSA correspond to overloaded conditions used in preparative chromatography of proteins. Four different carrier fluids were used: 0.0 M salt, 0.1 M LiCl, 0.1 M NaCl, and 0.1 M KCl. These three salts were chosen in order to determine the effects of the cation in solution. The results are presented in Table 6-1. A sample calculation is shown in Appendix A–9. Surface concentration values were obtained through isotherm measurements conducted by M.E. Thrash in our laboratory (Thrash *et al.*, 2003).

Surface Concentration (mg/g)	Salt	ΔH_{ads} (kcal/mol)
35.3	0.0	13.9
67.4	0.0	15.7
105.0	0.0	20.1
21.3	0.1 KCl	7.04
33.5	0.1 KCl	10.6
50.6	0.1 KCl	9.4
19.2	0.1 NaCl	8
30.2	0.1 NaCl	10.5
48.4	0.1 NaCl	11.2
21.1	0.1 LiCl	5
30.0	0.1 LiCl	6.9
43.3	0.1 LiCl	6.1

Table 6-1. Heats of adsorption for BSA on PEI–1000–10. Results were obtained using flow microcalorimetry at 26±3.0 C° and a flow rate of 1.65 mL/hr.

In all cases, endothermic heats of adsorption were observed. An example peak is shown in Figure 6-1. A plot of the heats of adsorption as a function of surface coverage is provided in Figure 6-2.

6.2 Discussion

Adsorption of charged proteins onto oppositely charged supports is exploited in ion exchange chromatography. Strong attractive forces between the adsorbate and the adsorbent typically result in exothermic heats of adsorption (Thrash and Pinto, 2002). In this study, negatively charged BSA (pH 6.0) adsorbed onto positively charged PEI–1000–10, and endothermic heats of adsorption were observed in all cases.

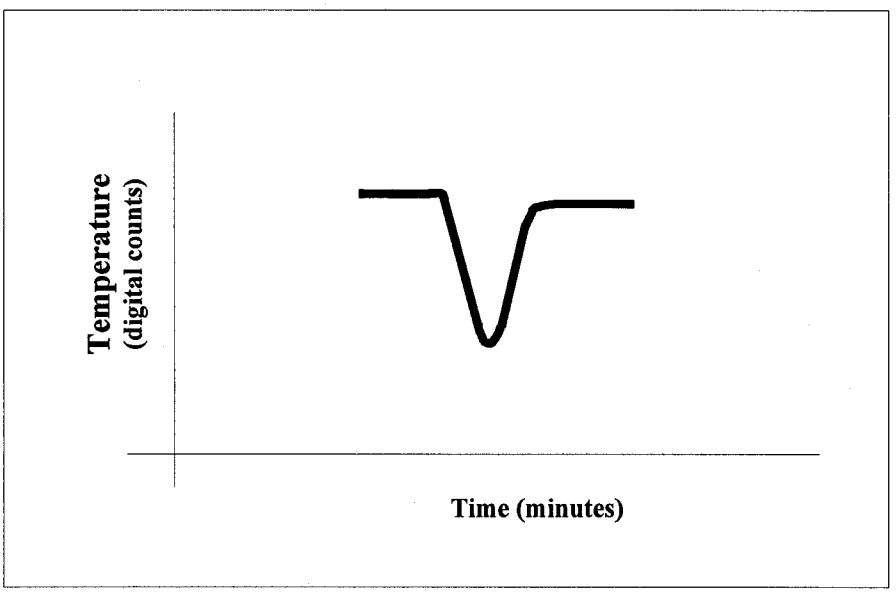

Figure 6-1. Example peak obtained for BSA adsorbing onto PEI–1000–10. This peak was obtained at the following conditions: flow rate, 1.65 mL/hr; sample, 20 mg/mL BSA solution in 0.0 M salt; pH, 6.0; temperature, 26.0° C.

The observed endothermic heats were strong enough to mask the exothermic heat associated with attraction between the oppositely charged adsorbent and protein. Endothermic heats of adsorption have been previously reported for the BSA/PEI system (Thrash and Pinto, 2001; Raje, 1997). In the literature, endothermic heats of adsorption have been attributed to several phenomena: water release from the surface and the molecule, repulsive interactions between adsorbed molecules and molecules in solution, and conformational changes of the target molecule (Welzel, 2002; Thrash

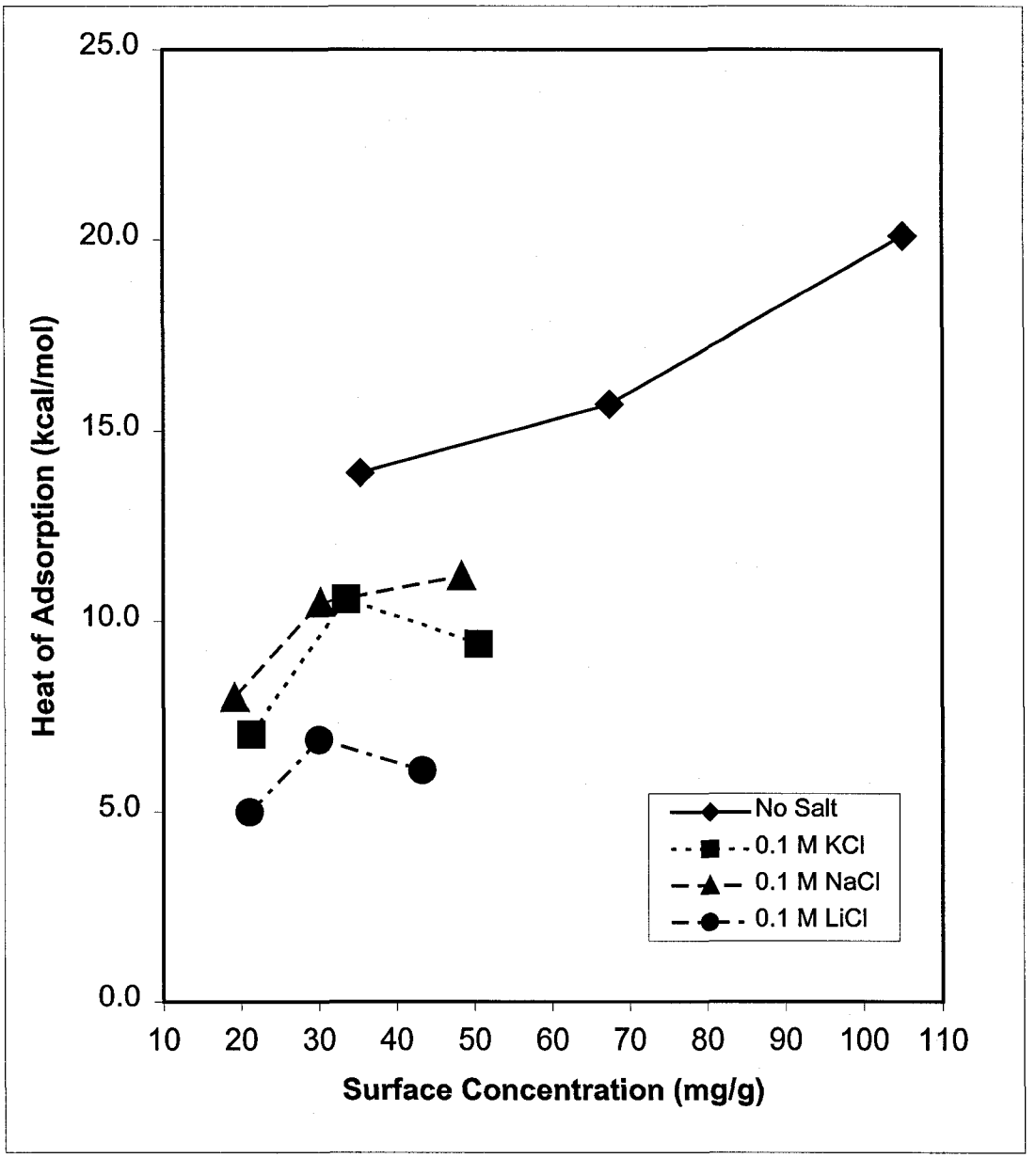

Figure 6-2. Heats of adsorption with respect to surface coverage. These data were obtained at the following conditions: flow rate, 1.65 mL/hr; pH, 6.0; temperature, 26±3.0° C.

and Pinto, 2002; Malmsten, 1998). Our data indicate that the observed endothermic heats of adsorption probably derive from a combination of these three effects.

Thrash and Pinto (2002) explored the effects of water release for this system by collecting retention data and applying the preferential interaction model described in Chapter 3. They obtained water release values of 149 for KCl, 112 for NaCl, and 59 for LiCl. Since a larger number of released water molecules generally correspond to an increase in surface dehydration, it would be expected that the endothermic heat of dehydration would increase as the number of water molecules released increases. The data obtained in this study fit this trend to some degree. Table 6-1 and Figure 6-2 indicate that the observed endothermic heats are consistently larger in the presence of KCl than in the presence of LiCl, regardless of surface coverage. Similarly, water release was significantly larger for KCl than LiCl. However, the observed endothermic heats in the presence of NaCl are consistently equal to or greater than those obtained in the presence of KCl. This aspect of our data cannot be explained through water release alone. Still, since the trends for the heats of adsorption correspond to the water release trends in some cases, it can be concluded that surface dehydration affects the observed positive enthalpy to some degree. Surface dehydration is clearly not the only effect contributing to the observed endothermic heats of adsorption, however.

Another possible source derives from repulsive interactions. Figure 6-2 shows that the endothermic heat of adsorption is much larger in the absence of salt than in the presence of salt. Furthermore, the endothermic heats increase in the absence of salt as the surface coverage increases. Because the heats of adsorption

decrease significantly in the presence of salt and increase with increasing surface coverage in the absence of salt, it is likely that repulsive interactions significantly contribute to the endothermic heats. As the surface becomes crowded with adsorbed BSA molecules, the BSA molecules in solution repulsively interact with those molecules adsorbed on the surface. Therefore for the BSA molecules in solution to adsorb, they must overcome this repulsive interaction, which contributes to the overall endothermic heat of adsorption (Thrash and Pinto, 2002; Müller *et al.*, 2001).

It has been reported that repulsive interactions decrease with increasing ionic strength, and that bivalent cations are more effective in reducing repulsive interactions than monovalent cations (Larsericsdotter *et al.*, 2001). Generally, the salt ions shield the adsorbed molecules from the molecules in solution, thus minimizing the repulsive interactions between them. It is believed that bivalent cations are more effective than monovalent cations at screening repulsive interactions because of their increased surface charge density, which results in a larger hydrated radius.

For the cations used in this study, the relative sizes of the hydrated radii are as follows: $Li^+ > Na^+ > K^+$ (Hearn *et al.*, 1988). It is generally believed that the cation with the largest hydrated radius screens repulsive interactions most effectively. For all surface coverages, larger endothermic peaks were observed at 0.1 M KCl than at 0.1 M LiCl. Accordingly, it appears that Li^+ screens the repulsive interactions between adsorbed molecules and molecules in solution more effectively, as expected. Because the magnitudes of the endothermic heats are significantly different for 0.0 M salt, 0.1 M KCl, and 0.1 M LiCl, the effect of repulsive interactions appears to be substantial.

Although water release calculations and repulsive interactions describe most of the observed trends, they do not adequately describe observed endothermic heats obtained at 0.1 M NaCl. However, it is possible that the combination of these two effects, along with an endothermic contribution due to conformational changes, could cause heats of adsorption in NaCl to be larger than those in LiCl and KCl.

One trend in particular suggests that conformational changes may be significant at the high surface concentrations studied. For KCl and LiCl the heats of adsorption decrease as the surface coverage increases from 30 mg/g to about 50 mg/g. If repulsive interactions were solely responsible for the observed endothermic heats, it would be expected that these heats would become more endothermic as the available surface decreases. Additionally, the heats of adsorption for 0.0 M salt and 0.1 M NaCl increase slightly as surface coverage increases. These conflicting trends can be interpreted in terms of the orientation of the adsorbed molecule.

According to Haynes and Norde, the conformation of adsorbed protein is at least partially dependent upon the amount of available adsorbent surface (Haynes and Norde, 1995). In the case of BSA, it may assume a spread-out orientation or may adsorb "end-on" (Thrash and Pinto, 2002). It is likely that at low surface concentration the protein assumes the first orientation, but as surface concentration increases it adopts the second. Accordingly, the non-linearity of our data indicates that the adsorbed orientation for BSA changes significantly between 33 mg/g and 50 mg/g in 0.1 M KCl, and between 30 mg/g and 43 mg/g in 0.1 M LiCl. It can be postulated that a similar transition occurs at a surface coverage greater than 50 mg/g in NaCl.

In addition, the changes in conformation that the adsorbed protein undergoes after adsorption may also account for larger heats of adsorption in NaCl solution than in KCl. It has been documented that changes in mobile phase conditions can contribute to the heat requirements for structural rearrangement of proteins on the surface (Lin *et al.*, 2001). In this study, it is possible that changing the cation in the mobile phase significantly affects protein conformation. Although conformational changes are typically considered to primarily contribute to an entropy change, it is possible that the conformational changes after adsorption are significant enough to contribute to a change in enthalpy through an endothermic heat effect (Haynes and Norde, 1995; Bowen and Hughes, 1993).

Since the net heat of adsorption observed in all cases is endothermic, the ion-exchange adsorption process must be entropically driven. Through preferential interaction analysis, Thrash and Pinto (2002) demonstrated that the release of water could be a significant contributor to the entropic driving force. In addition, several research groups have demonstrated that the increase in entropy associated with conformational changes of adsorbed BSA contributes to an increase in the overall entropy of the system (Norde and Giacomelli, 2000; Esquibel-King *et al.*, 1999). It can therefore be presumed that, for this system, the increase in the enthalpy change of adsorption is due to a combination of surface dehydration, repulsive interactions, and conformational changes that are overcome by the increase in entropy resulting from water release and conformational changes.

6.3 Summary

Heats of adsorption measured through flow microcalorimetry for BSA on PEI–1000–10 are endothermic for 0.0 M salt and 0.1 M LiCl, NaCl, and KCl. The source of these endothermic heats derives from a combination of surface dehydration, repulsive interactions between adsorbed molecules and molecules in solution, and changes in adsorbed protein orientation and conformation. This statement is supported by several observations. First, heats of adsorption for two of the three salts studied correspond to water release trends obtained through preferential interaction analysis. Second, heats of adsorption are greatest in the absence of salt and decrease in the presence of salt, indicating that repulsive interactions are significant. And finally, heats of adsorption decrease with increasing surface coverage for some salts, indicating that adsorbed orientation and conformational changes may contribute to the observed endothermic heats of adsorption.

One of the primary purposes of this study was to correlate endothermic heat of adsorption data collected through flow microcalorimetry with pertinent data obtained through preferential interaction analysis. Combining these two methods provides insight into sources of endothermic enthalpic events and positive entropic contributions to the overall change in Gibb's free energy. Analyzing these data in conjunction proved useful not only for the BSA/PEI–1000–10 system, but also for the homo-deoxyoligonucleotide/Sepharose CL–6B system.

7. Conclusions and Recommendations for Future Work

7.1 Conclusions

Heat of adsorption data analyzed in combination with water release data calculated through preferential interaction analysis provides a means for uncovering thermodynamic driving forces for adsorption of biomolecules onto chromatographic supports. Preferential interaction analysis specifically determines the amount of water released during adsorption, which makes it particularly useful when endothermic heats of adsorption are detected, as was generally the case in this study. Furthermore, preferential interaction analysis requires chromatographic retention times and, in its general form, can be used for both ion exchange and hydrophobic interaction chromatography. For these reasons, water release data calculated from the preferential interaction model is best utilized in conjunction with heats of adsorption obtained through flow microcalorimetry, which mimics the conditions in a chromatographic column.

Heats of adsorption for the nitrogen bases adenine and thymine and for the nucleoside thymidine on Sepharose CL–6B were endothermic. However, heats of adsorption for 2'-deoxyadenosine were exothermic, indicating that another effect besides adsorption to the adsorbent was significant.

It was determined that enthalpy changes associated with base stacking self-interactions contribute considerably to the observed heats of adsorption. It appears that the magnitude of the base stacking contribution to the observed heat of adsorption depends on the biomolecule's relative affinities for binding to the adsorbent and self-interacting. Accordingly, the base stacking heats contribute most significantly to the observed heats of adsorption for the molecule with the highest association constant, in

this case 2'-deoxyadenosine. However, data for the other three compounds studied suggest that self-interactions cannot be overlooked for any nitrogen base or nucleoside.

Endothermic heats of adsorption were observed for all four homo-deoxyoligonucleotides studied. The results indicate that these biomolecules likely adsorb "end-on," and that the increase in retention factor with increasing ammonium sulfate concentration derives from an increase in the entropic contribution to the overall change in Gibb's free energy. For poly(T) 6mer, poly(A) 6mer, and poly(T) 30mer, the observed peaks were Gaussian in shape, indicating that the hydrophobic effect alone predominated. However, the poly(A) 30mer peaks were not Gaussian, and the heats of adsorption were much larger than for the other three homo-deoxyoligonucleotides studied. This large endothermic enthalpic contribution stems from a combination of hydrophobic interactions and repulsion between charged phosphate groups and the hydrophobic surface, since the charge spacing for poly(A) 30mer is the smallest of any of the oligonucleotides studied. Water release data obtained through preferential interaction analysis further supported these conclusions.

In general, it appears that the predominant effect in the adsorption of homo-deoxyoligonucleotides poly(A) and poly(T) onto Sepharose CL–6B is hydrophobic interaction. However, structural features of each individual oligonucleotide can influence the adsorption thermodynamics and thus the retention behavior of these biomolecules. At this time, the understanding of oligonucleotide structure and conformation in aqueous solution is limited. Because of the pharmaceutical relevance of these biomolecules, an understanding of these structures will begin to be elucidated in the coming years.

One particularly daunting task in oligonucleotide purification is to uncover successful methods of purifying synthetic oligonucleotides whose main impurities include (n-1) and other deletion sequences. The results of this study indicate that HIC is probably not a viable process for this type of purification, since it appears that these biomolecules adsorb "end-on" to hydrophobic adsorbents. Thus, small changes in molecular hydrophobicity would not appreciably influence retention behavior. However, HIC has already proven successful in the purification of biological mixtures and future researchers should explore further applications of this kind.

Through analysis of calorimetric data and water release calculations, it was determined that adsorption of the protein BSA onto PEI–1000–10 is entropically driven. Endothermic heats of adsorption were obtained in the absence of salt and in 0.1 M KCl, LiCl, and NaCl. Sources of the positive entropy term are likely conformational changes of the protein and surface dehydration. The endothermic heats of adsorption detected through FMC probably derive from a combination of repulsive interactions, water release, and reorientation/conformational changes.

7.2 Recommendations for Future Work

1. It would be useful to gather additional data for poly(A) 30mer in order to observe the changes in the endothermic heat of adsorption with changing ammonium sulfate concentration. Although the oligonucleotides utilized in this study were purchased and used without further purification, in future studies it would be advisable to purify the poly(A) 30mer before gathering FMC data in light of the difficulties we had in obtaining reproducible results.

2. Heat of adsorption data for poly(T) at base lengths of 6 and 30 clearly demonstrate that the heat of adsorption does not correlate linearly with the base length/hydrophobicity. With additional heat of adsorption data at other base lengths, i.e. 10, 15, 20, and 25, the relationship between heat of adsorption and base length/hydrophobicity could be established. It would be advisable to collect these data at a relatively high temperature, i.e. 30–35° C, to ensure that the secondary structure of the poly(T) homo-deoxyoligonucleotide does not significantly affect the heat of adsorption.
3. While studying homo-deoxyoligonucleotides is useful in that it minimizes the experimental variables, heterogeneous oligonucleotides are the realistic candidates for anti-sense drugs. Accordingly, it would be useful to relate the results for the 6mers of this study to FMC data collected for the following deoxyoligonucleotides:
    a. 5' AAA TTT 3'
    b. 5' ATA TAT 3'
    c. 5' AAT TAA 3'
    d. 5' TTA ATT 3'

    Future researchers could further extend this to oligonucleotides containing all four bases.
4. It has been postulated in this thesis that charge spacing of oligonucleotides affects adsorption thermodynamics and therefore retention behavior. Kontturi and coauthors (2002) reported charge spacing data for four oligonucleotides at two different temperatures. It would be useful to collect retention data and flow

microcalorimetry data for the same four oligonucleotides studied by Kontturi and coworkers in order to determine the relationship between charge spacing, adsorption thermodynamics, and HIC retention behavior.

BIBLIOGRAPHY

S. Agrawal, R.P. Iyer, *Current Opinion in Biotechnology*. (1995) 12–19.

T. Arakawa, *Archives of Biochemistry and Biophysics*. 248 (1986) 101–105.

T. Arakawa, S.N. Timasheff, *Biochemistry*. 23 (1984) 5912–5923.

T. Arakawa, S.N. Timasheff, *Biochemistry*. 21 (1982) 6545–6552.

C.F. Bennett, *Biochemical Pharmacology*. (1998) 9–19.

V.A. Bloomfield, D.M. Crothers, I.Tinoco, Jr., *Physical Chemistry of Nucleic Acids*, Harper and Row, New York, 1974.

W.R. Bowen, D.T. Hughes, *Journal of Colloid and Interface Science*. 158 (1993) 395–402.

A.D. Broom, M.P. Schweizer, P.O.P. Ts'o, *Journal of the American Chemical Society*. 89 (1967) 3612–3622.

P.R. Brown, E. Grushka, *Analytical Chemistry*. 52 (1980) 1210–1215.

S. Budavari, M.J. O'Neil, A. Smith, P.E. Heckelman, ed., *The Merck Index: an Encyclopedia of Chemicals, Drugs, and Biologicals*, Merck & Co., Inc., Rahway, New Jersey, 1989.

C.E. Bugg. "Solid-State Stacking Patterns of Purine Bases." *The Jerusalem Symposia on Quantum Chemistry and Biochemistry*, E.D. Bergmann and B. Pullman, ed. Israel Academy of Sciences and Humanities, Jerusalem (1972).

S.I. Chan, M.P. Schweizer, P.O.P Ts'o, G.K. Helmkamp, *Journal of the American Chemical Society*. 86 (1964) 4182–4188.

J.R. Conder, B.O. Hayek, *Biochemical Engineering Journal 6*. (2000) 225–232.

R.R. Deshmukh, T.N. Warner, F. Hutchison, M. Murphy, W.E. Leitch, P.De Leon, G.S. Srivasta, D.L. Cole, Y.S. Sanghvi, *Journal of Chromatography A*. (2000) 179–192.

R.R. Deshmukh, W.E. Leitch, D.L. Cole, *Journal of Chromatography A*. (1998) 77–92.

M.M. Diogo, J.A. Queiroz, G.A. Monteiro, S.A.M. Martins, G.N.M. Ferreira, D.M.F. Prazares, *Biotechnology and Bioengineering*. (2000) 576–583.

M.M. Diogo, J.A. Queiroz, N.G. Pinto, D.M.F. Prazeres, *Journal of Chromatography A*. In publication (2003).

M.M. Diogo, J.A. Queiroz, D.M.F. Prazares, *Journal of Chromatography A*. (2002) 119–128.

J. Duchesne, ed., *Physico-chemical Properties of Nucleic Acids*, Vol. 2–3, Academic Press Inc., London, 1973.

M.A. Esquibel-King, A.C. Dias-Cabral, J.A. Queiroz, N.G. Pinto, *Journal of Chromatography A*. 865 (1999) 111–122.

E.L. Farquhar, M. Downing, S.J. Gill, *Biochemistry*. 7 (1968) 1224–1225.

G. Felsenfeld, H.T. Miles, *Annual Review of Biochemistry*. 36 (1967) 407–491.

G-L. Friedli. *Protein Structure.* http://www.cmbi.kun.nl/gvteach/alg/infopages/proteins.shtml. Gert Vriend, 2000.

M. Gilar, E.S.P. Bouvier, *Journal of Chromatography A*. 890 (2000) 167–177.

S.J. Gill, M. Downing, G.F. Sheats, *Biochemistry*. 6 (1967) 272–276.

S.J. Gill, D.B. Martin, M. Downing, *Journal of the American Chemical Society*. 85 (1963) 706–708.

K.M. Gooding, F.E. Regnier, ed., *HPLC of Biological Macromolecules: Methods and Applications*, Marcel Dekker, Inc., New York, 1990.

G. Guiochon, S.G. Shirazi, A.M. Katti, *Fundamentals of Preparative and Nonlinear Chromatography*, Academic Press, Boston, 1994.

J-H. Ha, M.W. Capp, M.D. Hohenwalter, M. Baskerville, M.T. Record, *Journal of Molecular Biology*. 228 (1992) 252–264.

D. Haidacher, A. Vailaya, C. Horvath, *Proceedings of the National Academy of Science USA*. (1996) 2290–2295.

C.A. Haynes, W. Norde, *Journal of Colloid and Interface Science*. (1995) 313–328.

M.T. Hearn, A.N. Hodder, M.I. Aguilar, *Journal of Chromatography*. 443 (1988) 97–118.

H. Husi, M.D. Walkinshaw, *Journal of Chromatography B*. (2001) 367–371.

S. Ikuta, R. Chattopadhyaya, R.E. Dickerson, *Analytical Chemistry*. (1984) 2256–2257.

G. Karlsson, S. Winge, *Protein Expression and Purification.* (2001) 149–155.

J. Kim, P.S. Cremer, *Chemphyschem.* (2001) 543–546.

I.M. Klotz, *Ligand–Receptor Energetics: A Guide for the Perplexed*, John Wiley & Sons, Chichester, 1997.

A.K. Kontturi, K.Kontturi, A. Urtti, *European Journal of Pharmaceutical Sciences.* 15 (2002) 379–385.

J.E. Ladbury, B.Z. Chowdry, ed., *Biocalorimetry: Applications of Calorimetry in the Biological Sciences*, John Wiley & Sons, Chichester, 1998.

M.R. Ladisch, *Bioseparations Engineering: Principles, Practice, and Economics*, John Wiley & Sons, New York, 2001.

H. Larsericsdotter, S. Oscarsson, J. Buijs, *Journal of Colloid and Interface Sciences.* 237 (2001) 98–103.

D.P. Lee, J.H. Kindsvater, *Analytical Chemistry.* (1980) 2425–2428.

N.B. Leontis, J. SantaLucia, Jr., ed., *Molecular Modeling of Nucleic Acids*, American Chemical Society, Washington, D.C., 1998.

F.Y. Lin, C-S. Chen, W.Y. Chen, S. Yamamoto, *Journal of Chromatography A.* 912 (2001) 281–289.

F.Y. Lin, W.Y. Chen, M.T.W. Hearn, *Analytical Chemistry.* (2001) 3875–3883.

F.Y. Lin, W.Y. Chen, M.T.W. Hearn, *Journal of Molecular Recognition.* 15 (2002) 55–93.

F.Y. Lin, W.Y. Chen, R.C. Ruaan, H.M. Huang, *Journal of Chromatography A.* (2000) 37–47.

M. Malmsten, *Journal of Colloid and Interface Science.* 207 (1998) 186–199.

C.K. Mathews, K.E. van Holde, *Biochemistry*, Benjamin/Cummings Publishing Company, Inc., Redwood City, CA, 1990.

W.R. Melander, C. Horvath, *Archives of Biochemistry and Biophysics.* (1977) 200–215.

W.R. Melander, D. Corrandini, C. Horvath, *Journal of Chromatography.* (1984) 67–85.

W.R. Melander, Z. El Rassi, C. Horvath, *Journal of Chromatography*. (1989) 3–27.

Microscal Flow Adsorption Microcalorimetery. http://www.microscal.com/fmc. Microscal Limited, 2001.

M. Müller, T. Rieser, P.L. Dubin, K. Lunkwitz, *Macromolecular Rapid Communications*. 22 (2001) 390–395.

National Human Genome Research Institute, Division of Intramural Research. *Ribonucleic Acid (RNA)*. http://www.accessexcellence.org/AB/GG/nhgri_PDFs/rna2.pdf. Access Excellence@The National Health Museum, 2003.

S. Neidle, ed., *Oxford Handbook of Nucleic Acid Structure*, Oxford University Press, New York, 1999.

S. Neidle, ed., *DNA Structure and Recognition*, IRL Press at Oxford University Press, New York, 1994.

W. Norde, C.E. Giacomelli, *Journal of Biotechnology*. 79 (2000) 259–268.

W. Norde. "Driving Forces for Protein Adsorption at Solid Surfaces." *Biopolymers at Interfaces*, M. Malmsten, ed., Marcel Dekker Inc., New York (1998).

R.W.A. Oliver, ed., *HPLC of Macromolecules: A Practical Approach*, IRL Press at Oxford University Press, New York, 1989.

R.W.A. Oliver ed., *HPLC of Macromolecules: A Practical Approach, Second Edition*, IRL Press at Oxford University Press, New York, 1998.

T.W. Perkins, D.S. Mak, T.W. Root, E.N. Lightfoot, *Journal of Chromatography A*. (1997) 1–14.

O. Pitiot, L. Folley, M.A. Vijayalakshmi, *Journal of Chromatography B*. (2001) 163–172.

O. Pitiot, E. Nedonchelle, C. Legallais, M.A. Vijayalakshmi, *Journal of Chromatography B*. (2001) 173–182.

B. Pullman, ed., *Molecular Associations in Biology*, Academic Press Inc., New York, 1968.

J.A. Queiroz, C.T. Tomaz, J.M.S. Cabral, *Journal of Biotechnology*. 87 (2001) 143–159.

J.A. Queiroz, F.A.P. Garcia, J.M.S. Cabral, *Journal of Chromatography A*. (1995) 137–142

P. Raje. *Effect of Heat of Adsorption on Modeling Preparative Protein Chromatography.* Master's Thesis, University of Cincinnati, Cincinnati, OH, 1997.

P.Raje, N.G. Pinto, *Journal of Chromatography A.* (1998) 141–156.

P.Raje, N.G. Pinto, *Journal of Chromatography A.* (1997) 89–103.

M.T. Record, Jr., C.F. Anderson, *Biophysical Journal.* 68 (1995) 786–794.

P. Ritter. *Biochemistry: A Foundation.* Brooks/Cole Publishing Company, Pacific Grove, CA, 1996.

D.R. Robinson, M.E. Grant, *Journal of Biological Chemistry.* 241 (1966) 4030–4042.

P. Russell. *Nucleotide Chemical Structure.* http://dlab.reed.edu/projects/vgm/vgm/VGMProjectFolder/VGM/RED/RED.ISG/chem1.html. Peregrine Publishers, Inc., 1997.

W. Saenger, *Principles of Nucleic Acid Structure*, Springer-Verlag, New York, 1984.

M.P. Schweizer, S.I. Chan, P.O.P. Ts'o, *Journal of the American Chemical Society.* 87 (1965) 5241–5247.

H.A. Scoble. "Structures, Properties, and Chromatographic Behavior of Nucleic Acid Constituents." *HPLC in Nucleic Acid Research*, P.R. Brown, ed. Marcel Dekker, Inc., New York (1984).

J.E. Seely, C.W. Richey, *Journal of Chromatography A.* (2001) 235–241.

S.R. Shepard, R.Boucher, J. Johnston, R. Boerner, G. Koch, J.W. Madsen, D.Grella, B.K.L. Sim, J.F. Schrimsher, *Protein Expression and Purification.* (2000) 216–227.

R.R. Sinden, *DNA Structure and Function*, Academic Press Inc., New York, 1994.

T.N. Solie, J.A. Schellman, *Journal of Molecular Biology.* 33 (1968) 61–77.

M.E. Thrash, J.M. Phillips, N.G. Pinto, *Journal of Chromatography A.* In Publication (2003).

M.E. Thrash, N.G. Pinto, *Journal of Chromatography A.* 944 (2002) 61–68.

M.E. Thrash, N.G. Pinto, *Journal of Chromatography A.* 908 (2001) 293–299.

M.E. Thrash, N.G. Pinto. "Proteins and Peptides Purification in Pharmaceuticals Analysis." *Encyclopedia of Analytical Chemistry*, R.A. Meyers, ed. John Wiley & Sons Ltd, Chichester (2000).

C.T. Tomaz, D.Duarte, J.A. Queiroz, *Journal of Chromatography A.* (2002) 211–216.

L.B. Townsend, *Chemistry of Nucleosides and Nucleotides*, Vol. 2, Plenum Press, New York, 1991.

Y.S. Tsai, F.Y Lin, W.Y. Chen, C.C. Lin, *Colloids and Surfaces.* (2002) 111–118.

P.O.P. Ts'o, ed., *Basic Principles in Nucleic Acid Chemistry*, Vol. 1, Academic Press, Inc., New York, 1974.

P.O.P. Ts'o, S.I. Chan, *Journal of the American Chemical Society.* 86 (1964) 4176–4181.

P.O.P. Ts'o, N.S. Kondo, R.K. Robins, A.D. Broom, *Journal of the American Chemical Society.* 91 (1969) 5625–5631.

P.O.P. Ts'o, I.S. Melvin, A.C. Olsen, *Journal of the American Chemical Society.* 85 (1963) 1289–1296.

N. Tugcu, R.R. Deshmukh, Y.S. Sanghvi, S.M. Cramer, *Reactive and Functional Polymers.* 54 (2003) 37–47.

N. Tugcu, R.R. Deshmukh, Y.S. Sanghvi, J.A. Moore, S.M Cramer, *Journal of Chromatography A.* (2001) 65–73.

R.B. van Breemen, Y.Tan, J. Lai, C.R. Huang, X. Zhao, *Journal of Chromatography A.* (1998) 67–76.

V.L. Vilker, C.K. Colton, K.A. Smith, *Journal of Colloid and Interface Science.* 79 (1981) 548–566.

P.B. Welzel, *Thermochimica Acta.* 382 (2002) 175–188.

J.B. Wheatley, D.E Schmidt, *Journal of Chromatography A.* (1999) 1–12.

S-L. Wu, K. Benedek, B.L. Karger, *Journal of Chromatography.* 359 (1986) 3–27.

S-L. Wu, A. Figueroa, B.L. Karger, *Journal of Chromatography.* 371 (1986) 3–27.

Appendix A

Appendix A–1: Sample Calculations for Thymine Adsorption to and Desorption from Sepharose CL–6B

Conditions:

Biomolecule:	Thymine
Molecular Weight:	126.1 *g/mol*
Solution:	2.0 M ammonium sulfate, pH = 8.0
Temperature:	26.9° C
Loop Volume:	0.52 *mL*
Flow rate:	1.65 *mL/hr*

Calibration Curve Equation (UV Spectrophotometer at 264 nm):

$y = 58.036x + 0.0021$
y = UV absorbance value
x = Concentration (*mg/mL*)

Heat Calibration Value: $\frac{9mJ}{19.735boxes} = 0.456\frac{mJ}{box}$

Conversion Factor (to convert *mJ/mg* to *kcal/mol*):

$$\left(\frac{1cal}{4.18J}\right)\left(\frac{1J}{1000mJ}\right)\left(\frac{1kcal}{1000cal}\right)\left(\frac{1000mg}{1g}\right)\left(\frac{126.1g}{1mol}\right) = 0.030167\frac{kcal \cdot mg}{mJ \cdot mol}$$

UV Measurements:

Prepared Solution: Dilution ratio→30
Absorbance values: 0.598
0.598
0.601

Effluent: Dilution ration→10
Effluent Volume→1.95 mL
Absorbance values: 0.483
0.490
0.484

Calculating the Amount Injected:

Average of the UV absorbance values: $\frac{0.598+0.598+0.601}{3}=0.599$

Inserting the average UV absorbance value into the calibration curve equation:

$$\frac{0.599-0.0021}{58.036}=0.0096\frac{mg}{mL}$$

Multiplying this concentration by the dilution factor: $0.0096\times 30=0.29\frac{mg}{mL}$

Multiplying the solution concentration by the sample volume:

$$0.29\frac{mg}{mL}\times 0.52mL=0.151mg$$

Amount injected: 0.151 *mg*

Calculating the Amount Recovered:

Average of the UV absorbance values: $\frac{0.483+0.490+0.484}{3}=0.486$

Inserting the average UV absorbance value into the calibration curve equation:

$$\frac{0.486-0.0021}{58.036}=0.0080\frac{mg}{mL}$$

Multiplying this concentration by the dilution factor: $0.0080\times 10=0.080\frac{mg}{mL}$

Multiplying the solution concentration by the effluent volume:

$$0.080\frac{mg}{mL}\times 1.95mL=0.156mg$$

Amount recovered: 0.156 *mg*

Notice that the amount recovered is within 5% of the amount injected. Therefore, heats of adsorption and heats of desorption were calculated using the amount injected.

Calculating the Heat of Adsorption and the Heat of Desorption:

A strip chart recorder was used to obtain the original thermograms. Example peaks shown in Chapters 4, 5, and 6 are reproductions rendered using Microsoft Word. Gridlines used to reproduce the peaks in these drawings represented the original gridlines

on the strip chart recorder paper. However, for aesthetic purposed these gridlines were deleted from the peaks shown in the body of the thesis.

The same example peak shown in Figure 4-1 is shown with gridlines in Figure A-1-1. Peaks were integrated by counting the number of boxes included in each peak. The base of each peak is represented by a gray line. The number of boxes was used to calculate heat of adsorption and heat of desorption values, as shown below.

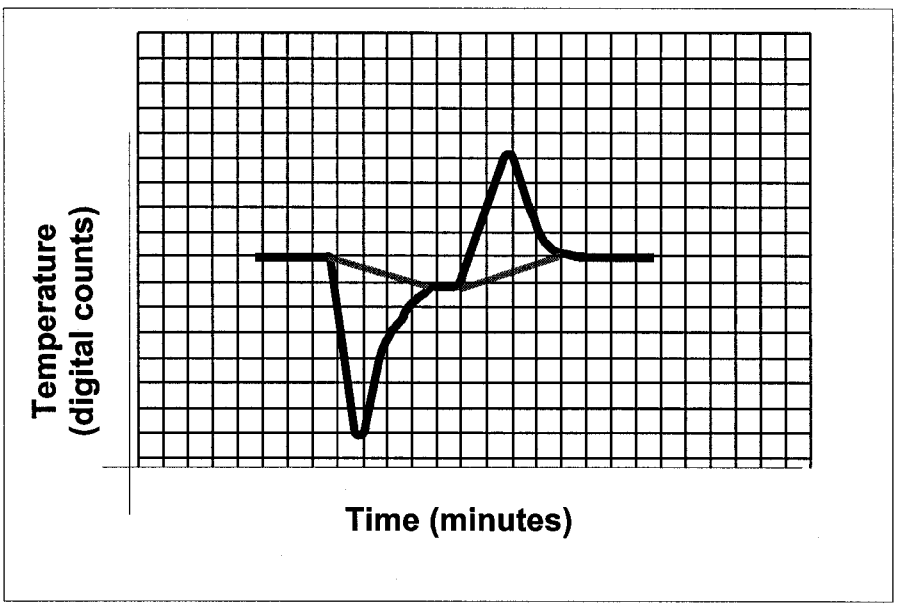

Figure A-1-1. Example of a thermogram drawing including gridlines. The original peaks were obtained on strip chart recorder paper, which included gridlines. This peak is a reproduction rendered using Microsoft Word, and is the same example peak shown in Figure 4-1. (Conditions: flow rate, 1.65 mL/hr; sample, 0.25 mg/mL thymine in 2.0 M ammonium sulfate; pH, 8.0; temperature, 26.9° C.) Peaks are integrated by counting the number of boxes in each peak, with the gray lines indicating the base of each peak.

Calculating the Heat of Adsorption (see Figures 4-1 and A-1-1):

Number of boxes in heat signal: 10.35 *boxes*

Calculating the heat and converting to *kcal/mol*:

$$\frac{0.456\frac{mJ}{box}\times 10.35 boxes\times 0.030167\frac{kcal\cdot mg}{mJ\cdot mol}}{0.151 mg}=0.943\frac{kcal}{mol}$$

Calculating the Heat of Desorption(see Figures 4-1 and A-1-1):

Number of boxes in heat signal: -9.5 *boxes*

Calculating the heat and converting to *kcal/mol*:

$$\frac{0.456\frac{mJ}{box}\times -9.5 boxes\times 0.030167\frac{kcal\cdot mg}{mJ\cdot mol}}{0.151 mg}=-0.865\frac{kcal}{mol}$$

Appendix A

Appendix A–2: Sample Calculations for Thymidine Adsorption to and Desorption from Sepharose CL–6B

Conditions:

Biomolecule:	Thymidine
Molecular Weight:	242.2 *g/mol*
Solution:	1.5 M ammonium sulfate, pH = 8.0
Temperature:	26.2° C
Loop Volume:	0.52 *mL*
Flow rate:	1.65 *mL/hr*

Calibration Curve Equation (UV Spectrophotometer at 264 nm):

$y = 41.488x + 0.0034$
y = UV absorbance value
x = Concentration (*mg/mL*)

Heat Calibration Value: $\frac{9mJ}{19.735boxes} = 0.456\frac{mJ}{box}$

Conversion Factor (to convert *mJ/mg* to *kcal/mol*):

$$\left(\frac{1cal}{4.18J}\right)\left(\frac{1J}{1000mJ}\right)\left(\frac{1kcal}{1000cal}\right)\left(\frac{1000mg}{1g}\right)\left(\frac{242.2g}{1mol}\right) = 0.057943\frac{kcal \cdot mg}{mJ \cdot mol}$$

UV Measurements:

Prepared Solution: Dilution ratio→100
Absorbance values: 0.809
0.806
0.802

Effluent: Dilution ration→30
Effluent Volume→1.95 mL
Absorbance values: 0.711
0.712
0.710

Calculating the Amount Injected:

Average of the UV absorbance values: $\frac{0.809+0.806+0.802}{3}=0.806$

Inserting the average UV absorbance value into the calibration curve equation:

$$\frac{0.806-0.0034}{41.488}=0.0193\frac{mg}{mL}$$

Multiplying this concentration by the dilution factor: $0.0193\times 100=1.93\frac{mg}{mL}$

Multiplying the solution concentration by the sample volume:

$$1.93\frac{mg}{mL}\times 0.52mL=1.00mg$$

Amount injected: 1.00 *mg*

Calculating the Amount Recovered:

Average of the UV absorbance values: $\frac{0.711+0.712+0.710}{3}=0.711$

Inserting the average UV absorbance value into the calibration curve equation:

$$\frac{0.711-0.0034}{41.488}=0.0171\frac{mg}{mL}$$

Multiplying this concentration by the dilution factor: $0.0171\times 30=0.513\frac{mg}{mL}$

Multiplying the solution concentration by the effluent volume:

$$0.513\frac{mg}{mL}\times 1.95mL=1.00mg$$

Amount recovered: 1.00 *mg*

Notice that the amount recovered is within 5% of the amount injected. Therefore, heats of adsorption and heats of desorption were calculated using the amount injected.

Calculating the Heat of Adsorption (see Figure 4-2):

Number of boxes in heat signal: 5.7 *boxes*

Calculating the heat and converting to *kcal/mol*:

$$\frac{0.456\frac{mJ}{box}\times 5.7boxes\times 0.057943\frac{kcal\cdot mg}{mJ\cdot mol}}{1.00mg}=0.151\frac{kcal}{mol}$$

Calculating the Heat of Desorption (see Figure 4-2):

Number of boxes in heat signal: -5.1 *boxes*

Calculating the heat and converting to *kcal/mol*:

$$\frac{0.456\frac{mJ}{box}\times -5.1 boxes\times 0.057943\frac{kcal\cdot mg}{mJ\cdot mol}}{1.00mg}=-0.135\frac{kcal}{mol}$$

Appendix A

Appendix A–3: Sample Calculations for Adenine Adsorption to and Desorption from Sepharose CL–6B

Conditions:

Biomolecule:	Adenine
Molecular Weight:	135.1 *g/mol*
Solution:	1.7 M ammonium sulfate, pH = 8.0
Temperature:	26.7° C
Loop Volume:	0.52 *mL*
Flow rate:	1.65 *mL/hr*

Calibration Curve Equation (UV Spectrophotometer at 254 nm):

$y = 89.14x + 0.0029$
y = UV absorbance value
x = Concentration (*mg/mL*)

Heat Calibration Value: $\frac{9mJ}{19.735boxes} = 0.456\frac{mJ}{box}$

Conversion Factor (to convert *mJ/mg* to *kcal/mol*):

$$\left(\frac{1cal}{4.18J}\right)\left(\frac{1J}{1000mJ}\right)\left(\frac{1kcal}{1000cal}\right)\left(\frac{1000mg}{1g}\right)\left(\frac{135.1g}{1mol}\right) = 0.032321\frac{kcal \cdot mg}{mJ \cdot mol}$$

UV Measurements:

Prepared Solution: Dilution ratio→30
Absorbance values: 0.740
0.745
0.748

Effluent: Dilution ration→10
Effluent Volume→2.0 mL
Absorbance values: 0.586
0.597
0.595

Calculating the Amount Injected:

Average of the UV absorbance values: $\frac{0.740+0.745+0.748}{3}=0.744$

Inserting the average UV absorbance value into the calibration curve equation:

$$\frac{0.744-0.0029}{89.14}=0.00831\frac{mg}{mL}$$

Multiplying this concentration by the dilution factor: $0.00831\times 30=0.249\frac{mg}{mL}$

Multiplying the solution concentration by the sample volume:

$$0.249\frac{mg}{mL}\times 0.52mL=0.129mg$$

Amount injected: 0.129 *mg*

Calculating the Amount Recovered:

Average of the UV absorbance values: $\frac{0.586+0.597+0.595}{3}=0.593$

Inserting the average UV absorbance value into the calibration curve equation:

$$\frac{0.593-0.0029}{89.14}=0.00662\frac{mg}{mL}$$

Multiplying this concentration by the dilution factor: $0.00662\times 10=0.0662\frac{mg}{mL}$

Multiplying the solution concentration by the effluent volume:

$$0.0662\frac{mg}{mL}\times 2.0mL=0.132mg$$

Amount recovered: 0.132 *mg*

Notice that the amount recovered is within 5% of the amount injected. Therefore, heats of adsorption and heats of desorption were calculated using the amount injected.

Calculating the Heat of Adsorption (see Figure 4-7):

Number of boxes in heat signal: 6.15 *boxes*

Calculating the heat and converting to *kcal/mol*:

$$\frac{0.456\frac{mJ}{box}\times 6.15boxes\times 0.032321\frac{kcal\cdot mg}{mJ\cdot mol}}{0.129mg}=0.703\frac{kcal}{mol}$$

Calculating the Heat of Desorption (see Figure 4-7):

Number of boxes in heat signal: -5.6 *boxes*

Calculating the heat and converting to *kcal/mol*:

$$\frac{0.456\frac{mJ}{box}\times -5.6 boxes\times 0.032321\frac{kcal\cdot mg}{mJ\cdot mol}}{0.129mg}=-0.640\frac{kcal}{mol}$$

Appendix A

Appendix A–4: Sample Calculations for 2'-deoxyadenosine Adsorption to and Desorption from Sepharose CL–6B

Conditions:

Biomolecule:	2'-deoxyadenosine
Molecular Weight:	251.2 *g/mol*
Solution:	1.5 M ammonium sulfate, pH = 8.0
Temperature:	26.2° C
Loop Volume:	0.52 *mL*
Flow rate:	1.65 *mL/hr*

Calibration Curve Equation (UV Spectrophotometer at 254 nm):

$y = 49.925x + 0.0061$
y = UV absorbance value
x = Concentration (*mg/mL*)

Heat Calibration Value: $\frac{9mJ}{19.735boxes} = 0.456\frac{mJ}{box}$

Conversion Factor (to convert *mJ/mg* to *kcal/mol*):

$$\left(\frac{1cal}{4.18J}\right)\left(\frac{1J}{1000mJ}\right)\left(\frac{1kcal}{1000cal}\right)\left(\frac{1000mg}{1g}\right)\left(\frac{251.2g}{1mol}\right) = 0.060096\frac{kcal \cdot mg}{mJ \cdot mol}$$

UV Measurements:

Prepared Solution: Dilution ratio→100
Absorbance values: 1.123
1.136
1.137

Effluent: Dilution ration→30
Effluent Volume→2.15 mL
Absorbance values: 0.916
0.919
0.915

Calculating the Amount Injected:

Average of the UV absorbance values: $\frac{1.123+1.136+1.137}{3}=1.132$

Inserting the average UV absorbance value into the calibration curve equation:

$$\frac{1.132-0.0061}{49.925}=0.0226\frac{mg}{mL}$$

Multiplying this concentration by the dilution factor: $0.0226\times100=2.26\frac{mg}{mL}$

Multiplying the solution concentration by the sample volume:

$$2.26\frac{mg}{mL}\times0.52mL=1.18mg$$

Amount injected: 1.18 *mg*

Calculating the Amount Recovered:

Average of the UV absorbance values: $\frac{0.916+0.919+0.915}{3}=0.917$

Inserting the average UV absorbance value into the calibration curve equation:

$$\frac{0.917-0.0061}{49.925}=0.0182\frac{mg}{mL}$$

Multiplying this concentration by the dilution factor: $0.0182\times30=0.546\frac{mg}{mL}$

Multiplying the solution concentration by the effluent volume:

$$0.546\frac{mg}{mL}\times2.15mL=1.17mg$$

Amount recovered: 1.17 *mg*

Notice that the amount recovered is within 5% of the amount injected. Therefore, heats of adsorption and heats of desorption were calculated using the amount injected.

Calculating the Heat of Adsorption (see Figure 4-10):

Number of boxes in heat signal: -13.8 *boxes*

Calculating the heat and converting to *kcal/mol*:

$$\frac{0.456\frac{mJ}{box}\times-13.8boxes\times0.060096\frac{kcal\cdot mg}{mJ\cdot mol}}{1.18mg}=-0.320\frac{kcal}{mol}$$

Calculating the Heat of Desorption (see Figure 4-10):

Number of boxes in heat signal: 13.9 *boxes*

Calculating the heat and converting to *kcal/mol*:

$$\frac{0.456\frac{mJ}{box}\times 13.9 boxes\times 0.060096\frac{kcal\cdot mg}{mJ\cdot mol}}{1.18mg}=0.323\frac{kcal}{mol}$$

Appendix A

Appendix A–5: Sample Calculations for Poly(T) 6mer Adsorption to and Desorption from Sepharose CL–6B

Conditions:

Biomolecule:	Poly(T) 6mer
Molecular Weight:	1,763.2 *g/mol*
Solution:	1.0 M ammonium sulfate, pH = 8.0
Temperature:	26.1° C
Loop Volume:	0.52 *mL*
Flow rate:	1.65 *mL/hr*

Heat Calibration Value: $\frac{9mJ}{19.735boxes} = 0.456\frac{mJ}{box}$

Conversion Factor (to convert *mJ/mg* to *kcal/mol*):

$$\left(\frac{1cal}{4.18J}\right)\left(\frac{1J}{1000mJ}\right)\left(\frac{1kcal}{1000cal}\right)\left(\frac{1000mg}{1g}\right)\left(\frac{1{,}763.2g}{1mol}\right) = 0.421818\frac{kcal \cdot mg}{mJ \cdot mol}$$

Calculating the Amount Injected:

Dividing the mass of dry oligonucleotide by the volume of carrier fluid added:

$$\frac{4.6mg}{4.6mL} = 1.0\frac{mg}{mL}$$

Multiplying the solution concentration by the sample volume:

$$1.0\frac{mg}{mL} \times 0.52mL = 0.52mg$$

Amount injected: 0.52 *mg*

Calculating the Heat of Adsorption (see Figure 5-1):

Number of boxes in heat signal: 3.35 *boxes*

Calculating the heat and converting to *kcal/mol*:

$$\frac{0.456\frac{mJ}{box}\times 3.35 boxes\times 0.421818\frac{kcal\cdot mg}{mJ\cdot mol}}{0.52mg}=1.24\frac{kcal}{mol}$$

Calculating the Heat of Desorption (see Figure 5-1):

Number of boxes in heat signal: -4.6 *boxes*

Calculating the heat and converting to *kcal/mol*:

$$\frac{0.456\frac{mJ}{box}\times -4.6 boxes\times 0.421818\frac{kcal\cdot mg}{mJ\cdot mol}}{0.52mg}=-1.70\frac{kcal}{mol}$$

Appendix A

Appendix A–6: Sample Calculations for Poly(A) 6mer Adsorption to and Desorption from Sepharose CL–6B

Conditions:

Biomolecule:	Poly(A)
Molecular Weight:	1,817.3 *g/mol*
Solution:	1.0 M ammonium sulfate, pH = 8.0
Temperature:	25.9° C
Loop Volume:	0.52 *mL*
Flow rate:	1.65 *mL/hr*

Heat Calibration Value: $\frac{9mJ}{19.735boxes} = 0.456\frac{mJ}{box}$

Conversion Factor (to convert *mJ/mg* to *kcal/mol*):

$$\left(\frac{1cal}{4.18J}\right)\left(\frac{1J}{1000mJ}\right)\left(\frac{1kcal}{1000cal}\right)\left(\frac{1000mg}{1g}\right)\left(\frac{1{,}817.3g}{1mol}\right) = 0.434761\frac{kcal \cdot mg}{mJ \cdot mol}$$

Calculating the Amount Injected:

Dividing the mass of dry oligonucleotide by the volume of carrier fluid added:

$$\frac{4.6mg}{4.6mL} = 1.0\frac{mg}{mL}$$

Multiplying the solution concentration by the sample volume:

$$1.0\frac{mg}{mL} \times 0.52mL = 0.52mg$$

Amount injected: 0.52 *mg*

Calculating the Heat of Adsorption (see Figure 5-6) :

Number of boxes in heat signal: 3.6 *boxes*

Calculating the heat and converting to *kcal/mol*:

$$\frac{0.456\frac{mJ}{box}\times 3.6 boxes\times 0.434761\frac{kcal\cdot mg}{mJ\cdot mol}}{0.52mg}=1.37\frac{kcal}{mol}$$

Calculating the Heat of Desorption (see Figure 5-6):

Number of boxes in heat signal: -3.5 *boxes*

Calculating the heat and converting to *kcal/mol*:

$$\frac{0.456\frac{mJ}{box}\times -3.5 boxes\times 0.434761\frac{kcal\cdot mg}{mJ\cdot mol}}{0.52mg}=-1.33\frac{kcal}{mol}$$

Appendix A

Appendix A–7: Sample Calculations for Poly(T) 30mer Adsorption to and Desorption from Sepharose CL–6B

Conditions:

Biomolecule:	Poly(T) 30mer
Molecular Weight:	9,063.9 *g/mol*
Solution:	1.5 M ammonium sulfate, pH = 8.0
Temperature:	26.1° C
Loop Volume:	0.52 *mL*
Flow rate:	1.65 *mL/hr*

Heat Calibration Value: $\frac{9mJ}{19.735boxes} = 0.456\frac{mJ}{box}$

Conversion Factor (to convert *mJ/mg* to *kcal/mol*):

$$\left(\frac{1cal}{4.18J}\right)\left(\frac{1J}{1000mJ}\right)\left(\frac{1kcal}{1000cal}\right)\left(\frac{1000mg}{1g}\right)\left(\frac{9,063.9g}{1mol}\right) = 2.1684\frac{kcal \cdot mg}{mJ \cdot mol}$$

Calculating the Amount Injected:

Dividing the mass of dry oligonucleotide by the volume of carrier fluid added:

$$\frac{3.70mg}{3.70mL} = 1.0\frac{mg}{mL}$$

Multiplying the solution concentration by the sample volume:

$$1.0\frac{mg}{mL} \times 0.52mL = 0.52mg$$

Amount injected: 0.52 *mg*

Calculating the Heat of Adsorption:

Number of boxes in heat signal: 1.4 *boxes*

Calculating the heat and converting to *kcal/mol*:

$$\frac{0.456\frac{mJ}{box}\times 1.4 boxes\times 2.1684\frac{kcal\cdot mg}{mJ\cdot mol}}{0.52mg}=2.66\frac{kcal}{mol}$$

Calculating the Heat of Desorption:

Number of boxes in heat signal: -1.6 *boxes*

Calculating the heat and converting to *kcal/mol*:

$$\frac{0.456\frac{mJ}{box}\times -1.6 boxes\times 2.1684\frac{kcal\cdot mg}{mJ\cdot mol}}{0.52mg}=-3.04\frac{kcal}{mol}$$

Appendix A

Appendix A–8: Sample Calculations for Poly(A) 30mer Adsorption to and Desorption from Sepharose CL–6B

Conditions:

Biomolecule:	Poly(A) 30mer
Molecular Weight:	9,344.3 *g/mol*
Solution:	1.5 M ammonium sulfate, pH = 8.0
Temperature:	25.9° C
Loop Volume:	0.52 *mL*
Flow rate:	1.65 *mL/hr*

Heat Calibration Value: $\frac{9mJ}{19.735boxes} = 0.456\frac{mJ}{box}$

Conversion Factor (to convert *mJ/mg* to *kcal/mol*):

$$\left(\frac{1cal}{4.18J}\right)\left(\frac{1J}{1000mJ}\right)\left(\frac{1kcal}{1000cal}\right)\left(\frac{1000mg}{1g}\right)\left(\frac{9{,}334.3g}{1mol}\right) = 2.23309\frac{kcal \cdot mg}{mJ \cdot mol}$$

Calculating the Amount Injected:

Dividing the mass of dry oligonucleotide by the volume of carrier fluid added:

$$\frac{1.79mg}{2.5mL} = 0.716\frac{mg}{mL}$$

Multiplying the solution concentration by the sample volume:

$$0.716\frac{mg}{mL} \times 0.52mL = 0.37mg$$

Amount injected: 0.37 *mg*

Calculating the Heat of Adsorption (see Figure 5-9):

Number of boxes in heat signal: 4.35 *boxes*

Calculating the heat and converting to *kcal/mol*:

$$\frac{0.456\frac{mJ}{box}\times 4.35 boxes\times 2.23309\frac{kcal\cdot mg}{mJ\cdot mol}}{0.37 mg}=12.0\frac{kcal}{mol}$$

Appendix A

Appendix A–9: Sample Calculations for BSA Adsorption onto PEI–1000–10

Conditions:

Biomolecule:	Bovine Serum Albumin (BSA)
Molecular Weight:	69,000 *g/mol*
Solution:	0.1 M KCl, pH = 6.0
Temperature:	26° C
Loop Volume:	0.32 *mL*
Flow rate:	1.65 *mL/hr*

Calibration Curve Equation (UV Spectrophotometer at 280 nm):

$$y = 0.6313x + 0.0156$$

y = UV absorbance value

x = Concentration (*mg/mL*)

Heat Calibration Value: $\dfrac{9mJ}{17.2boxes} = 0.52\dfrac{mJ}{box}$

Conversion Factor (to convert *mJ/mg* to *kcal/mol*):

$$\left(\frac{1cal}{4.18J}\right)\left(\frac{1J}{1000mJ}\right)\left(\frac{1kcal}{1000cal}\right)\left(\frac{1000mg}{1g}\right)\left(\frac{69{,}000g}{1mol}\right) = 16.5072\frac{kcal \cdot mg}{mJ \cdot mol}$$

UV Measurements:

Prepared Solution: Dilution ratio→20

Absorbance values: 0.640
0.663
0.673

Effluent: Dilution ration→20
Effluent Volume→3.30 mL

Absorbance values: 0.045
0.046
0.045

Calculating the Amount Injected:

Average of the UV absorbance values: $\frac{0.640+0.663+0.673}{3}=0.659$

Inserting the average UV absorbance value into the calibration curve equation:

$$\frac{0.659-0.0156}{0.6313}=1.02\frac{mg}{mL}$$

Multiplying this concentration by the dilution factor: $1.02\times 20=20.4\frac{mg}{mL}$

Multiplying the solution concentration by the sample volume:

$$20.4\frac{mg}{mL}\times 0.32mL=6.53mg$$

Amount injected: 6.53 *mg*

Calculating the Amount Recovered:

Average of the UV absorbance values: $\frac{0.045+0.046+0.045}{3}=0.0453$

Inserting the average UV absorbance value into the calibration curve equation:

$$\frac{0.0453-0.0156}{0.6313}=0.047\frac{mg}{mL}$$

Multiplying this concentration by the dilution factor: $0.047\times 20=0.94\frac{mg}{mL}$

Multiplying the solution concentration by the effluent volume:

$$0.94\frac{mg}{mL}\times 3.30mL=3.1mg$$

Amount recovered: $3.1mg$

Calculating the Amount Adsorbed:

$$6.53mg-3.1mg=3.43mg$$

Calculating the Heat of Adsorption:

Number of boxes in heat signal: 3.8 *boxes*

Calculating the heat and converting to *kcal/mol*:

$$\frac{0.52\frac{mJ}{box}\times 3.8boxes\times 16.5072\frac{kcal\cdot mg}{mJ\cdot mol}}{3.43mg}=9.51\frac{kcal}{mol}$$

Appendix A

Appendix A–10: Sample Error Analysis

UV Measurements:

Prepared Solution: Dilution ratio→30

Smallest volume increment of pipette: ±0.002 *mL*

Absorbance values: 0.853
0.865
0.860

Effluent: Dilution ratio→ 3.5

Effluent Volume:→3.30±0.05 *mL*

Absorbance values: 0.595
0.602
0.589

Loop Volume: 0.320±0.003 *mL*

Calibration Curve Equation: $y = 0.6313x + 0.0156$

Error in Calculated Concentration, Injected Solution:

Mean Absorbance: $\frac{(0.853 + 0.865 + 0.860)}{3} = 0.8593$

Error of Mean:

$$\sqrt{\frac{(0.853 - 0.8593)^2 + (0.865 - 0.8593)^2 + (0.860 - 0.8593)^2}{3}} = \pm 0.0049$$

Error of Product (from calibration curve): $\frac{1}{0.6313} \times 0.0049 = \pm 0.0078$

Diluted Concentration (from calibration curve):

$$\frac{(0.8593 - 0.0156)}{0.6313} = 1.337$$

Total Concentration: $1.337 \times 30.0 = 40.1 mg/mL$

Error in Total Concentration:

$$E_P = 30.0 \times 1.337 \times \sqrt{\left(\frac{0.002}{30.0}\right)^2 + \left(\frac{0.0078}{1.337}\right)^2} = \pm 0.23$$

Error in Calculated Concentration, Effluent:

The error in calculated concentration for the effluent is calculated in the same way as that for the injected solution. Using the UV absorbance values above, the calculated values are:

Total Concentration: $3.21 mg/mL$

Error in Total Concentration: ±0.030.

Error in Calculated Mass, Injected Solution:

Error in injected Mass:

$$E_P = (0.320)\times(40.1)\sqrt{\left(\frac{0.003}{0.320}\right)^2 + \left(\frac{0.23}{40.1}\right)^2} = \pm 0.14$$

Error in Effluent Mass:

$$E_P = (3.30)\times(3.21)\sqrt{\left(\frac{0.05}{3.30}\right)^2 + \left(\frac{0.030}{3.21}\right)^2} = \pm 0.19$$

Error in Amount Adsorbed:

$$E_{diff} = \sqrt{0.14^2 + 0.19^2} = \pm 0.24$$

Error in Heat of Adsorption:

Number of Boxes: 4.00±0.02 *boxes*
Calibration Factor: 0.52±0.01 *mJ/box*
Amount Adsorbed: $(0.32\times 40.1)-(3.3\times 3.21) = 2.24 mg$
Conversion Factor (converting *mJ/mg* to *kcal/mol*): $16.5072 \frac{kcal \cdot mg}{mJ \cdot mol}$

Error in Product (Heat of Adsorption):

$$\sqrt{(4\times 0.01)^2 + (0.52\times 0.02)^2} = \pm 0.041$$

Error in Quotient (Heat of Adsorption):

$$\frac{4.00\times 0.52}{2.24}\sqrt{\left(\frac{0.041}{4.00\times 0.52}\right)^2+\left(\frac{0.24}{2.24}\right)^2}=\pm 0.10$$

Total Error (Heat of Adsorption):

$$E_{Total}=16.5072\times 0.10=\pm 1.65 kcal/mol$$